25

UNCLASSIFIED

[redacted]

BMI-1288

MASTER

GCRE CRITICAL-ASSEMBLY STUDIES

[redacted]

AEC RESEARCH AND DEVELOPMENT REPORT

BATTELLE MEMORIAL INSTITUTE

[redacted]

UNCLASSIFIED

1 4133

UNCLASSIFIED

[redacted] Report No. BMI-1288
~~C-83 - Reactors - Special Features of Military Package Power Reactors (M-3679, 21st Ed.)~~

Contract No. W-7405-eng-92

MASTER

GCRE CRITICAL-ASSEMBLY STUDIES

by

David A. Dingee
William C. Ballowe
Raymond W. Klingensmith
Richard A. Egen
Francis J. Jankowski
Joel W. Chastain

September 10, 1958

Classification cancelled (or changed to UNCLASSIFIED)
by authority of Ltr. fr. Decl. Br., dtd 7/24/59
by JB TIE, date 8/31/59

[redacted]

This document is PUBLICLY RELEASABLE
H. Kinser
Authorizing Official
Date 8/24/06

BATTELLE MEMORIAL INSTITUTE
505 King Avenue
Columbus 1, Ohio

[redacted]

UNCLASSIFIED

[redacted]

TABLE OF CONTENTS

Page

[redacted]

[redacted]

TABLE OF CONTENTS
(Continued)

[redacted]

GCRE CRITICAL-ASSEMBLY STUDIES

David A. Dingee, William C. Ballowe, Raymond W. Klingensmith,
Richard A. Egen, F. J. Jankowski, and Joel W. Chastain

Critical-assembly studies were made to provide engineering and physics data to aid in developing the Gas Cooled Reactor Experiment-1 (GCRE-1). Measurements of critical mass, flux and power distributions, and shutdown worth of the GCRE-1 mock-up safety and control blades were obtained.

The critical assembly consists of aluminum tubes containing four concentric stainless steel cylinders wrapped with highly enriched uranium foil. These tubes are supported at each end by grid plates and arranged to approximate a right circular cylinder. The entire core structure is supported within a tank which can be filled remotely with moderator water. A void beneath the core structure and the air above it represent the gas plenums of the GCRE-1 reactor.

Critical mass and flux power distributions were determined for several cases of four basic cores. The thermal utilization, measured in two core configurations, was 0.780 for the reactor without burnable poison or a lead reflector. The temperature coefficient of reactivity, measured in two cores, was positive at room temperature but negative in the proposed operating-temperature range. The total reactivity effect in going from 20 to 80 C was a positive 0.22 per cent $\Delta k/k$.

The worth of control and safety-shutdown blades of several compositions and sizes in various locations was determined for a number of core configurations; blades having a sandwich construction of cadmium, tungsten, and indium had the greatest shutdown worth.

To date these studies have resulted in a 61-element core (critical with 54 elements) with a 4-in. lead reflector which has 2.5 per cent $\Delta k/k$ excess reactivity for startup and for override of poison and burnup. A mock-up blade configuration has been determined which will control the excess reactivity introduced by flooding the elements with mineral oil (to simulate water flooding when fuel elements are changed in GCRE-1).

INTRODUCTION

A program to develop a transportable nuclear power plant is being carried out by the Army Reactors Branch of the Atomic Energy Commission. As part of this program Aerojet-General Corporation is conducting experiments to investigate compact gas-cooled reactors for this application.

In this program a test reactor, Gas Cooled Reactor Experiment-1 (GCRE-1), will be constructed at the National Reactor Testing Station (NRTS) in Idaho to study the reactor components at operating conditions. To provide data for developing the reactor core, critical-assembly studies have been conducted at Battelle's Nuclear Research Center during the past 8 months.

The test-reactor facility and the critical-assembly mock-up are briefly described below. Further details regarding the test reactor may be found in another report(1); the critical assembly is described more completely in later sections of this report.

Gas Cooled Reactor Experiment-1

The core assembly will consist of two plenum chambers connected by pressure tubes containing fuel elements. The entire assembly will be submerged in water which will serve as moderator and primary radiation shield. A fast-neutron reflector of lead 4 in. thick will surround the core assembly. The plenums and pressure tubes will be insulated from the gas coolant on the inside and cooled by the surrounding unpressurized water moderator; only the gas passages and the fuel elements will be operated at high temperature. A flanged head in the upper plenum will allow access to the core for fuel-element replacement and for instrumentation connections.

Core materials and operating characteristics for a nominal 60-element assembly are listed below. The tube sheet will accommodate up to 73 fuel elements.

Core size	An approximate cylinder 21 in. in diameter and 28 in. long
Reflector	
Top	2 in. water
Bottom	Aluminum
Sides	1/2 in. of water surrounded by 4 in. of lead
Reactor power (heat)	2 megawatts
Coolant	Nitrogen gas
Coolant temperature (inlet)	800 F
Coolant-temperature rise	400 F
Moderator temperature (inlet)	100 F
Average thermal flux	3×10^{12} n/(cm^2)(sec)
Average fast flux	1.9×10^{13} n/(cm^2)(sec)
Uranium loading	19 kg
Volume fractions of materials in active core regions	
UO_2	1 per cent
Stainless steel	11 per cent
Aluminum	7 per cent
Water moderator	51 per cent

(1) References at end.

[redacted]

Insulation	9 per cent
Void	21 per cent

The fuel elements will be formed from plates of UO_2 dispersed in Type 316 stainless steel and clad with Type 318 stainless steel. The plate is 0.045 in. thick with a 0.033-in. core of 30 w/o UO_2-stainless steel and a 0.006-in. cladding. These plates are rolled to form 120-deg sectors of the cylindrical fuel tubes; each fuel tube is made up of three of these rolled sections.

The fuel element will be comprised of four concentric fuel tubes contained in an aluminum pressure tube. The spacing of the fuel tubes is varied to provide larger coolant passages where the heat generation is the greatest. A layer of insulating material will provide a thermal barrier between the coolant gas and the pressure tube. Metal liners will be provided on each side of the fuel-element insulation. The active portion of the fuel elements will be 1.25 in. in diameter and 28 in. long. The pressure tube is 1.875 in. in OD with 0.058-in. wall.

GCRE-1 will be controlled by poison blades inserted horizontally between the pressure tubes. The insertion of the shim-control blades in the reactor core during operation will be held to a minimum; the highly absorbing safety and shutdown blades will be completely withdrawn. A 6-in.-long cylinder of steel containing samarium-oxide will be placed on the insulation liner as a burnable poison to balance fuel burnup and buildup of fission products other than xenon.

Critical-Assembly Mock-Up

The core assembly, fuel elements, and control systems of the GCRE-1 were mocked-up in the critical assembly. The fuel tubes were simulated by wrapping highly enriched uranium foil on stainless steel tubes of four different diameters. A concentric arrangement of these "fuel" tubes and other tubes which mocked-up structural components was placed within an aluminum tube simulating the pressure-tube wall. These aluminum tubes were positioned at top and bottom by aluminum support plates. This entire assembly was contained in a tank mounted on the assembly stand shown in Figure 1.

The gas-plenum assemblies were mocked-up at one end by a stainless steel cylinder 2 ft in diameter and 2 ft high located under the core and at the other end by the air space above the core.

Mock-up control blades of the proper materials were supported rigidly at the periphery of the critical-assembly core. They could not be driven remotely. The critical-assembly control rods were vertically acting driven rods; a sandwich construction of stainless steel and cadmium sheets was used. For loading and making other adjustments to the core, shutdown safety was assured by draining water from the core tank.

The critical assembly was normally operated at room temperature but facilities for heating the moderator-water were incorporated so that temperature coefficients could be obtained.

[redacted]

[redacted]

N47623

FIGURE 1. CRITICAL-ASSEMBLY STAND SHOWING MAJOR COMPONENTS

[redacted]

Purpose of the Experiments

The objectives of the program were (1) to provide engineering information which would aid in the final design of the test-reactor facility, (2) to provide a test facility for optimizing this design, and (3) to furnish information to check the physics design calculations and permit logical extrapolations. Consequently, the critical assembly was designed so that a number of engineering modifications could be simulated. Several core configurations were tried in an effort to increase the excess reactivity available from a given UO_2 loading.

The minimum program undertaken for each core configuration included a critical-mass determination, power-distribution measurements, and mock-up control-blade studies. In studies of several core configurations, detailed measurements were made of flux distributions in typical "cells" around and within a fuel element, and power distributions were measured in the vicinity of interesting regions such as those of mock-up control blades or the core-reflector interface.

The program was redirected frequently as a result of the experiments. Experiments were discontinued for a core configuration when results indicated that it was not practicable in the program. As a consequence, the program of experiments may be better understood if described chronologically rather than topically. This approach is used in the sections describing the test conditions and, where possible, in the other sections.

DESCRIPTION OF THE CRITICAL ASSEMBLY AND FACILITY

Location

The critical assembly was located in the assembly room of the Battelle Critical-Assembly Laboratory. This room is approximately 40 ft square and 50 ft high. The reactor was operated from the console in the control room on the second floor adjacent to the assembly room.

Critical-Assembly Stand

The complete assembly stand and associated facility is shown in Figure 1. The stand has three working levels; the floor level for the dump tanks, filling pump, and heating unit, the core level for the reactor core and instruments, and the upper level for the critical-assembly control-rod-drive units.

Reactor Tank

The reactor tank, a cylinder 52 in. in diameter and 71 in. high, is mounted on the assembly stand with its bottom about 7 ft above the floor level. It is drained through two quick-acting air-to-close spring-to-open 4-in. dump valves into the storage tanks at the floor level.

Core Structure

Figures 2, 3, and 4 show the core assembly and give the nomenclature and location of core components. The core consisted of the mocked-up gas plenum, fuel elements, support and positioning plates, mocked-up and operating control elements, and water moderator – all contained in the reactor tank. During normal operation the bottom of the upper support plate was at the same level as the top of the fuel region. The water level in the critical condition was also at this level for most experiments.

The core assembly provided space for 69 fuel elements supported and positioned between 2-3/4-in.-thick aluminum plates. In later experiments a fast-neutron reflector of 4-in.-thick lead billets was placed around the core perimeter, which restricted the maximum number of fuel elements to 61. The location of the lead is shown in Figure 4.

The fuel-element lattice was hexagonal; the distance between adjacent fuel elements differed along the core radii denoted as AA and BB in Figure 4; i.e., the center-to-center spacing between fuel elements in Positions 1, 5, 14, 29, and 50 was 2.375 in., while the spacing between fuel elements in Positions 1, 4, 12, 29, and 46 was 2.656 in.

The location of the critical-assembly control rods (vertically acting) and the mocked-up GCRE control blades (horizontally mounted) can be seen in Figures 2 and 4.*

Fuel-Element Assembly

Figure 5, a drawing of a fuel-element assembly, shows the aluminum pressure tube, the stainless steel liner on the inside of the insulation, the aluminum positioning cylinder, the four fueled stainless steel tubes, and the central aluminum support mandrel. Three layers of highly enriched uranium foil 0.001 in. by 28 in. and of the required width were wrapped onto each of the four stainless steel fuel tubes to simulate the UO_2-stainless steel GCRE-1 fuel tubes. The foil fuel was held in position by tape (Mystik 7300 Mylar with silicone adhesive). The photograph of Figure 6 shows a tube being wrapped with fuel.

*Readers familiar with GCRE-1 will note that the critical-assembly core is inverted when compared with the prototype reactor. This is significant when the location of the control blades is considered.

[redacted]

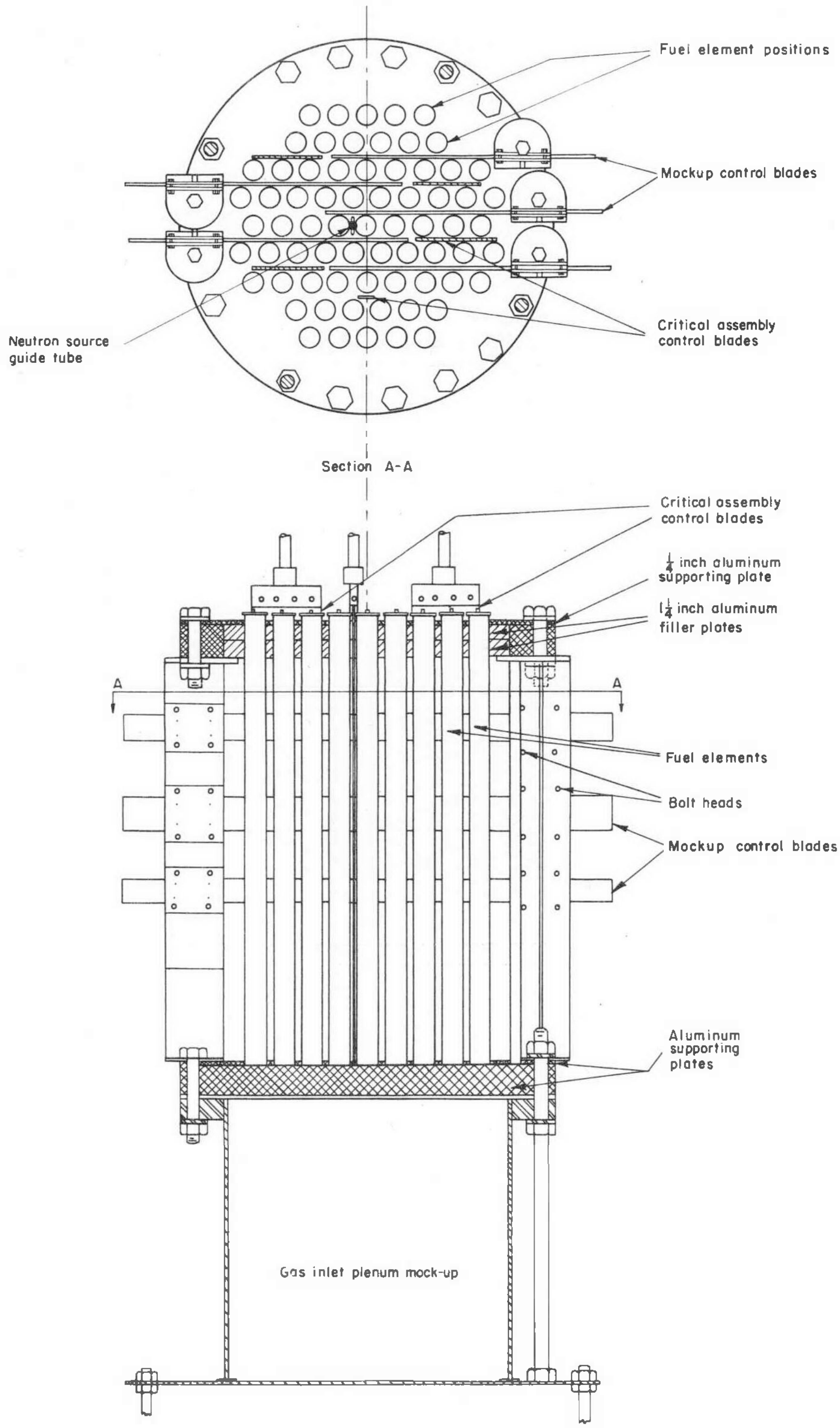

FIGURE 2. GCRE-1 CRITICAL-ASSEMBLY CORE STRUCTURE

[redacted]

[redacted]

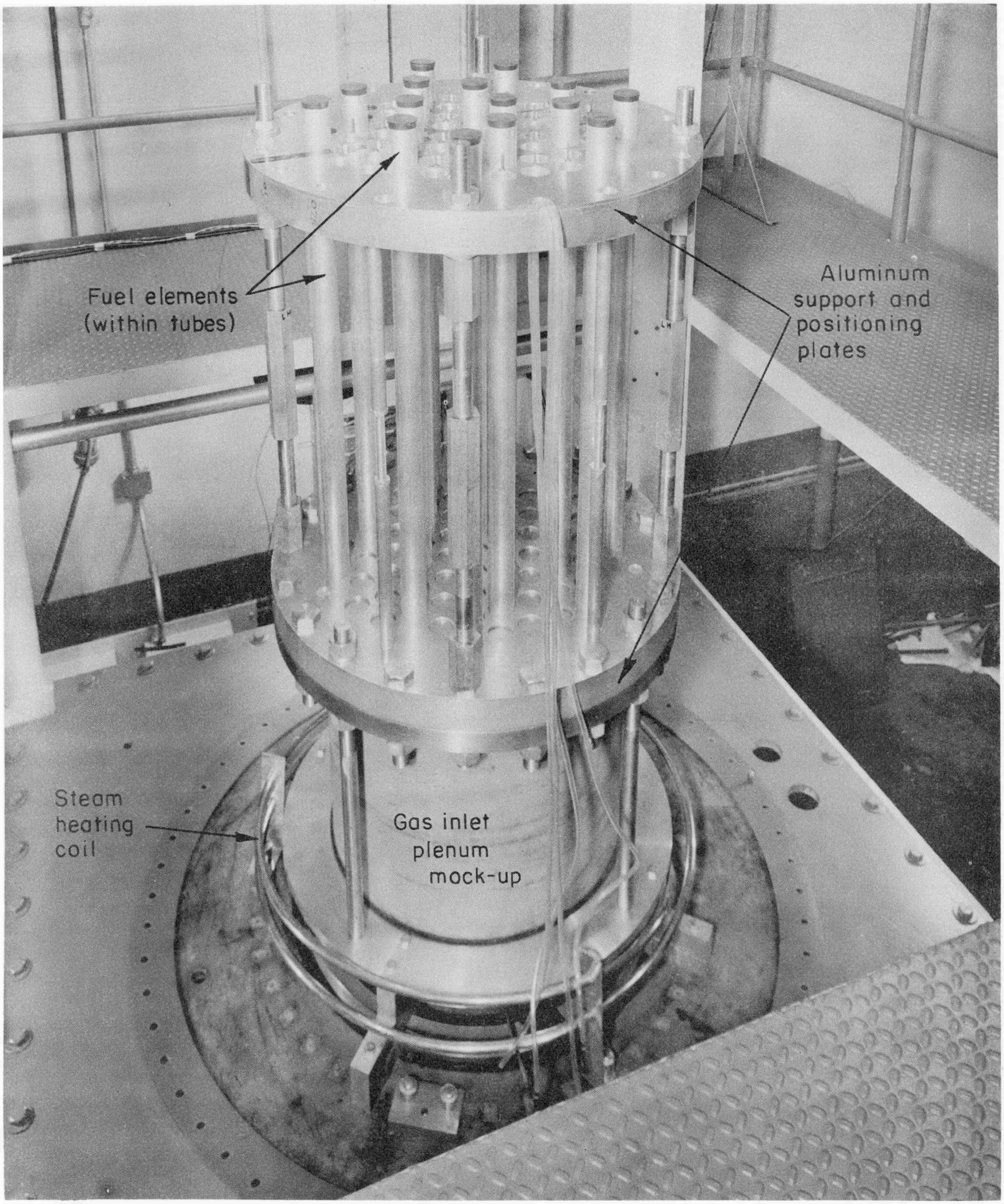

N46767

FIGURE 3. INSTALLATION OF GCRE-1 CRITICAL-ASSEMBLY CORE

[redacted]

[redacted]

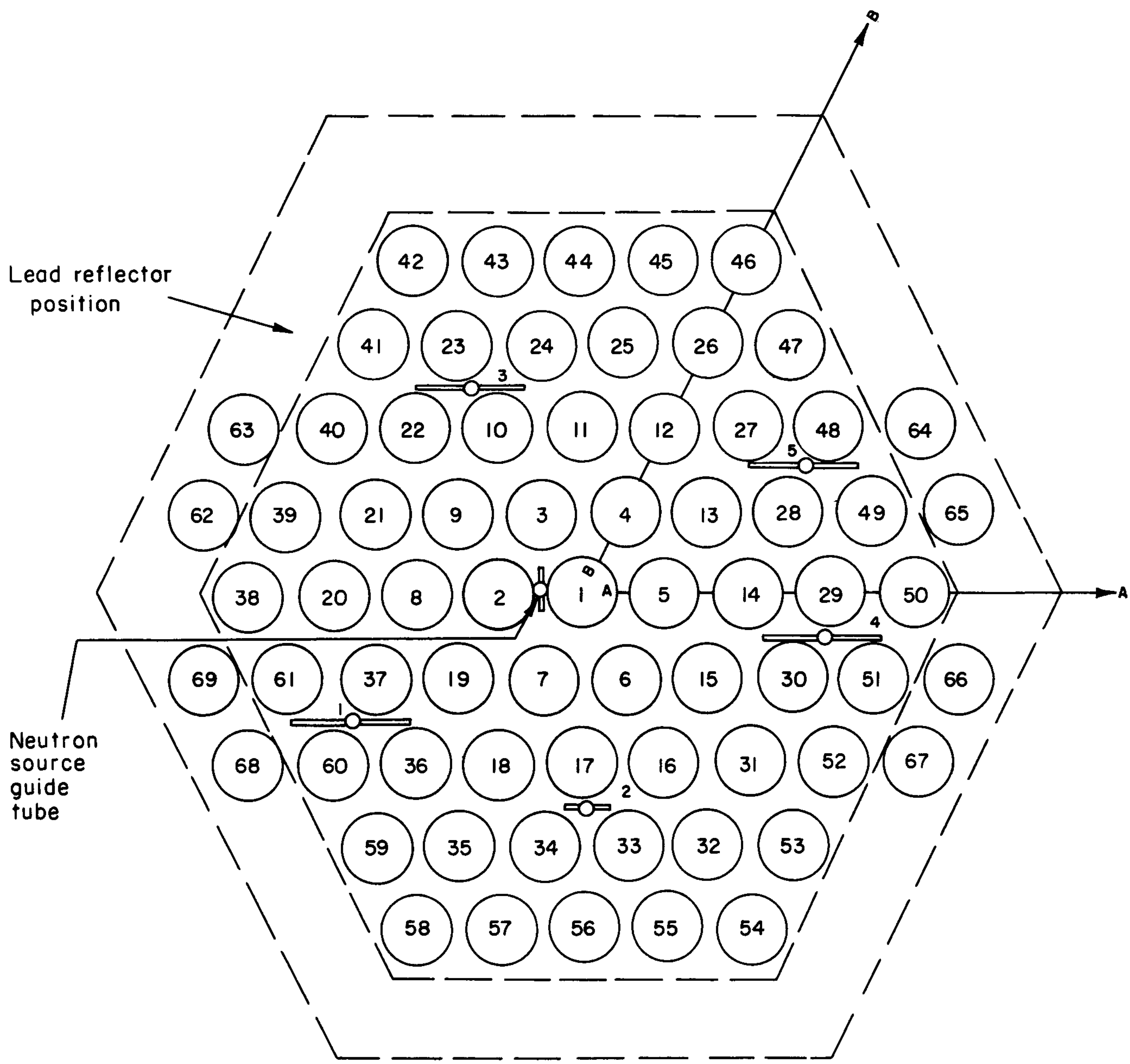

FIGURE 4. GCRE-1 CRITICAL-ASSEMBLY CORE NOMENCLATURE

Fuel-element position numbers are given. Critical-assembly control-rod positions are denoted by numbers at the appropriate locations between fuel elements. Radii AA and BB were used for flux- and power-distribution measurements.

[redacted]

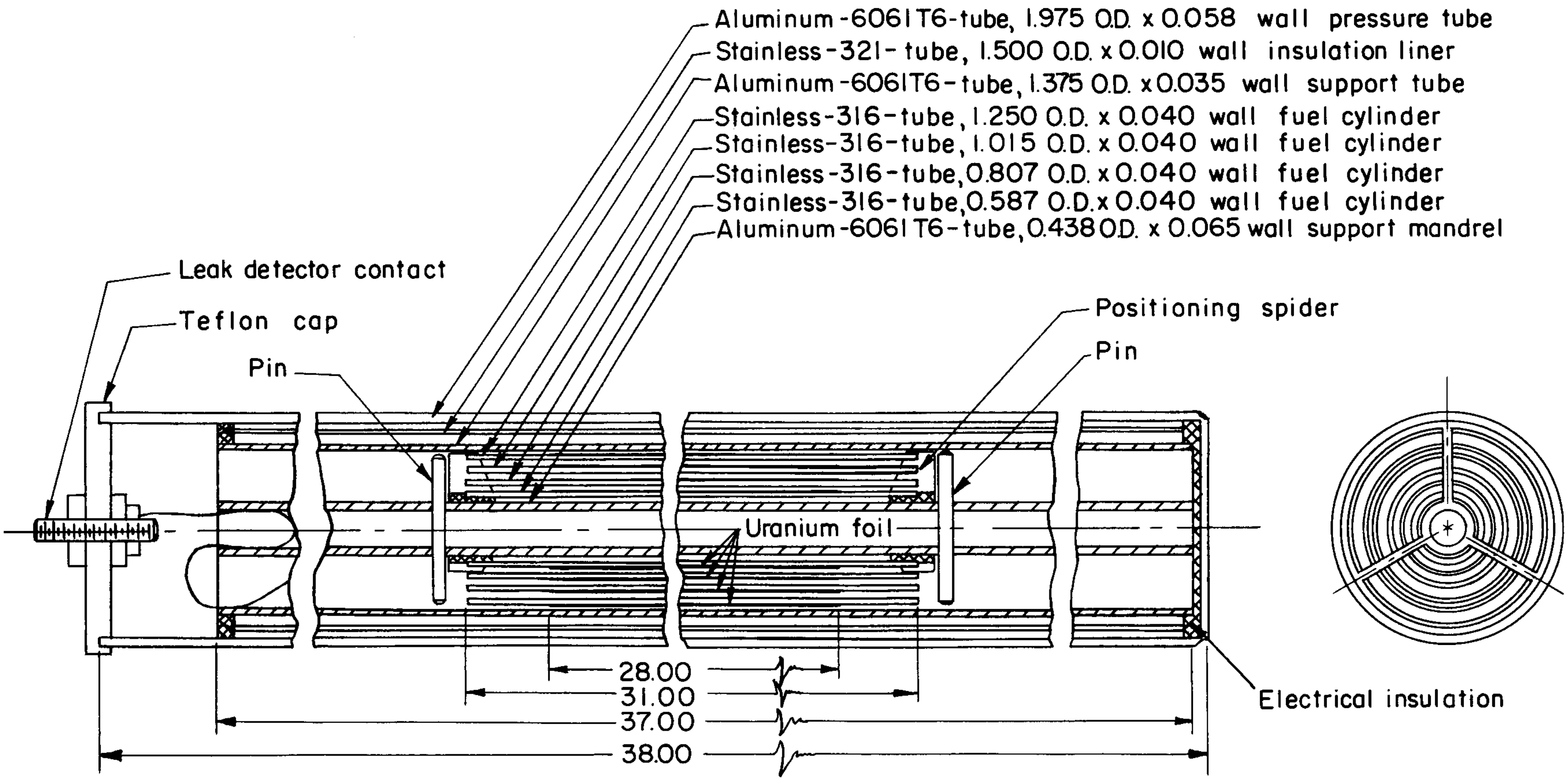

FIGURE 5. FUEL-ELEMENT ASSEMBLY

Burnable poison not shown.

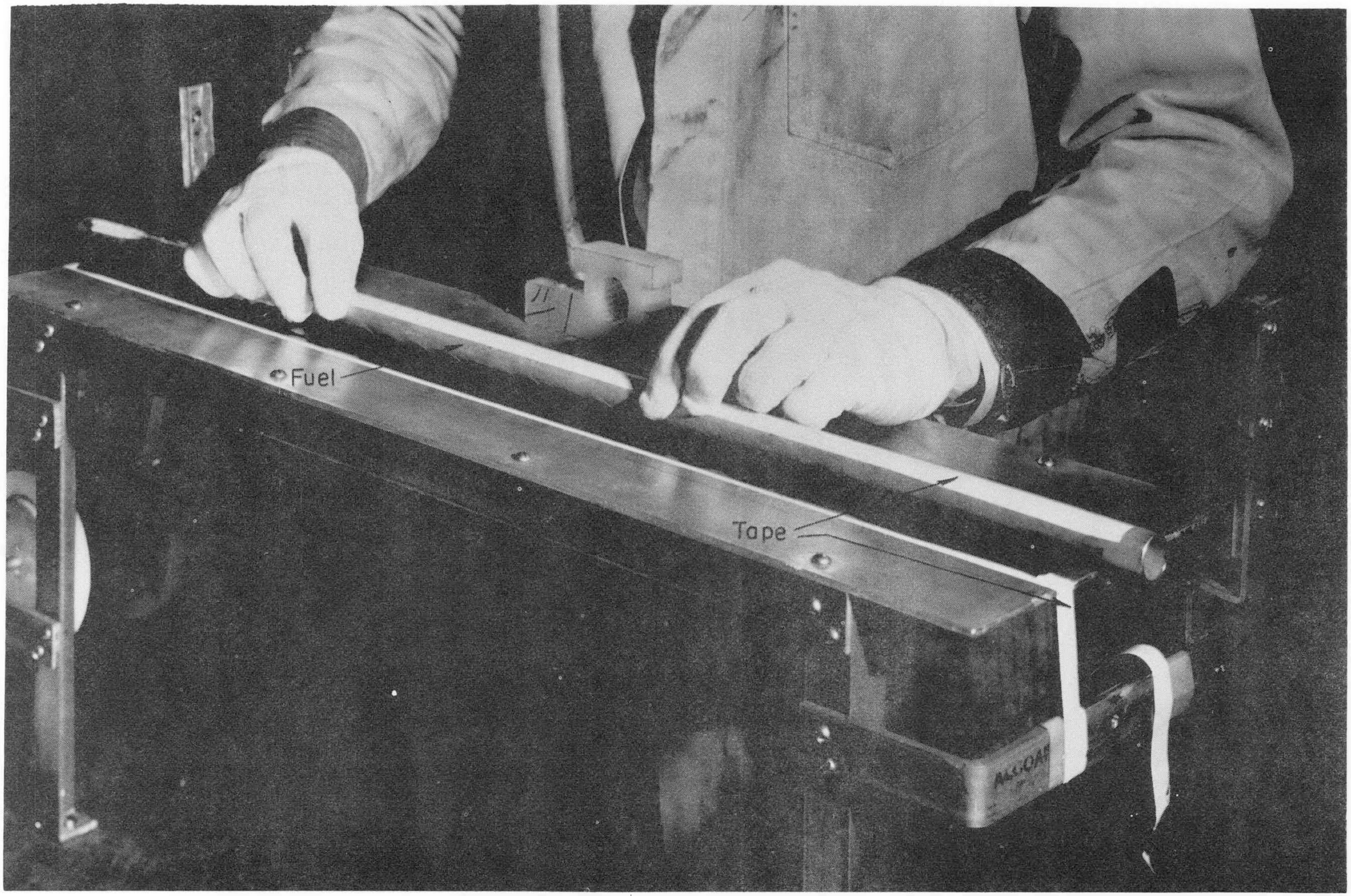

N46769

FIGURE 6. PREPARATION OF A FUEL CYLINDER

The average fuel loading per fuel element was 303.40 g (0.146 g per cm^2) with a maximum deviation of 28 g and a mean deviation of 7.8 g. The volume per cent of materials in the active core region of the critical assembly is given below.

Material	Cell Volume Fractions, per cent
Uranium metal	0.68
Stainless steel	8.63
Aluminum	9.84
Water	51.05
Void	29.80

The average hydrogen/uranium-235 atomic ratio is 111.

For most experiments the stainless steel insulation liner was wrapped with a 5-in.-wide band of cadmium-plated steel foil centered 15 in. up from the bottom of the fuel (approximately 0.12 mil of cadmium plated uniformly onto 15-mil-thick mild steel foil). The cadmium simulated the samarium-oxide cylinder which will be used as burnable poison in GCRE-1.

To prevent moisture from accumulating within the fuel tubes, they were capped with Teflon disks as shown in Figure 5. The contacts used in an electrical-resistance method of detecting water leaking into the tubes also appear in Figure 5. A checkout was made following each day of operation to insure that no water had entered any of the fuel tubes.

The Critical-Assembly Control Rods

Four critical-assembly control rods were used for the majority of the experiments. These were blades of a sandwich construction of 10-mil cadmium sheet between two 1/16-in.-thick stainless steel sheets. Three of the rods were 6 in. wide; the fourth was 1-1/2 in. wide and was used for fine control and accurate reactivity determinations. These rods passed through slots in the upper positioning plate assembly. For some experiments a fourth 6-in.-wide rod was used.

Simulated GCRE-1 Control Blades

GCRE-1 will use fine, setback, shim, shutdown and safety blades. The fine, setback, and shim blades will be constructed of tungsten to reduce distortion of the power distribution. The shutdown and safety blades will be a sandwich of tungsten and indium wrapped with cadmium. A number of different blade dimensions were investigated in the critical-assembly program. The individual blade shapes were constructed by silver soldering and/or brazing pieces of 0.2-in.-thick tungsten. Where required, a combination of 1/16-in. indium sheet and 0.2-in. tungsten was wrapped in 10-mil cadmium sheets which were soft soldered to form an integral unit. For one experiment 1/16-in.-thick tungsten was used. The blades were held rigidly at the core perimeter by the blade supports shown in Figure 2 and could not be moved remotely.

Instrumentation and Controls

Nuclear Instrumentation

Three neutron-sensitive ionization chambers and one photomultiplier tube with a sodium-iodide-thallium activated scintillation crystal were used for control and safety. Two of the ionization-chamber circuits gave outputs proportional to the logarithm of the power level. These outputs were differentiated to give period signals. The remaining ionization chamber was connected to a d-c amplifier to give a linear power indication. The scintillation detector was connected in series with a selenium rectifier to yield a logarithmic-type output signal. Scram circuits were associated with each of the four level and two period outputs.

In addition to the operating instruments, BF_3 and fission counters were used with scalers. These two pulse-counting channels provided information on the low-level operation of the reactor and also provided a means of accurately measuring reactor periods.

With the exception of the scintillation head, all nuclear detectors were located in the reactor tank in watertight containers.

Safety- and Regulating-Rod Drives

Each control-rod drive consisted of a motor, a magnetic clutch, two Selsyn position indicators, a rack-and-pinion gear, and a hydraulic shock absorber. A rod-drive unit is pictured in Figure 7.

Each of the rods had its own drive unit; only one rod was operated at a time. The rods could be driven up or down at 10 in. per min. When the power to the magnetic clutch was interrupted the control rods fell under the action of gravity with an acceleration of approximately 0.7 G to scram the reactor.

Moderator-Water Controls

The reactor tank was filled by a 20-gpm pump. A Tank-o-Meter indicator provided a rough value (±1/20 in.) of the liquid level while an electrical liquid-contact device gave values of the liquid level to within ±0.01 in. when a more accurate measurement was required. For most operations the water level was fixed by an overflow pipe so that the level was reproducible. Criticality was achieved by withdrawing the control rods with the water at the fixed level.

As a secondary shutdown means, water was rapidly drained from the reactor tank through the two quick-acting air-to-close spring-to-open 4-in. dump valves. The active core region was drained in approximately 20 sec. Fine control on the liquid level for other than full-tank levels was achieved by draining water back through the fill lines.

[redacted]

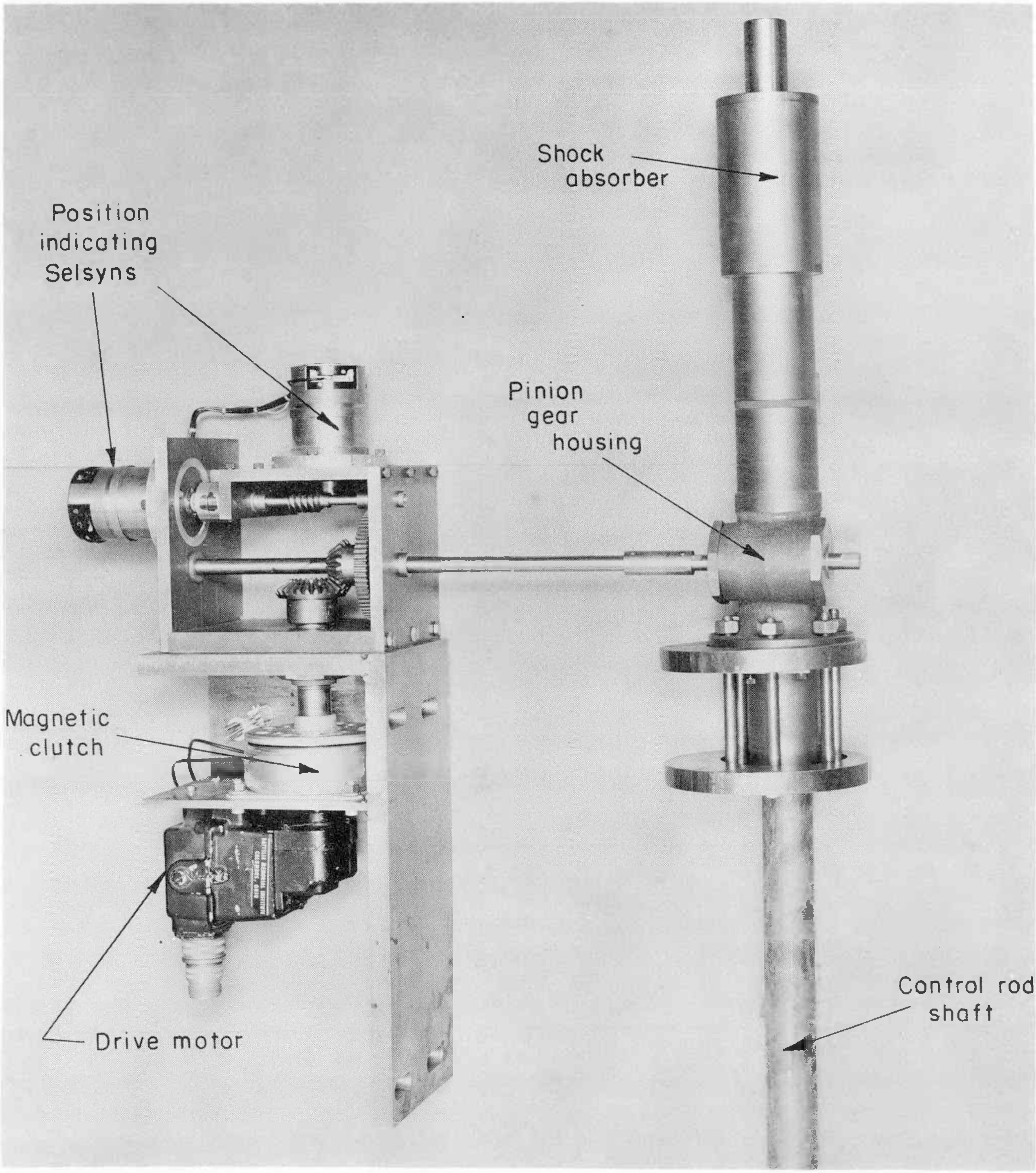

N31849

FIGURE 7. CONTROL-ROD-DRIVE ASSEMBLY

[redacted]

[redacted]

The water temperature was monitored during the experiments by three Thermohm resistance thermometers. One was placed in the reflector region, one in the core between fuel elements at the core midplane, and one in the top of a fuel element (Position 12) between the outer aluminum can and the stainless steel insulation liner. The water was heated by electrical immersion heaters and by a steam coil (1-in. -OD copper tubing 15 ft long). Measurements were made when the entire moderator and reflector regions were at the same temperature.

Water-purity checks were made periodically throughout the course of the experiments. The resistivity of the water averaged 40,000 ohm-cm. The activity of the water was checked weekly; at no time did the activity indicate the presence of contaminants.

Startup Source and Drive

A remotely controlled polonium-beryllium neutron source was used for loading measurements, startup, and experimental purposes. The source position in the core was indicated by Selsyn units.

The source box is shown in Figure 1. The shield box was filled with borax mixed with paraffin to minimize radiation to personnel as well as leakage to the reactor. The source was attached to a long flexible cable which was pushed through a stainless steel tube to position the source within the core.

Counting Facilities

The counting equipment included three photomultiplier channels. Two of these had print-out devices which automatically printed the total shown on the scaler at the end of a counting period. The third channel operated control circuits at the end of a preset count and was used for timing the other two counting channels, which automatically compensated for decay time of the activated foil or wire.

A sample changer moved the foils from a storage hopper to a position under the first counter. The foil was counted and moved to a second counter where it was counted a second time; the foil was then moved to a storage hopper, all automatically.

TEST CONDITIONS AND PROCEDURES

To conduct the critical-assembly research a number of core and reflector configurations were set up. In some cases detailed engineering-type studies were performed while in other cases physics-type information was required. This section of the report discusses the various critical-assembly experiments and the procedures used. Where possible, an estimate of the accuracy associated with the experiments is also given.

[redacted]

Core Configurations Tested

The order in which the core configurations were tested represents an approach toward a core for GCRE-1 which will meet the following specifications: (1) it will have enough excess reactivity to meet power, lifetime, and operating requirements, and (2) it will be adequately shut down when the coolant regions are flooded for fuel-element removal.

Four different cores were constructed during the course of the program. These are the (1) Experimental Core, (2) Clean Core, (3) Lead-Reflected Core, and (4) Simulated-Flooded Core. All these reactors had a 4-1/2-in. lower axial water reflector surrounding the fuel-tube extensions. Except for one reflector-worth experiment, the upper 2-3/4-in. -thick aluminum positioning plate had its lower surface aligned with the top edge of the fuel, which was also the water height in normal operation. The cores differed only in the fuel-element details and in the radial reflector design.

Experimental Core

The Experimental Core consisted of an array of fuel elements without the cadmium strip of burnable poison. There were 69 fuel-element positions available. A water reflector surrounded the core. The Experimental Core provided immediate data to aid in "normalizing" physics calculations and a basis to evaluate the worth of the simulated burnable-poison sheets.

When the burnable poison sheets became available, this core configuration was dismantled to set up the Clean Core.

Clean Core

The simulated burnable poison was added to the fuel elements in this core. A cadmium layer approximately 0.00012 in. thick was plated on a steel foil and wrapped on the insulation-liner tube of each fuel element. The midplane of foils was 1 in. above the horizontal midplane of the fuel.

This core was a good mock-up of the GCRE design at the time of the experiments and therefore a considerable amount of testing was done with the Clean Core. However the excess reactivity of this core was not sufficient to provide for poison override, burnup, and operating control, so a modified reactor design was suggested to overcome this difficulty. This modification led to the construction of the Lead-Reflected Core.

Lead-Reflected Core

The fuel elements in this core were identical with the Clean Core elements. A 4-in. -thick lead reflector was added at the core perimeter 1/2-in. from the fuel elements. The lead billets making up the reflector were 24 in. long and their midplane coincided with the fuel midplane.

Two lead-reflected configurations were constructed. In the first, the lead surrounded 51 fuel elements. When this did not provide a critical configuration, the reflector was rearranged to roughly surround 61 elements. After preliminary tests with this arrangement the lead was reoriented to surround the 61 elements with a more uniform 1/2-in. gap between the lead and perimetral fuel elements. The predicted reactivity effect of the lead reflector was borne out, so this reactor design became the new reference GCRE-1 concept. Accordingly, a number of experiments, primarily of an engineering nature, were performed with this reactor configuration.

The Simulated-Flooded Core

Whenever fuel elements are changed in the GCRE-1 core the upper gas plenum will be removed and all the fuel elements will be flooded. The reactivity worth of the control blades must be sufficient to maintain the core in a noncritical condition. To simulate flooding, each fuel element was filled with 1100 cm^3 of mineral oil with a molecular formulation approximating $C_{20}H_{42}$ and a density of 0.83 g per cm^3. A water-simulating material was used because uranium foil corrodes rapidly in water. The volumetric hydrogen density of mineral oil is about 10 per cent greater than that of water. The tests were performed with the lead reflector surrounding 61 element positions.

Table of Experiments

Table 1 presents a summary of the experiments performed during the present critical-assembly program.

Experimental Procedures

In general the experimental procedures used in this study have been used in previous critical-assembly work. Nevertheless, the procedures used in each of the major study areas are given below so that the results can be properly interpreted.

Critical Mass

In a heterogeneous reactor system such as the GCRE critical assembly, the exact critical mass is not easily determined. Experimentally, the number of fuel elements and the excess reactivity in the critical core are measured and are the quantities reported here.

The total uranium-235 in the core was obtained from the weights of the individual uranium foils which were recorded by the fuel fabricator to the nearest one hundredth gram. A maximum variation of about 7 per cent occurred in the uranium loadings in the various fuel elements; the mean variation throughout the core was less than 3 per cent. No estimate was made of the influence of this nonuniformity on the critical condition.

TABLE 1. EXPERIMENTS PERFORMED IN THE CRITICAL-ASSEMBLY PROGRAM

	Measurements Obtained With Designated Core		
Experimental Core	Clean Core	Lead-Reflected Core	Simulated-Flooded Core
Worth of 1. Upper axial annular reflector 2. Upper axial reflector 3. Peripheral fuel elements 4. Peripheral empty fuel cans	Worth of 1. Peripheral fuel elements	Worth of 1. Peripheral fuel elements 2. Polyethylene, paraffin, and mineral oil as compared with water in an element position	Worth of 1. Peripheral fuel elements
M^2 in two configurations	--	--	--
--	Temperature coefficient of reactivity (20-75 C)	Temperature coefficient of reactivity (20-75 C)	--
Worth of mock-up shim and shutdown blades at two positions in the core	Effects of changes in size and position of a mock-up shutdown blade	Worth and geometric effect of mock-up shim and shutdown blades at one location in the reactor	Critical configuration with a variety of mock-up shutdown-blade configurations
2-D flux distribution with bare and cadmium-covered wire	2-D flux distribution with bare and cadmium-covered wires	2-D power distribution	Axial flux distribution in the center fuel element
2-D power distribution with catcher foils	Axial, radial and azimuthal power variation in the vicinity of the cadmium band on two fuel elements	Detailed power distribution within fuel elements at the center of the core and the periphery	Detailed flux distribution within and adjacent to the central fuel element with bare and cadmium-covered wires
Detailed flux distribution within and adjacent to fuel element with bare and cadmium-covered wires		Detailed perturbed power distribution near a mock-up shim blade	

[redacted]

Reactivity Effects

Reactivity effects were measured by the change in the reactor period or by the change in the position of calibrated control rods. Since the control rods were calibrated by period measurements, all reactivity measurements are based on the period-reactivity relationship:

$$\rho = \frac{\ell^*}{T\, k_{eff}} + \sum_{i=1}^{6} \frac{\beta_i \epsilon_i}{1 + \lambda_i T} , \qquad (1)$$

where

ρ = reactivity = $k_{eff}-1/k_{eff}$

ℓ^* = neutron lifetime = 10^{-4} sec (assumed)

k_{eff} = multiplication constant

T = reactor period

β_i = fraction of fission neutrons in i^{th} delayed group[2]

ϵ_i = importance factor for i^{th} delayed neutron group = 1 (assumed)

λ_i = decay constant of the i^{th} delayed neutron emitter[2].

A large error in ℓ^* is not reflected as a large error in calculating the reactivity from the period since in these experiments the first term of Equation (1) is small compared with the summation term. Since very accurate determinations of absolute reactivity were not required, assuming $\epsilon_i = 1$ does not introduce a serious error. In general, reactivity effects caused by changes in core loading or mock-up control-blade position could compensate for the effect of change in other quantities such as temperature or water height. The error introduced by the assumed value for ϵ_i is the same for all reactivity determinations.

Reactor period was measured by several detectors. From these data the probable errors in the calculated reactivity were determined.[3] In some cases a control rod was calibrated by compensating for changes in its position with a calibrated rod. No additional errors are assumed when these "derived" rod-worth curves are used to evaluate reactivity changes.

Subcritical Reactivity Measurements

Measurements of the amount the reactor was subcritical were necessary in certain experiments where it was impossible to achieve a critical condition. Two methods were used for these measurements. The first consisted of plotting the reciprocal count rate versus fuel loading. Extrapolation of these data to zero gives the required critical loading. The inverse-count-rate method, while simple to perform, contains several inherent problems which affect the accuracy, an important one being the geometrical effect which additional fuel elements have on the instrumentation.

[redacted]

[redacted]

The second method used to measure subcriticality was the source-jerk method.(4) The subcritical reactor with a neutron source inserted is allowed to come to an equilibrium neutron level, C_1. Then the source is suddenly removed (at time zero) and the neutron level monitored as it decays. A plot of neutron level versus time extrapolated to t = 0 gives the neutron level, C_2. The neutron levels immediately before and after the removal of the source are related to the effective multiplication factor, k_{eff}, as follows:

$$\frac{C_1 - C_2}{C_2} = \frac{1 - k_{eff}}{\beta k_{eff}} . \tag{2}$$

The main disadvantage of the source-jerk method is the low neutron levels and, hence, the low counting rates. Another possible error arises from the finite time required for source removal, since Equation (2) assumes that the neutron level due to neutrons from the delayed precursors is the same immediately before and after the source is removed. It follows that the time of removal must be considerably shorter than the half-life of the shortest-lived delayed precursors. In the experiments described in this report, a source-removal time of about 0.1 sec was used. The method of source removal, though simple, proved effective. A 5/16-in.-ID stainless steel tube was inserted vertically into the source slot near the center of the core. A 2-curie polonium-beryllium source 1/4 in. in diameter and 1-1/4 in. long was lowered into this tube on a nylon cord. This cord was threaded over the test stand to a point outside the assembly room through a system of pulleys where it could be pulled by hand to remove the source. A monitoring system gave a signal in the control room when the source left the center position of the core, and when the source had reached a measured position well above the core. These signals were fed into the timing channel of a Sanborn Model 150 recorder. Another channel of the Sanborn was used to monitor the pulse signal from a fission chamber so that the count rate could easily be determined. The data on the Sanborn recorder gave a value of C_1 and permitted an extrapolation to zero time for obtaining a value of C_2 needed for Equation (2).

Axial-Reflector Worth

In one experiment the upper grid plate was raised approximately 2 in. so that the reactivity worth of the axial reflector could be measured. In another experiment with the aluminum grid plate in its normal position, the water level was raised so that the annular space around the grid plate could be filled with water to determine the reactivity worth of this region. In the GCRE-1 this region corresponds to the reflector surrounding the gas plenum; this experiment showed that the omitting of this reflector in the critical-assembly work was justified.

Since interlocks prevented raising the water level when the reactor was at or near critical, the water was raised above the desired level while the reactor was substantially subcritical and the reactor made slightly supercritical by withdrawing control rods. The water level was then dropped in small increments and the reactor period determined for each water level. Changes in reactivity corresponding to the reactor periods for a given change in water level can be used to determine the reactivity worth of the entire region.

[redacted]

[redacted]

Migration Area

The migration area was obtained by differentiating the one-group equation with respect to core height.[5] This gives

$$\frac{\partial \rho}{\partial H} = \frac{2\pi^2 M^2}{k_\infty} \frac{1}{H^3} , \qquad (3)$$

where

H = water height plus total extrapolation distance

k_∞ = infinite multiplication constant

M^2 = migration area

ρ = reactivity.

$\frac{\partial \rho}{\partial H}$ can be measured at known H and k_∞ can be estimated theoretically to obtain M^2.

The reactor was put on a period with all control rods out and the water level at the top of the fuel region. The water level was lowered in increments of about 0.05 in. and the change in period noted.

If the reflector savings is known or assumed, only one determination of differential water-height worth is required to determine $\frac{M^2}{k_\infty}$. However, if measurements are made with two or more configurations using the same core lattice, the reflector savings may be treated as a second unknown and determined from simultaneous solutions of two or more equations having the form of Equation (3).

If the differential water-height worth is determined for two different core radii, this worth may be integrated between the two critical heights to determine the total reactivity change. This reactivity change is also the worth of the increase in reactor diameter. The one-group criticality equations may be differentiated with respect to the radius to obtain

$$\frac{\Delta \rho}{\Delta R} = 11.58 \frac{M^2}{k_\infty} \frac{1}{R^3} , \qquad (4)$$

which is similar in form to Equation (3).

If the flux and migration areas are isotropic, the migration area as determined by Equation (3) and Equation (4) will be the same. If there are differences in these determinations they are indications of an anisotropic effect.

[redacted]

The determinations assume that the effective core height changes at the same rate as the water height, i.e., the extrapolation distance is not dependent on water height. The fuel exposed as the water is lowered has a positive effect on reactivity so that generally the measured migration area is low. No quantitative estimate of this effect was made.

Temperature Coefficient of Reactivity

The temperature coefficient of reactivity was measured by raising the water temperature in increments of 5 to 10 C and noting the change in position of a calibrated control rod. To degas the water it was heated and allowed to cool to room temperature prior to the measurements. Each water temperature was maintained for a time to insure that all reactor components were at the same temperature. However, the position of the calibrated control rod changed only slightly while awaiting temperature equilibrium; consequently, at the higher temperatures, which are difficult to maintain, this was not always done.

Two stirrers were used to circulate the water through the tank. These stirrers were shut off when measurements were made since they caused the water height to vary. At high temperatures the immersion heaters were operated during the measurements to maintain the temperature.

The moderator temperature was measured by two resistance thermometers (trade name, Thermohm). One was positioned between fuel cylinders about midway in the fuel region; the other was located in the reflector region. The reactivity was measured when these temperatures agreed to within 0.1 C.

A third Thermohm was located in a fuel element, about 8 in. from the top between the insulation liner and the outer aluminum can. The temperature at this point lagged the other readings by 2 to 6 C because of poor heat transfer between the fuel cylinders and the moderator. Tests showed that the fuel-element temperature did not affect the results.

Flux and Power Distributions

The flux was obtained by measuring the manganese activity in irradiated iron-manganese-molybdenum wires. These wires were 0.033 in. in diameter and contained approximately 15 w/o manganese and 2 w/o molybdenum. For two-dimensional core plots long lengths of wires were inserted in the mandrel in the individual fuel elements and in 0.038-in.-ID aluminum tubes which were located midway between the fuel elements on two radii. After radiation these wires were accurately cut to 1 in. lengths for counting.

Detailed flux maps were obtained in unit cells by irradiating many wires which were precut to 1-in. lengths. Within the element these wires were taped to fuel and structural cylinders. The wires were always separated from the fuel by a 1-mil aluminum foil to prevent contaminating the manganese activity with fission-product activity. In the water moderator region the individual wires were positioned by plastic holders.

[redacted]

Epicadmium flux was obtained by irradiating the same type wires in cadmium tubes having a wall thickness of 15 mils.

The wires were activated by operating the reactor at about 10 w for 30 to 60 min. An extra wire was always irradiated to serve as the source for the decay-correcting timing channel. When necessary, another wire was irradiated for normalization purposes.

The power at a given point in the core was determined by the catcher-foil technique. Aluminum foil placed adjacent to the uranium fuel caught the recoiling fission products, which could then be counted. Disks punched from the foil and counted give a direct measure of power since the fission-product activity in the catcher foil is directly proportional to the fissioning in the uranium fuel.

In some cases the aluminum foil was used with 3/4-in.-diameter 1-mil uranium foil. In other cases the catcher material was placed directly against the uranium foil wrapped on the tubes in the fuel elements. In both cases it was necessary to have the uranium foil clean at the location being measured so that the recoiling fission products would not be absorbed before reaching the catcher material. The catcher foils were 1/2 in. in diameter and were punched from the aluminum foil after the irradiation. In a few cases the uranium-foil combination was wrapped in cadmium to determine the epicadmium contribution to the power.

About 200 foils were activated in each run at a reactor power of 10 w. This builds up enough long-lived activity to permit counting the foils over a moderate period of time. Counting techniques were the same as those for flux determinations.

Before each run the counting facilities were checked to insure that they were operating within normal statistical error. During operation each wire or foil was counted at least once and sometimes twice on each of the two counting channels so that spurious counts could be detected; a few foils or wires were recounted at intervals to detect any long-term drift in the counting equipment. However, these steps were not sufficient to permit a reliable statistical analysis of the data. An estimated error based solely on comparison of data from the two counting channels is 5 per cent; the use of mean values and smoothed curves through the data should considerably reduce this error.

Thermal Utilization

Thermal utilization was determined for the Experimental Core and Simulated-Flooded Core from detailed flux data taken within unit cells at selected points in the core. An average value of thermal flux in each material was calculated from these flux data.

Ratios of material to fuel cross sections, volumes, and average fluxes were calculated for each material. The microscopic thermal-neutron absorption cross sections of the materials were corrected for application to a Maxwellian distribution and for non-1/v dependence (for uranium-235).

[redacted]

[redacted]

Thermal utilization was calculated using the equation:

$$f = \frac{1}{1 + \sum_j \left(\frac{\Sigma_j}{\Sigma_F} \frac{\phi_j}{\phi_F} \frac{V_j}{V_F} \right)} , \tag{5}$$

where

Σ_j = macroscopic thermal absorption cross section of the j^{th} material

ϕ_j = thermal neutron flux averaged over all of the j^{th} material in the unit cell

V_j = volume of j^{th} material per unit cell (assuming unit height)

F = fuel material (subscript).

The indices, j, vary over all materials in the unit cell other than fuel, i. e., water, stainless steel, aluminum, air, and, in the Simulated-Flooded Core, mineral oil.

EXPERIMENTAL RESULTS

Table 1 lists experiments performed during the program, and the fuel element position notation is shown in Figure 4.

The reactivity worths of the critical-assembly control rods were required as steps in measuring other changes, but are not of value in themselves in the GCRE-1 analyses. The calibrations of these rods are given in Appendix A.

Experimental Core

Critical Core Configuration

The Experimental Core was critical with 54 fuel elements arranged as shown in Figure 8. The core contained 16,383 g of uranium-235 and an excess reactivity of +0.250 ± 0.009 per cent $\frac{\Delta k}{k}$.

[redacted]

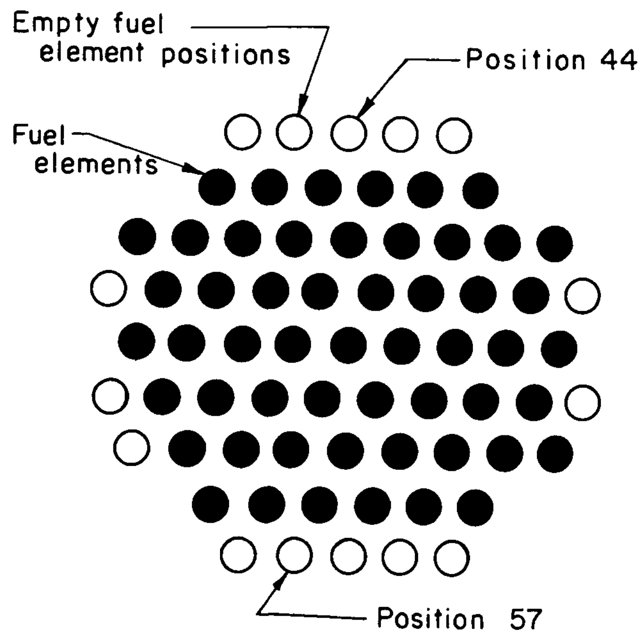

FIGURE 8. INITIAL CRITICAL CONFIGURATION, EXPERIMENTAL CORE – 54 FUEL ELEMENTS

Reactivity Worth of Peripheral Fuel Elements and Voids

Two additional fuel elements in Positions 44 and 57 were added to the core to provide excess reactivity for experiments. The reactivity worth was determined for the additional elements and for voids, i. e., a fuel can without fuel or structural material, at Positions 44 and 57. The results of these measurements are given in Table 2.

TABLE 2. NUMBER OF FUEL ELEMENTS, FUEL INVENTORY, AND EXCESS REACTIVITY IN EXPERIMENTAL CORE

Number of Fuel Elements	Fuel Inventory, g	Excess Reactivity, per cent $\Delta k/k$	Worth per Element, per cent $\Delta k/k$
54	16,383	$+0.250 \pm 0.009$	--
54 plus voids in Positions 44 and 57	16,383	$+0.107 \pm 0.010$	-0.070 ± 0.013
56 (additional elements in Positions 44 and 57)	16,978	$+0.949 \pm 0.023$	$+0.350 \pm 0.035$

Since the additional elements were added during the same run, the worth for each element was not determined separately. However, the elements were added to opposite faces of the core so that assuming they contributed to the total worth equallv is probably valid.

[redacted]

Migration-Area Measurements

The migration area was found by changing the water height in small increments and noting the change in reactivity. The one-group criticality equation contains the core height as the inverse square. However, for the small height changes which are possible about a single criticality point the reactivity change is approximately linear with height. The data taken in these experiments were analyzed both ways with identical results.

Figures 9 and 10 give the experimentally determined reactivities as functions of water height for the 54- and 56-element cores, respectively. Table 3 gives the critical height, the equivalent core radius, and the differential water-height worth as determined from the curves for each of these cases.

TABLE 3. DATA OBTAINED FROM M^2 EXPERIMENT

Water Height, h, cm	Equivalent Core Radius[a], r, cm	$\frac{\Delta\rho}{\Delta h}$, per cm	$\frac{\Delta\rho}{\Delta r}$, per cm
70.24	25.010	12.96×10^{-4}	162.0×10^{-4}
65.07	25.459	15.78×10^{-4}	

(a) Radius of circle having the same areas as the product of the number of elements times the core cross-sectional area associated with each element.

Extrapolating flux plots for the central core region gives a total axial reflector savings of approximately 12.7 cm for a core reflected by water at the bottom and by the aluminum plate at the top. Using this value and the data in Table 3, values of 59.3 and 59.7 cm^2 are obtained for M^2 for the 54- and 56-element cases. The value of k_∞ was taken as 1.59.

If Equation (3) is written for each of the experimental cases and the equations solved simultaneously for M^2 and reflector savings, the axial reflector savings is 11.03 cm and M^2 is 55.9 cm^2. The difference between the two values of reflector savings is in the expected direction; in the partial water-height experiment for M^2, the water is well below the aluminum plate and therefore there is less reflection from the aluminum, while the 12.7-cm reflector savings was obtained with full water height where the water and aluminum top plate were in contact.

Figure 11 shows the strong dependence of M^2 on reflector savings. The true value of reflector savings probably is between 11 and 13 cm, corresponding to values of M^2 between 55 and 59 cm^2.

With a 56-element core, if the water height is raised to the height which made the 54-element core critical, the increase in reactivity should equal the worth of the two additional elements added to the critical 54-element core. Thus a measure of the rate of change of reactivity with increasing core radius can be obtained. This change in reactivity and the corresponding radii are shown in Table 3. These data permit another determination of M^2 [using Equation (4)].

[redacted]

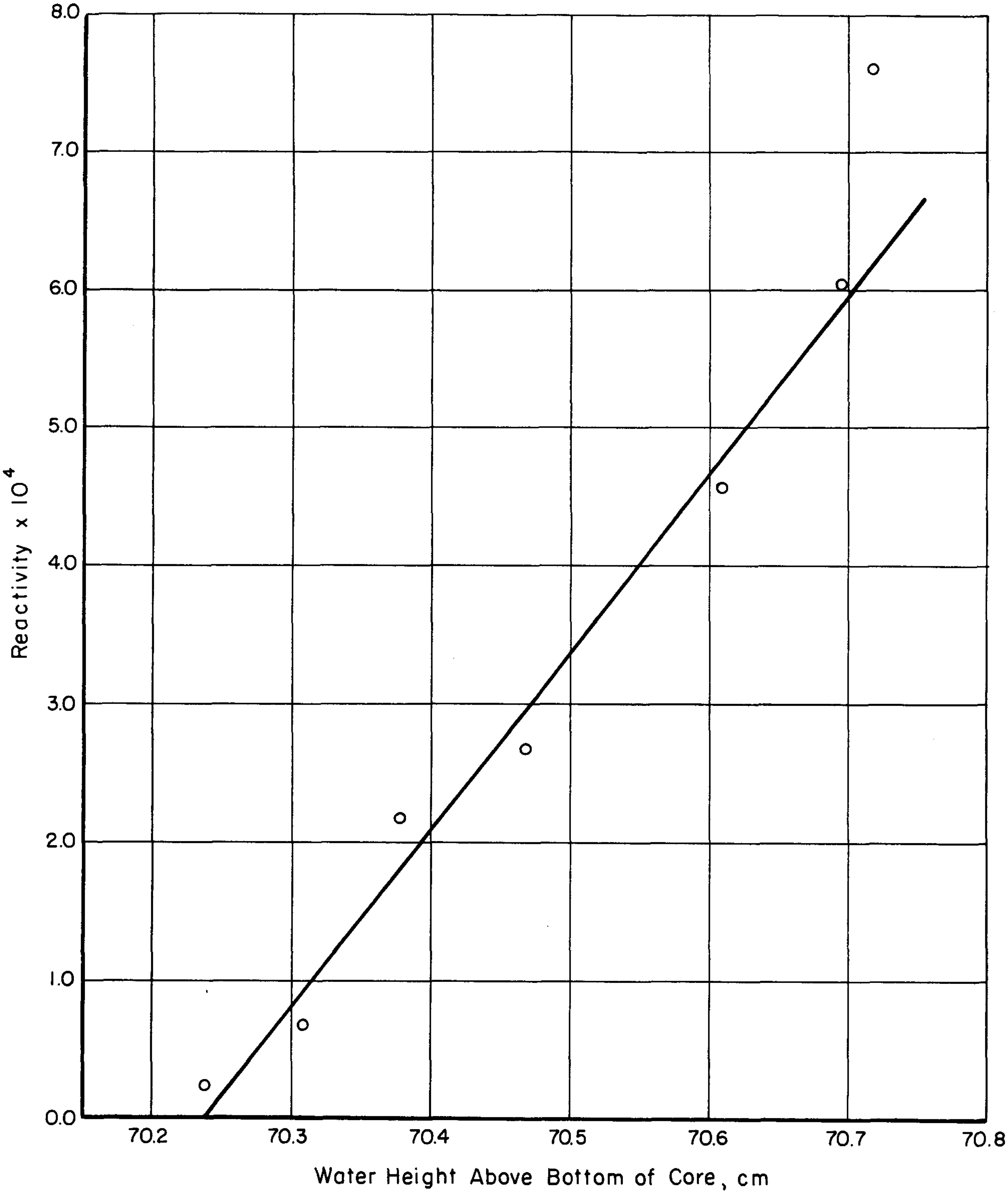

FIGURE 9. REACTIVITY VERSUS CORE HEIGHT, EXPERIMENTAL CORE – 54 FUEL ELEMENTS

[redacted]

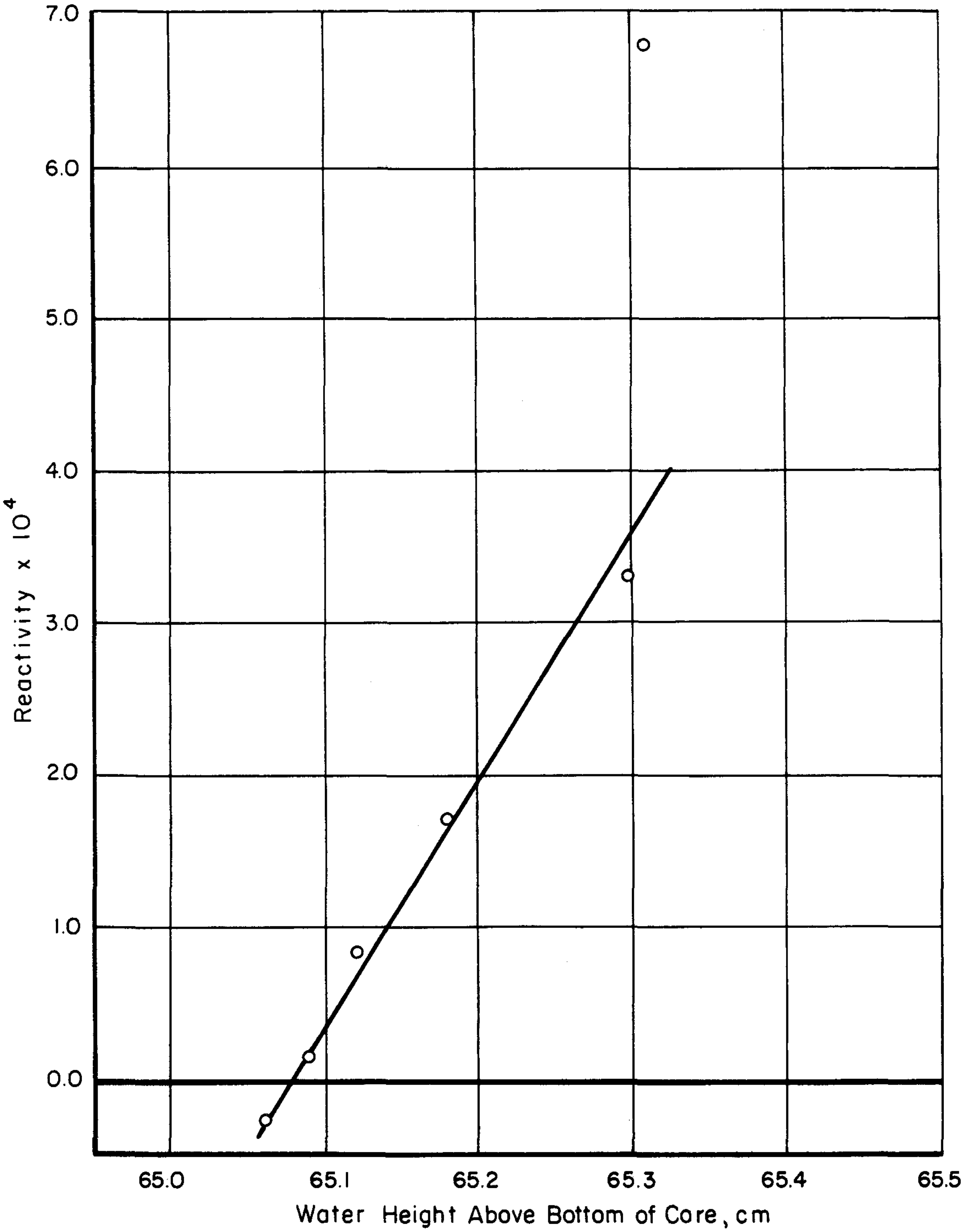

FIGURE 10. REACTIVITY VERSUS CORE HEIGHT, EXPERIMENTAL CORE — 56 FUEL ELEMENTS

[redacted]

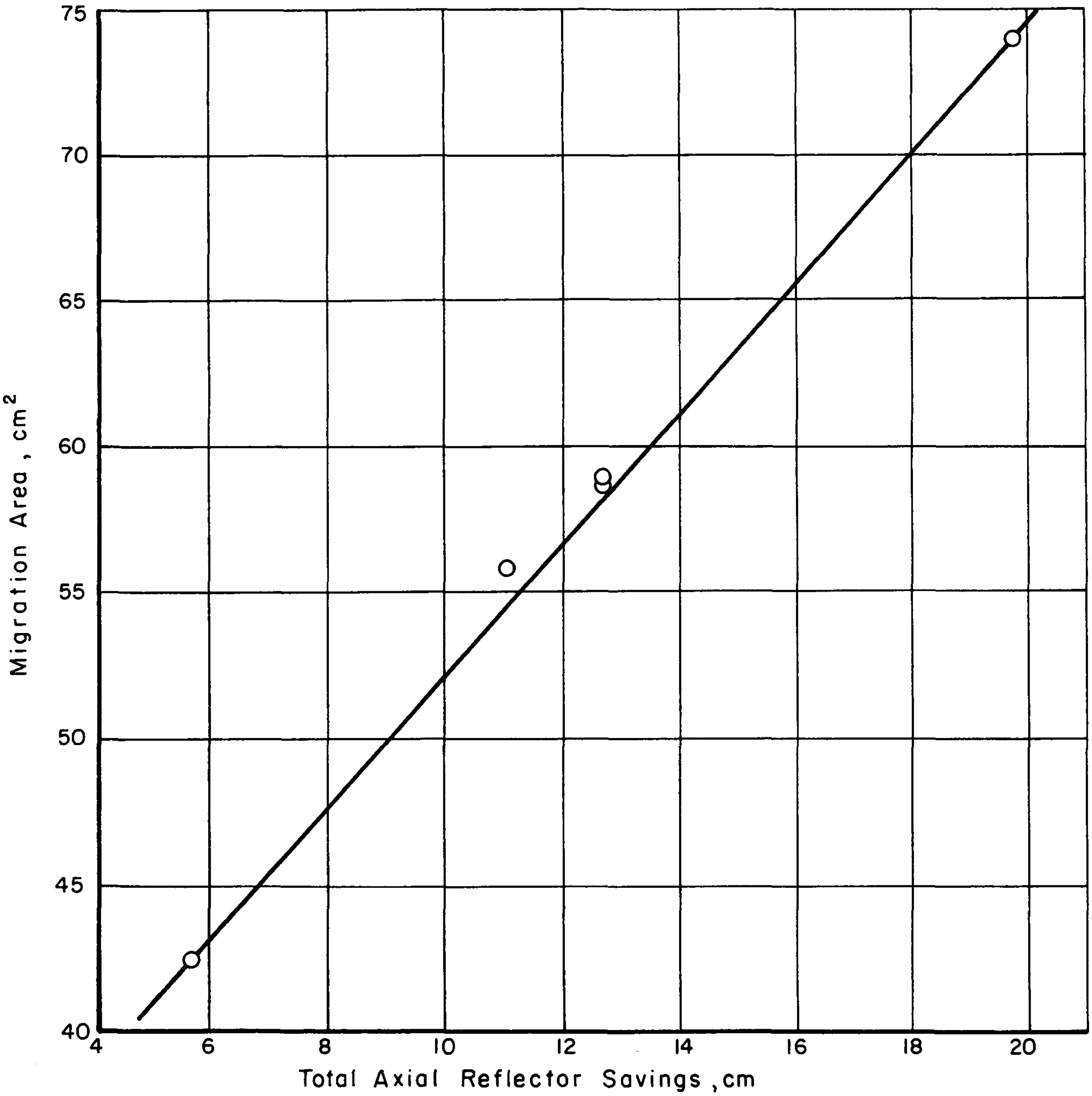

FIGURE 11. DEPENDENCE OF M^2 ON REFLECTOR SAVINGS, PARTIAL-WATER-HEIGHT METHOD, EXPERIMENTAL CORE

[redacted]

Most water-moderated and -reflected reactors have radial reflector savings of about 7 cm. If this value is used, the M^2 found by application of Equation (4) for change in reactivity with changing radius turns out to be 74 cm^2, which is not in agreement with the values found from increasing height. A value of radial reflector savings of approximately 4 cm will give a migration area of approximately 55 cm^2, in agreement with the values found previously.

Bessel functions were fitted graphically to the experimental points of the top three curves in Figure 17 shown in the section on flux and power-distribution measurements for this core below. The zero intercepts of these functions were compared with the core radius to obtain values of reflector savings. There is considerable uncertainty in this procedure because of the few points available for fitting the Bessel functions, the long extrapolation, and the uncertainty of the value of radius to assign to the core. In this case the core radius was taken to be the distance to the center of the last element along Radius AA (Figure 4) plus the radius of a unit cell in the core. By this means the radial reflector savings was found to be between 2-1/2 to 3-1/2 cm. If the 3-1/2-cm value is used, the value of M^2 becomes 52.5 cm^2. This again demonstrates the strong dependence of the value of M^2 on the value of the reflector savings. This dependence is shown in Figure 12.

From these experiments it is concluded that the migration area in the Experimental Core is in the range of 55 to 59 cm^2; the experiments performed were not sufficiently extensive to give an indication of whether anisotropy is present.

Reactivity Worth of Tungsten Mock-up Blades

Two tungsten blades, one 0.2 by 2 by 24 in. and the other 0.2 by 3 by 24 in., were used in this experiment. The reactivity worths were measured for the 2-in. blade at Positions B-1 and B-2 and for the 3-in. blade at Position B-1 (see Figure 13 for position nomenclature). Worth was measured for the 2-in. blade with and without a 10-mil cadmium jacket. The blades were inserted 15 in. into the core, measured from the perimeter of a reference circle with a 12-in. radius.

All measurements were made with the 56-element core containing an excess reactivity of +0.949 ± 0.23 per cent. Table 4 gives the results of these measurements.

TABLE 4. REACTIVITY WORTH OF TUNGSTEN BLADES

Blade Construction	Position	Blade Worth, per cent $\frac{\Delta k}{k}$
2-in.-wide tungsten blade	B-2	-0.700 ± 0.005
	B-1	-0.399 ± 0.005
2-in.-wide tungsten blade jacketed	B-2	-0.934 ± 0.005
with 10 mil of cadmium	B-1	-0.549 ± 0.005
3-in.-wide tungsten blade	B-1	-0.439 ± 0.005

[redacted]

[redacted]

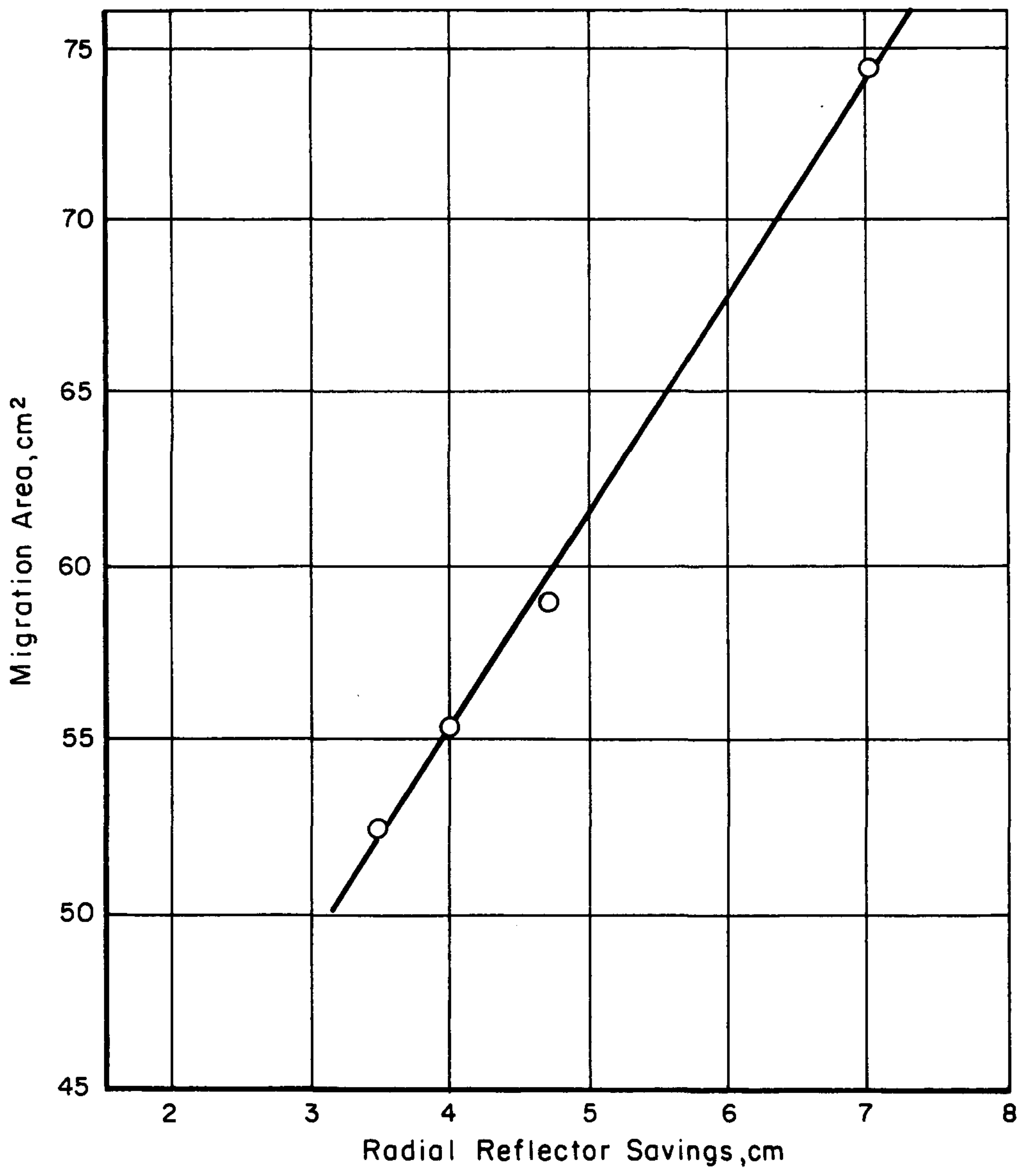

FIGURE 12. DEPENDENCE OF M^2 ON REFLECTOR SAVINGS, RADIAL-BUCKLING-VARIATION METHOD, EXPERIMENTAL CORE

[redacted]

[redacted]

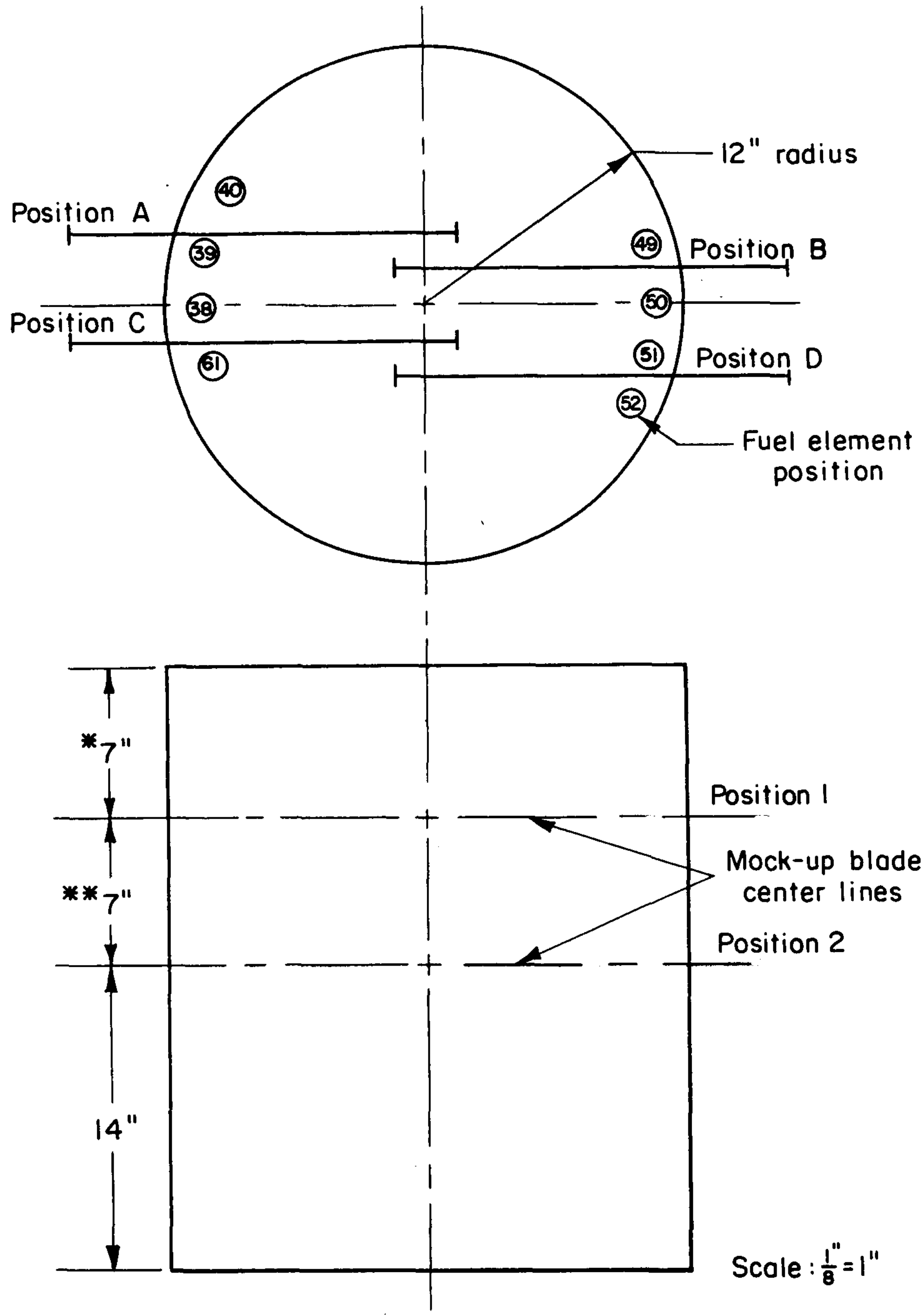

* This dimension 5.5 in. in the flooded core studies
** This dimension 8.5 in. in the flooded core studies

FIGURE 13. MOCK-UP BLADE POSITIONS

[redacted]

The shutdown capacity of a mock-up blade increases by a factor of about 1.7 when the blade is moved from Position B-1 to Position B-2. This increase is noted for both the cadmium-jacketed tungsten blade and the pure tungsten blade. The increase of 1.7 in blade worth is consistent with the higher flux level at Position B-2 than at Position B-1.

The results also show that jacketing the tungsten blade with 10-mil cadmium sheet increases its shutdown worth by a factor of 1.3. The shutdown worth for the pure tungsten blade increases by only 10 per cent for a 50 per cent increase in its width.

Miscellaneous Reactivity Measurements

Figure 2 shows the structure at the upper part of the critical-assembly core (which corresponds to the bottom of the GCRE-1 core). At the top of the core there are three aluminum plates which total 2-3/4 in. in thickness and 32 in. in diameter. These plates position the fuel elements. The bottom of this assembly of plates is at the level of the top of the fuel in the core, which is the same level as the surface of the water for normal operation. Several modifications were made with this arrangement to learn more of the operational characteristics of the core and to see what reactivity gains could be obtained.

One experiment was to raise this assembly of plates 1.97 in. and determine the change in reactivity. The result was a decrease in reactivity of 0.038 per cent $\frac{\Delta k}{k}$, showing the aluminum had some small worth as a reflector.

The next experiment started with the assembly of aluminum plates in the raised position, that is, 1.97 in. above the normal position. The water was then raised stepwise and the reactivity addition of each step measured to determine the worth of the water reflector above the core (actually the interlocks prevented addition of water when critical; the experiment was conducted by raising the water while subcritical, making the reactor supercritical by raising the controls rods, and then dropping the water in increments). Continued additions of water above the fueled region of the core gave decreasing positive increments to the reactivity as shown by the differential reactivity-worth curve in Figure 14. The total worth of the 1.97 in. of water above the active core region was approximately 0.37 per cent $\frac{\Delta k}{k}$.

The third experiment was done with the assembly of aluminum plates at the normal position, that is, the bottom of the plates level with the top of the fuel. If from this starting condition the water level is raised, the water directly above the core cannot rise higher because of the presence of the aluminum plates but in the region external to these plates the water level can rise. This region will be referred to as the upper axial annular reflector. This reflector region has an inner radius of 16 in. The water height in this annular region was changed in small increments and the reactivity changes associated with these water-height changes measured. The total worth of this region was small, approximately 0.07 per cent $\frac{\Delta k}{k}$, and will not be a significant quantity in the GCRE-1 operation.

The results of these miscellaneous reactivity measurements are summarized in Table 5.

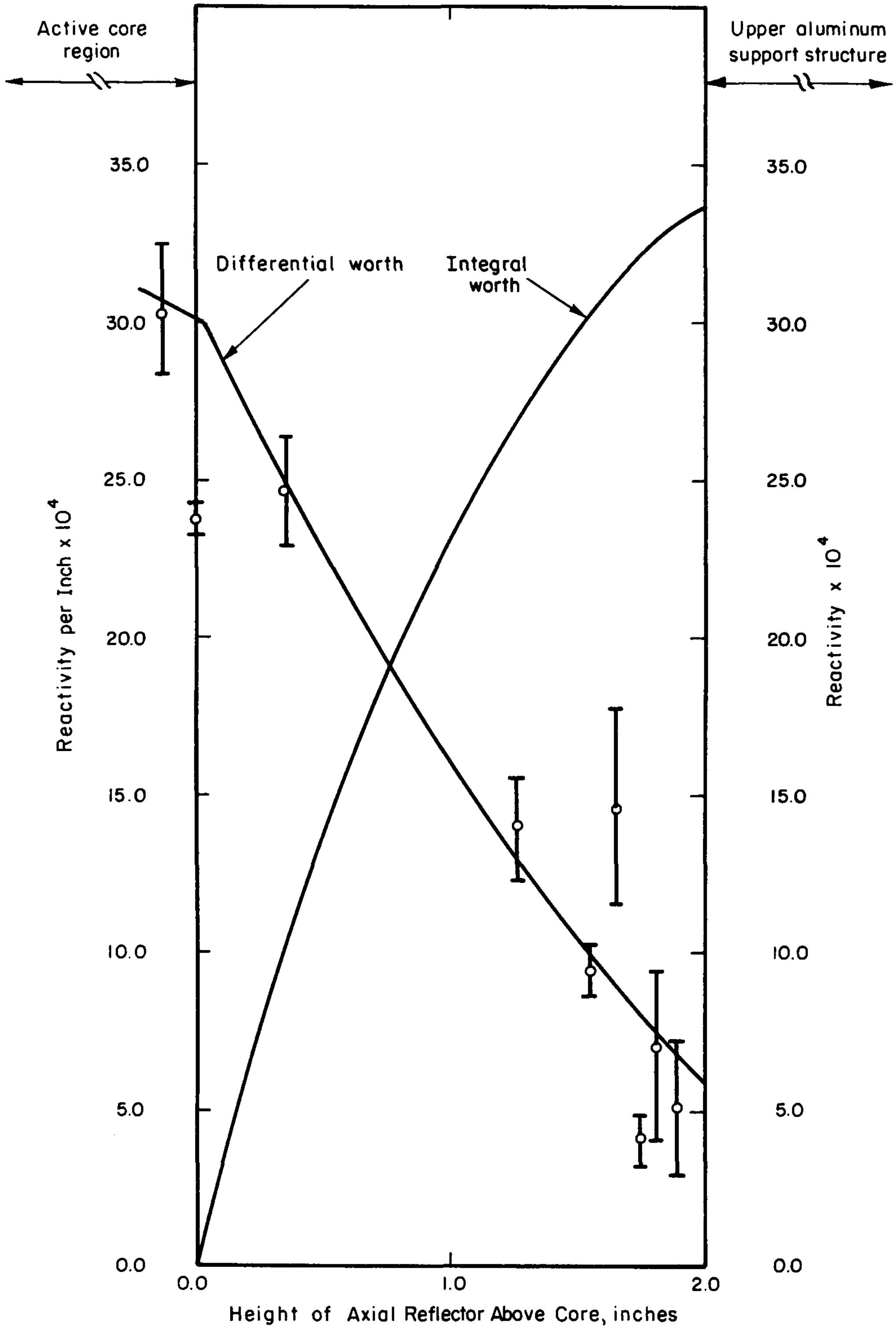

FIGURE 14. DIFFERENTIAL AND INTEGRAL WORTH OF UPPER AXIAL REFLECTOR

[redacted]

TABLE 5. MISCELLANEOUS REACTIVITY MEASUREMENTS

	Worth Measured by Water-Height Method, per cent $\frac{\Delta k}{k}$	Worth Measured by Calibrated-Rod Method, per cent $\frac{\Delta k}{k}$
Upper Axial Annular Reflector	+0.073 ± 0.013	+0.074 ± 0.005
Upper Axial Reflector	+0.336 ± 0.050	+0.377 ± 0.004
Upper Aluminum Support Assembly		+0.038 ± 0.008

Flux- and Power-Distribution Measurements

Two-dimensional flux and power measurements were made in vertical planes containing the central axis of the core and Radii AA and BB (Figure 4). The results are given in Figures 15 through 22.

Total flux was measured by the activation of bare manganese wires. Epicadmium flux was measured by the activation of cadmium-covered manganese wires. Power was measured by using aluminum catcher foils in combination with uranium fuel material.

The two-dimensional flux plots were obtained by activating wires located at the center of each element on the two radii, at points midway between pairs of fuel elements, and at points out into the reflector. The axial flux variations in the elements were found to have similar shapes. For Radius AA the axial flux distribution in Positions 1 and 50 are typical; these results are shown in Figure 15.

Likewise the axial flux variation in the moderator region is similar for various radii within the core but differs in the reflector region. Typical examples are given in Figure 16. These results are normalized to the same core condition as those in Figure 15 and are directly comparable.

The axial peak-to-average flux ratio within the core region is approximately 1.4 and is relatively independent of radius. The cadmium ratio in the core region is approximately 7.5 (in the moderator) and is about three times larger in the reflector region.

Figures 17 and 18 show the radial distribution of total flux along Radii AA and BB, respectively; fluxes in the fuel element and in the moderator region between the fuel elements are shown along each radii. Although the radii differ in length and in element spacing, the peak-to-average flux ratio is approximately the same in each case. Also the flux variation along the given radius is similar for each axial position.

Figure 19 gives the axial power variation along the outer fuel cylinder of the element at the center of the core. This is compared to the axial flux distribution in the moderator directly adjacent to this element. The two curves have been normalized to have the same peak value. In this case the agreement is excellent. This good agreement does not hold when the variation is plotted radially through the element, where the cadmium ratio changes rapidly, as is shown below.

[redacted]

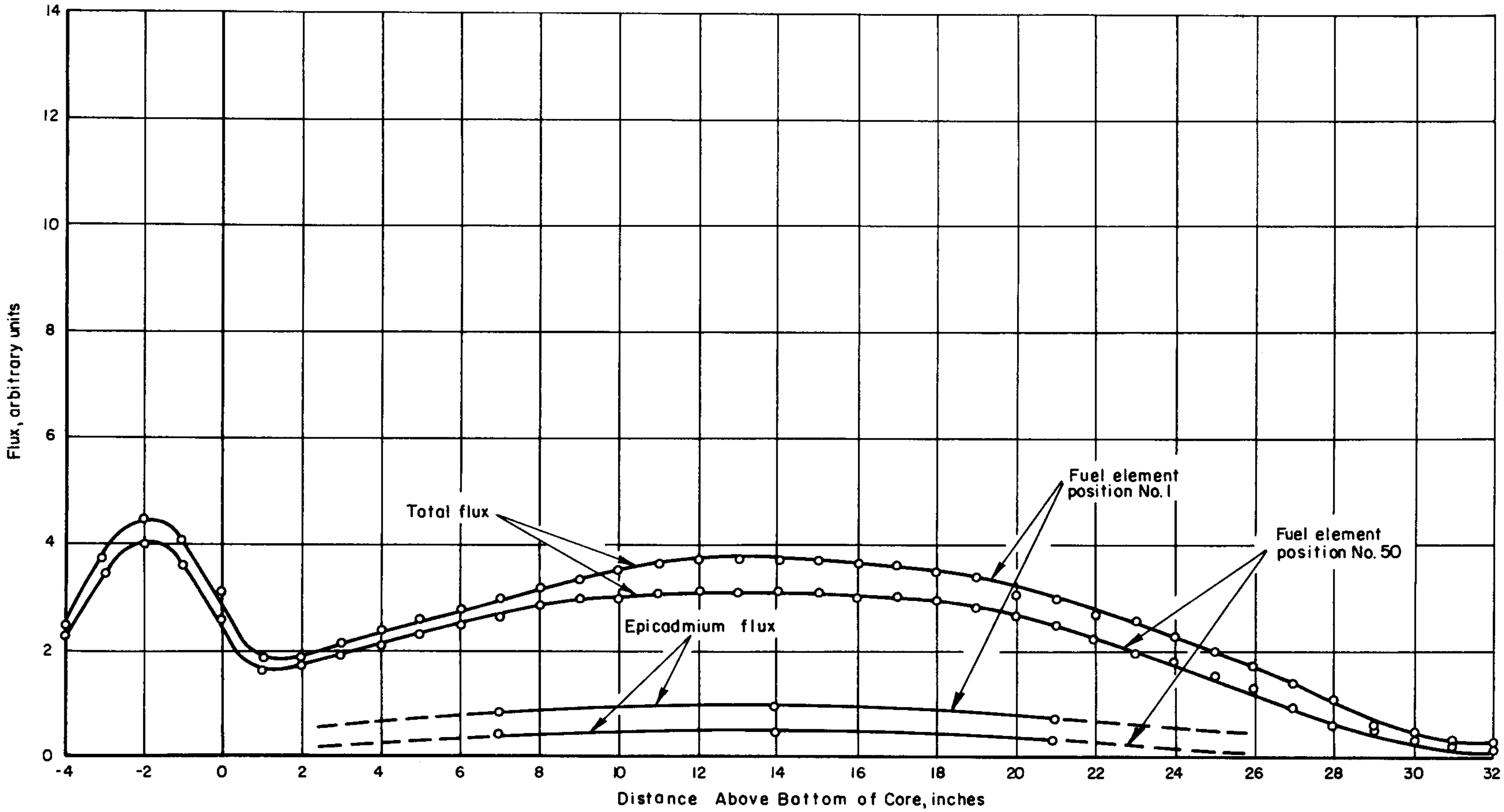

FIGURE 15. AXIAL FLUX DISTRIBUTION AT CENTER OF FUEL ELEMENTS ALONG RADIUS AA – EXPERIMENTAL CORE

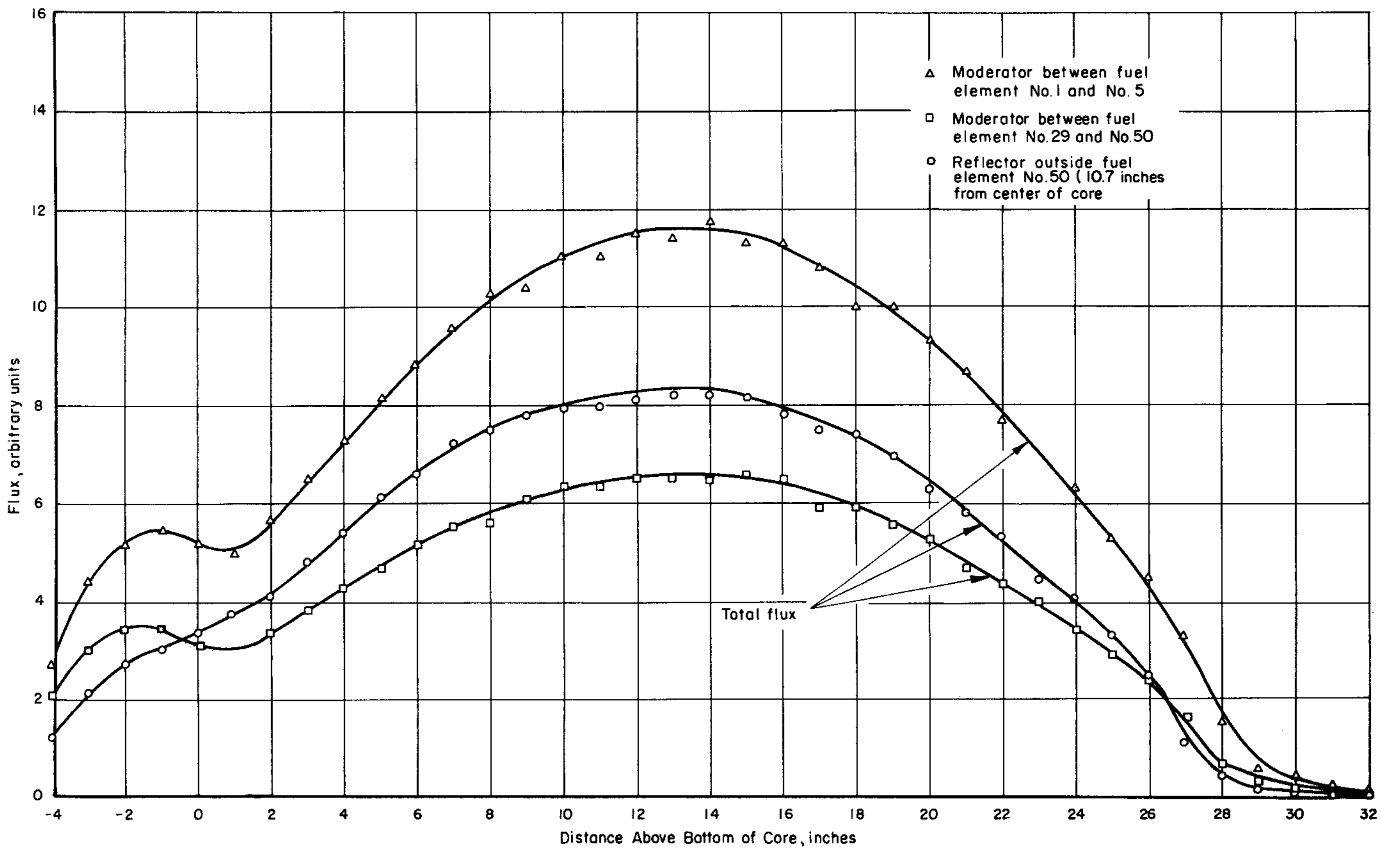

FIGURE 16. AXIAL FLUX DISTRIBUTION IN MODERATOR AND REFLECTOR ALONG RADIUS AA – EXPERIMENTAL CORE

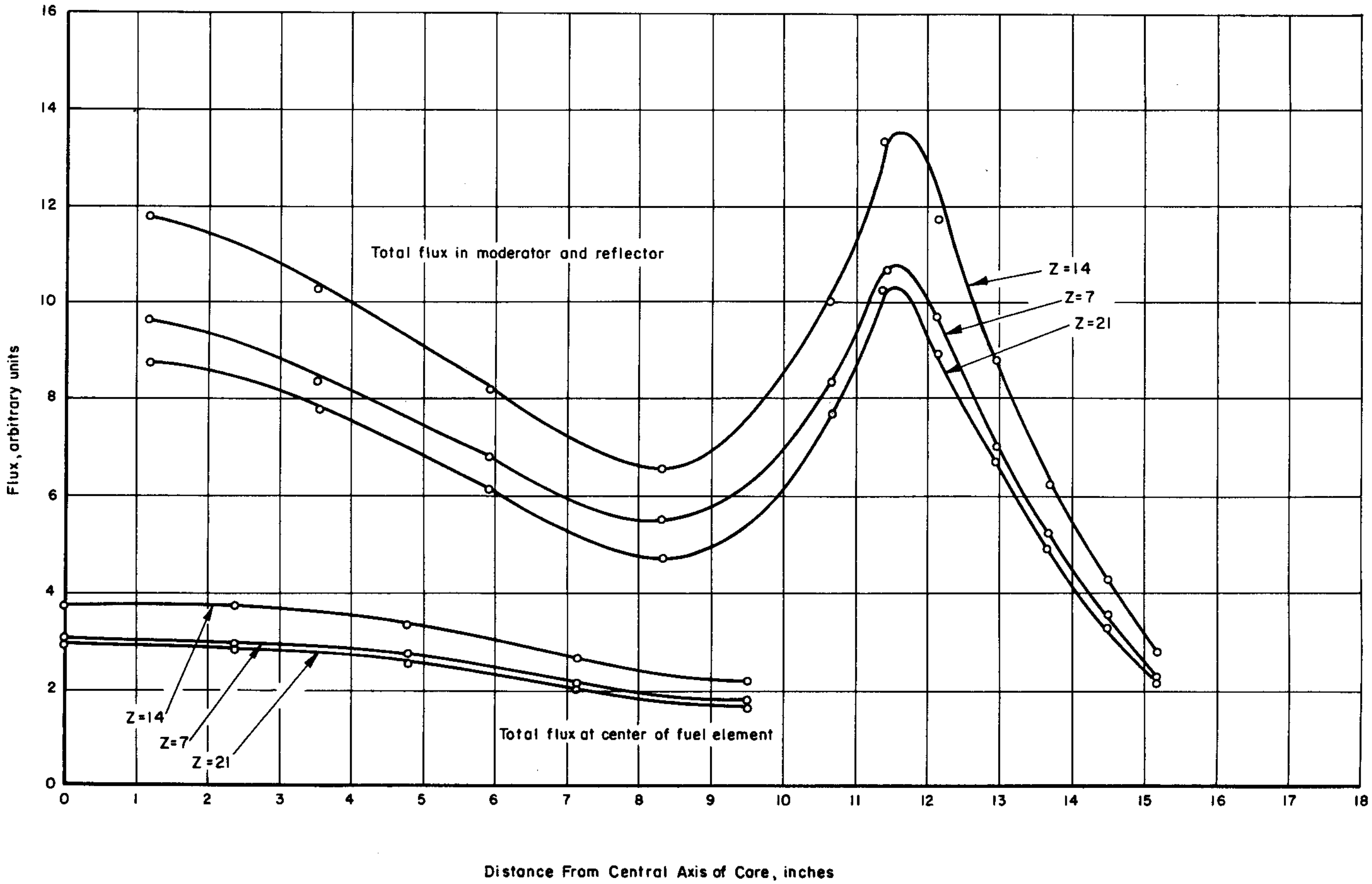

FIGURE 17. RADIAL FLUX DISTRIBUTION ALONG RADIUS AA - EXPERIMENTAL CORE

Z = distance above bottom of core, in.

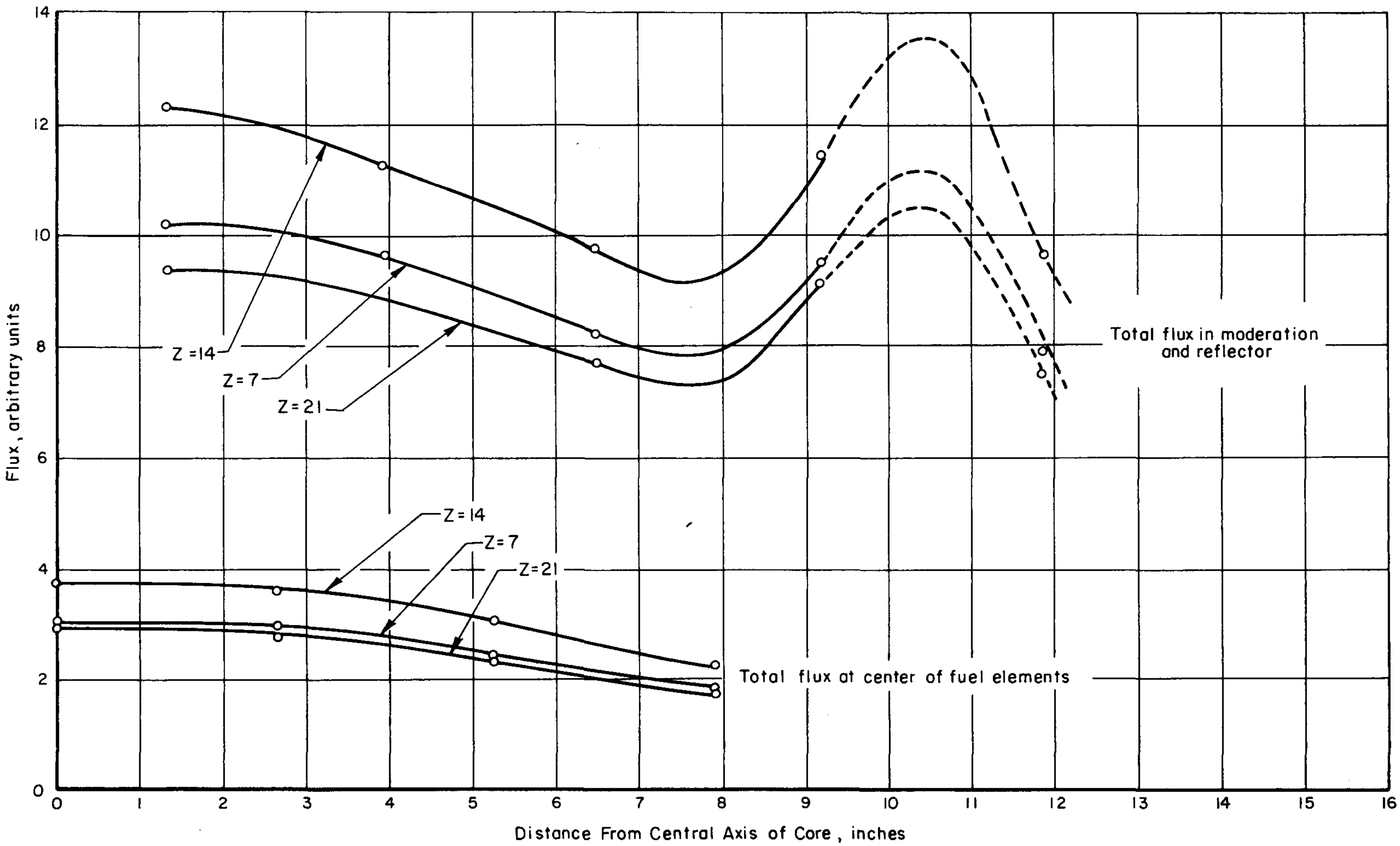

FIGURE 18. RADIAL FLUX DISTRIBUTION ALONG RADIUS BB – EXPERIMENTAL CORE

Z = distance above bottom of core, in.

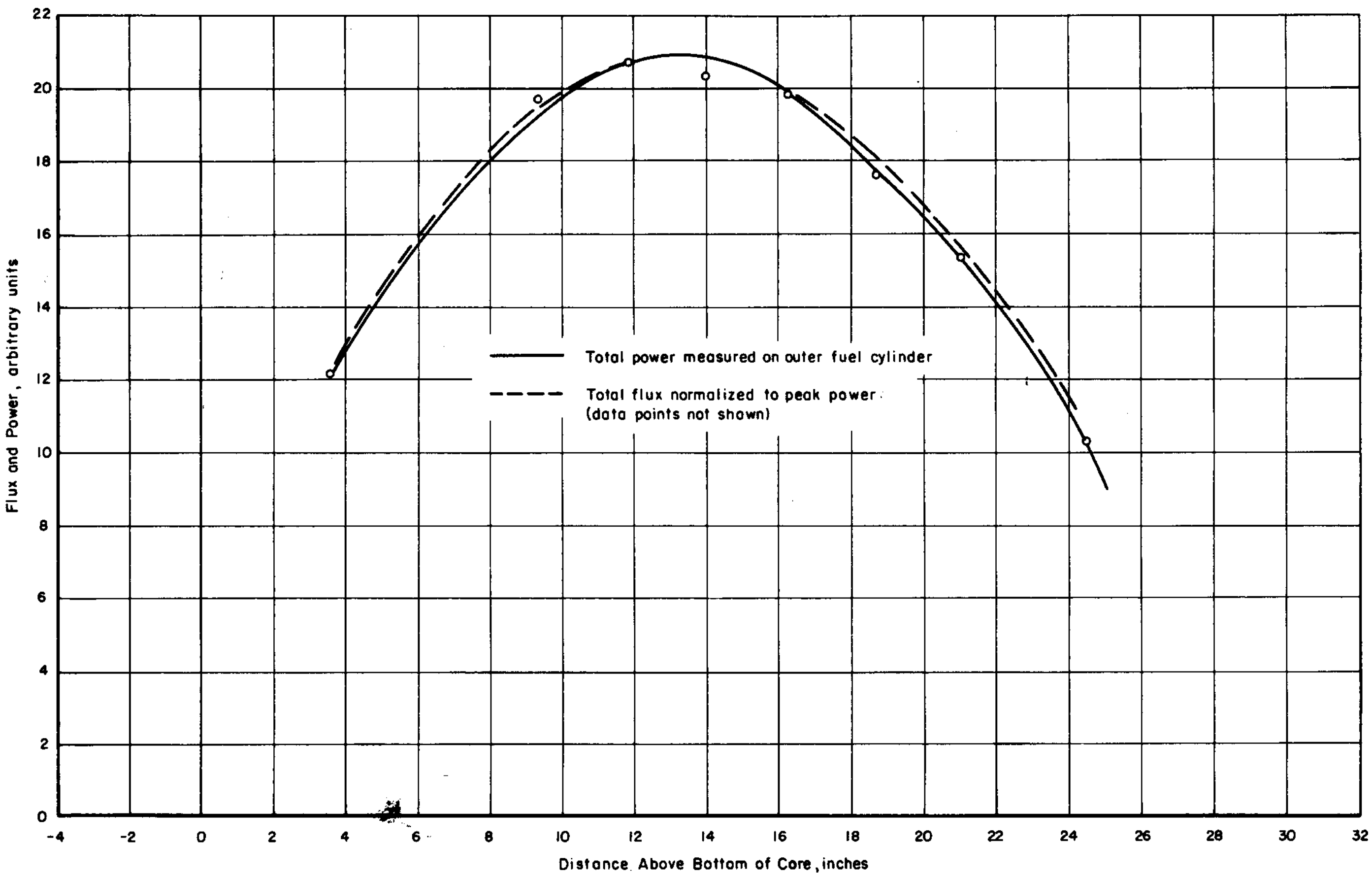

FIGURE 19. AXIAL FLUX AND POWER DISTRIBUTION WITHIN THE FUEL ELEMENTS ALONG RADIUS AA – EXPERIMENTAL CORE

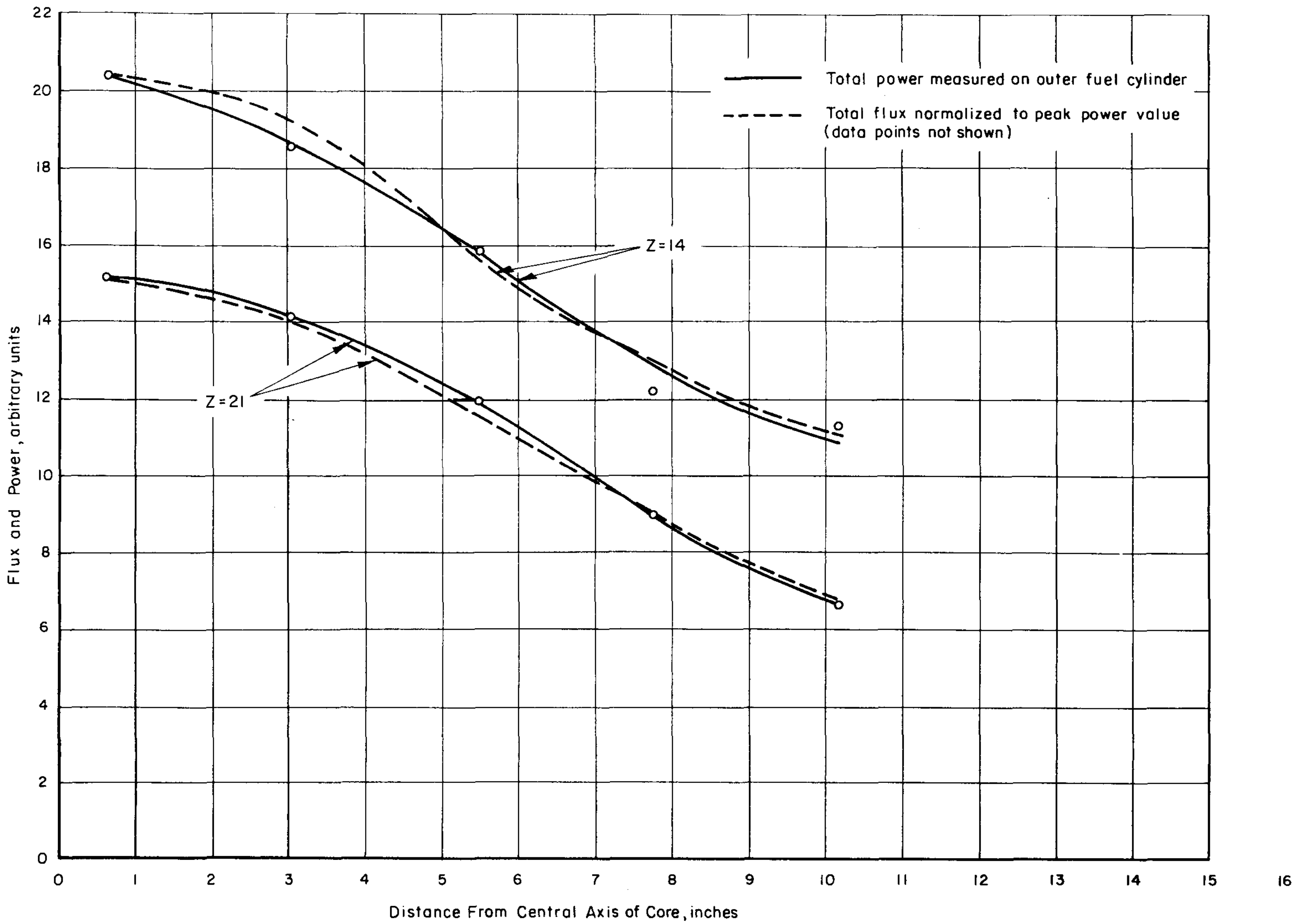

FIGURE 20. RADIAL FLUX AND POWER DISTRIBUTION ALONG RADIUS AA - EXPERIMENTAL CORE

Z = distance above bottom of core, in.

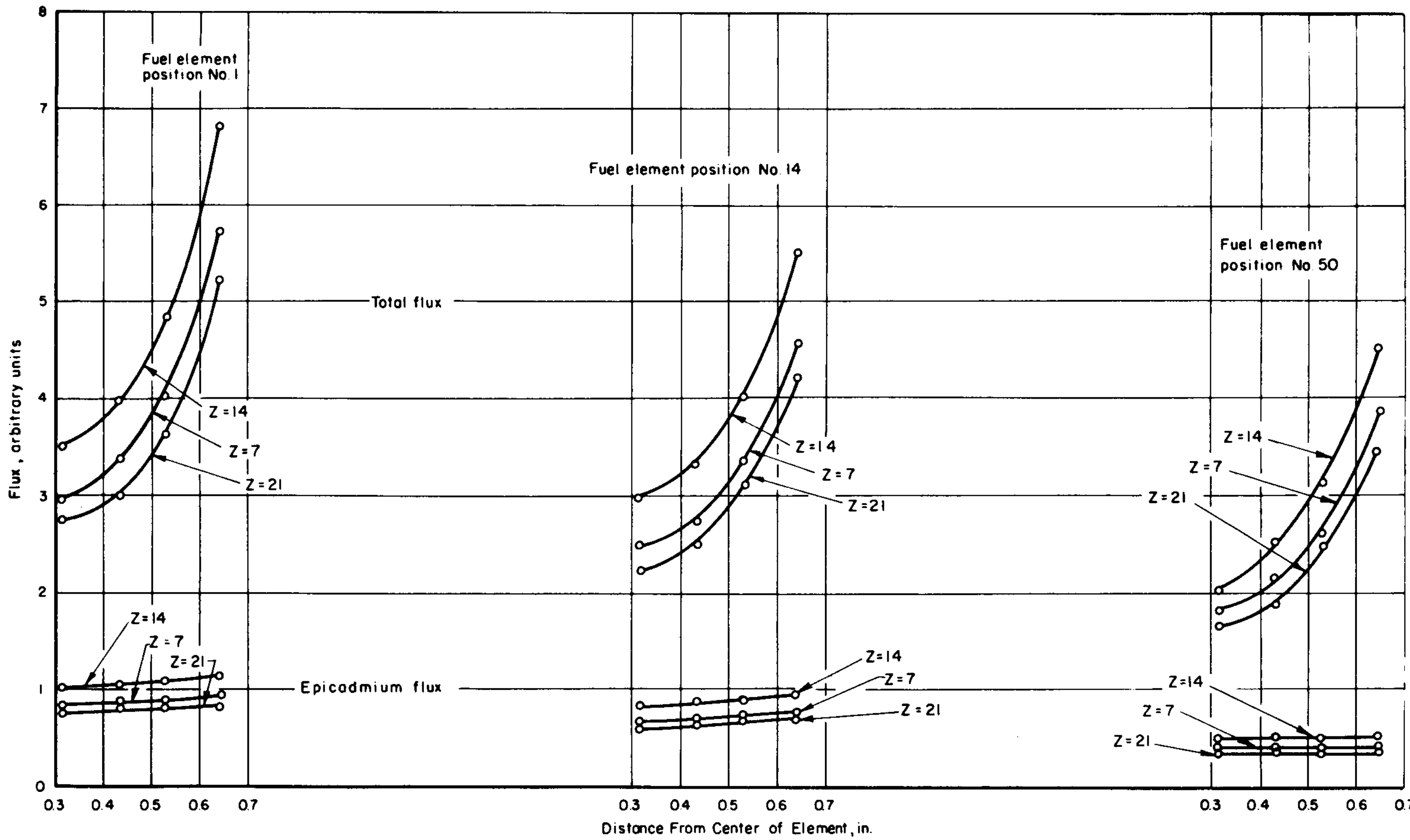

FIGURE 21. VARIATION OF FLUX WITHIN FUEL ELEMENTS ALONG RADIUS AA – EXPERIMENTAL CORE

Z = distance above bottom of core, in.

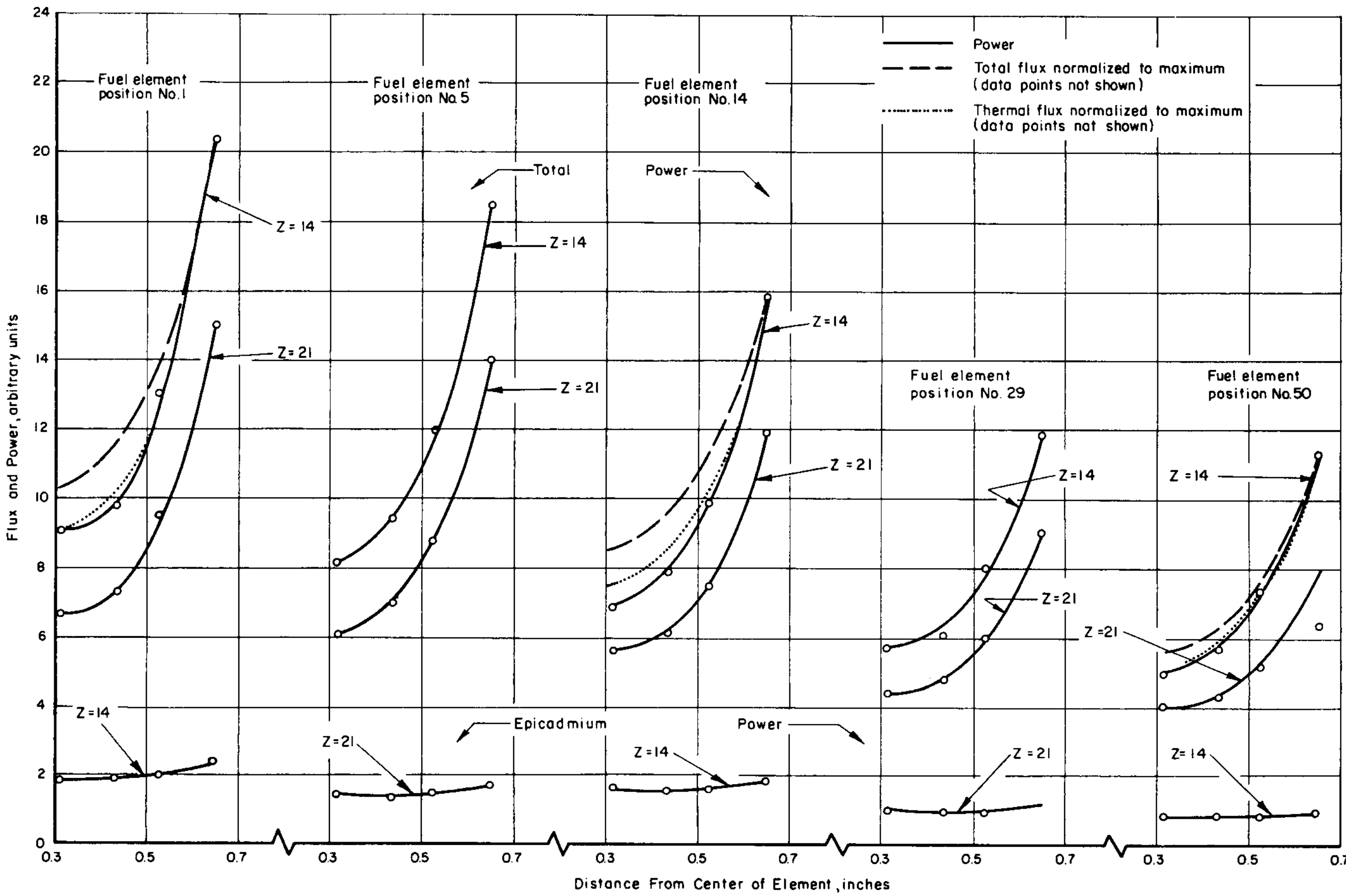

FIGURE 22. COMPARISON OF FLUX AND POWER WITHIN FUEL ELEMENTS ALONG RADIUS AA - EXPERIMENTAL CORE

Z = distance above bottom of core, in.

Figure 20 presents the radial power variation along Radius AA at two axial locations, 14 and 21 in. above the bottom of the fuel. The flux level at these same locations, as measured by the manganese activity and normalized to the same maximum value as the power, is given for comparison. Again the agreement is excellent over a region where the cadmium ratio is relatively constant.

From Figures 19 and 20 the peak-to-average power ratios are found to be 1.39 axially and 1.42 radially (computed from data along Radius AA).

Variations in flux and power were measured in detail across several fuel elements along Radius AA. The flux variations are shown in Figure 21. In Figure 22 the total flux and epicadmium flux through the fuel elements, as measured by bare and cadmium-covered manganese-wire activities, is compared with the corresponding power distribution. In each case the total flux depression within the element is less than the power depression, while the thermal flux has approximately the same variation as the power. The peak-to-average power ratio within the element is 1.42.

There are a number of factors contributing to the difference between the flux and power measurements shown in Figure 22. There is a hardening of the flux and a decrease in the cadmium ratio toward the center of the fuel element. In addition, the thermal manganese cross section is approximately $1/v$, while the fission cross section for uranium-235 drops more rapidly than $1/v$. Also the cross sections for manganese and uranium-235 are different in the resonance region and therefore the relative contributions to the total activity are likely to be different for different locations in the fuel elements. The peak-to-average power ratios in the core with and without the variation within the fuel element were computed and found to be 2.80 and 1.97, respectively.

Thermal-Utilization Measurements

Additional detailed flux measurements were made at axial positions 7, 14, and 21 in. above the bottom of the fuel in fuel elements in Positions 1 and 14 and in the moderator region adjacent to each element. Values for total and thermal flux were obtained. These data were used in calculating the thermal utilization. The flux variation in the moderator was obtained by using 1-in. (1.000 ± 0.002) wires placed in polyethylene holders clamped to the fuel cylinder at the proper axial position. The location of the wires with respect to the fuel element is shown in Figure 23. Typical radial thermal-flux variations within unit cells are shown in Figure 24.

The thermal-flux values were averaged over the area occupied by each material. In addition, the flux values taken at Position 14 were corrected for the radial variation of the flux at that position (see Figure 17). From these data thermal-flux ratios within various core materials were calculated. Thermal-utilization data for the experimental core appear in Tables 6 and 7. The average for the six determinations of thermal utilization is 0.780.

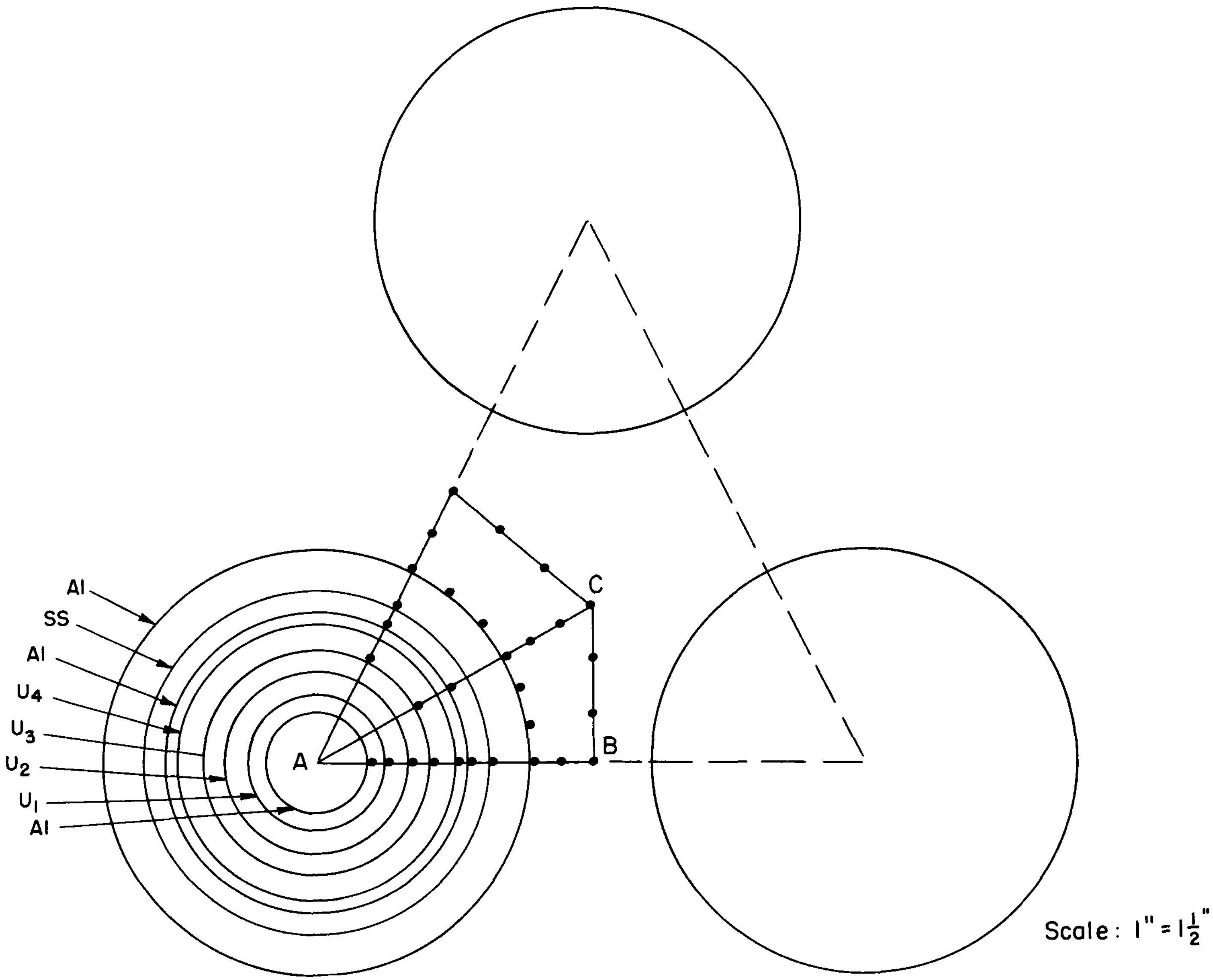

FIGURE 23. LOCATION OF MANGANESE WIRES FOR DETAILED FLUX MAPPING WITHIN AND ADJACENT TO A FUEL ELEMENT IN THE EXPERIMENTAL CORE

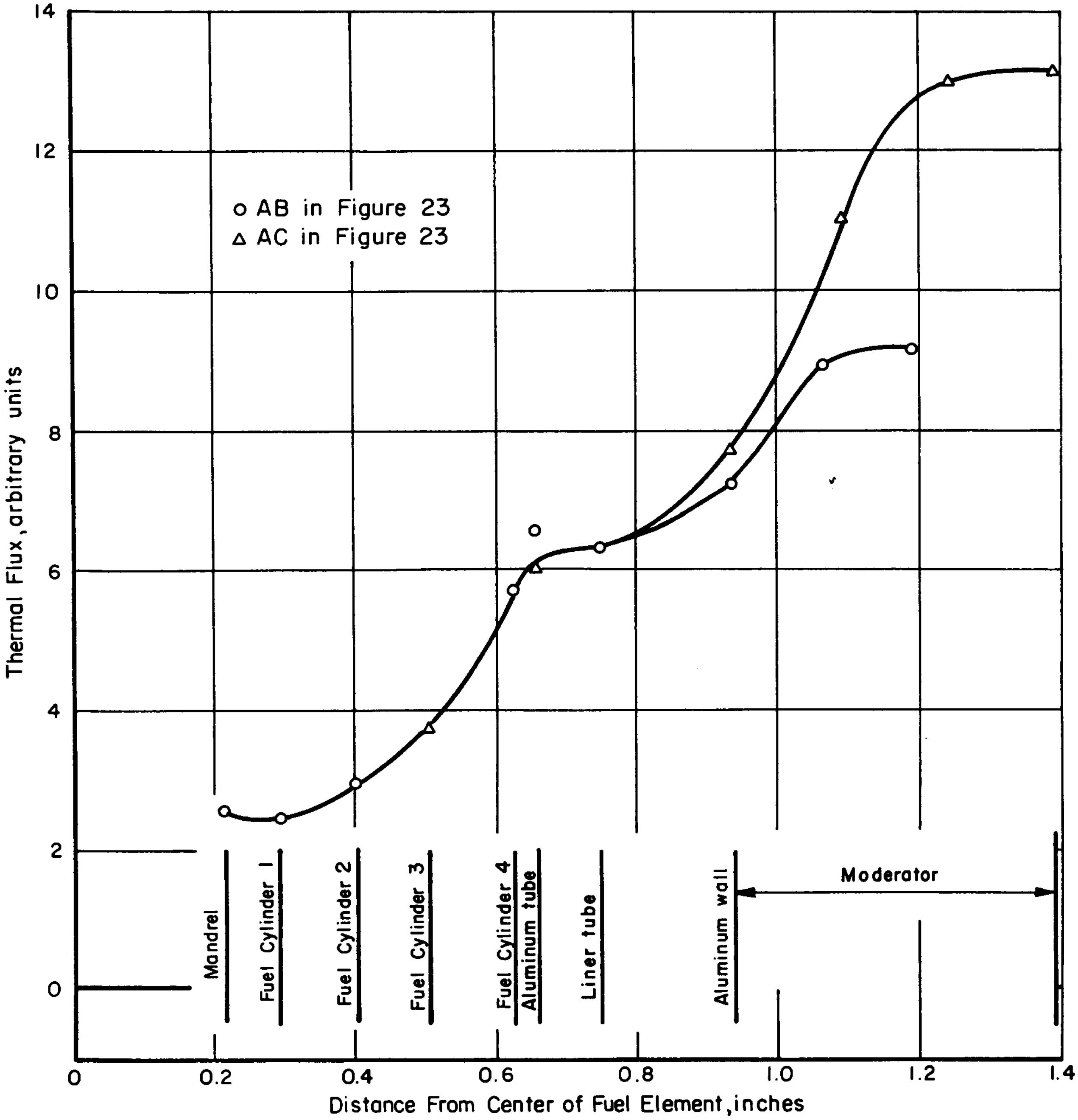

FIGURE 24. THERMAL FLUX THROUGH THE CENTRAL FUEL-ELEMENT CELL – EXPERIMENTAL CORE

Measurements made at Z = 14 in. Outer surface of element components shown.

[redacted]

TABLE 6. PARAMETERS USED IN THERMAL-UTILIZATION CALCULATIONS

Cell Material	Per Cent of Total Volume	Ratio to Fuel Volume	Cross Section $\sigma^{(a)}$, barns	Cross Section Σ, cm^{-1}	Ratio to Fuel Cross Section
Total cell	100.00	--	--	--	--
Moderator (water)	51.05	83.48	0.589	0.0197	0.000690
Aluminum	9.84	16.09	0.204	0.0123	0.000431
Stainless steel	8.63	14.12	2.66	0.222	0.00777
Air	29.80	48.73	--	--	--
Uranium	0.675	1.105	--	--	--
Fuel (uranium-235)	0.612	1.00	599[b]	28.56	1.0

(a) Corrected for Maxwellian distribution.
(b) Corrected for non-1/v dependence.

TABLE 7. THERMAL-UTILIZATION DATA

	Values for Indicated Axial Position Above Bottom of Fuel					
	Element Position 1			Element Position 14		
	7 In.	14 In.	21 In.	7 In.	14 In.	21 In.
Average Thermal Flux, Observed						
Uranium-235	3,440	4,071	3,153	2,820	3,399	2,617
Moderator	9,356	10,552	8,018	7,322	9,048	7,171
Aluminum	5,322	6,308	4,616	4,421	5,215	4,020
Stainless steel	3,613	4,262	3,269	2,958	3,528	2,700
Average Thermal Flux, Corrected for Radial Variation						
Uranium-235	3,440	4,071	3,153	2,978	3,588	2,763
Moderator	9,356	10,552	8,018	8,186	9,948	8,016
Aluminum	5,322	6,308	4,616	4,824	5,691	4,389
Stainless steel	3,613	4,262	3,269	3,136	3,739	2,861
Ratio of Flux in Material to Flux in Fuel						
Moderator	2.717	2.591	2.545	2.749	2.773	2.901
Aluminum	1.547	1.549	1.464	1.620	1.586	1.588
Stainless steel	1.050	1.047	1.037	1.053	1.042	1.035
Values of Thermal Utilization	0.779	0.784	0.787	0.778	0.778	0.774

[redacted]

Clean Core

Critical Core Configuration

The fuel inventory in the Clean Core was 19,453 g contained in 64 fuel elements arranged as shown in Figure 25. The excess reactivity was +0.258 ± 0.003 per cent $\frac{\Delta k}{k}$.

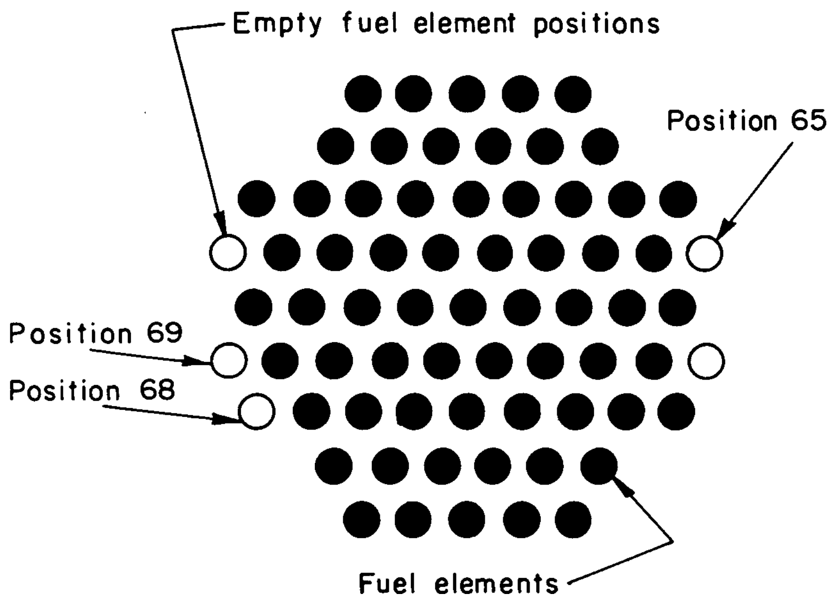

FIGURE 25. INITIAL CRITICAL CONFIGURATION, CLEAN CORE – 64 FUEL ELEMENTS

Reactivity Worth of Peripheral Fuel Elements

Three additional fuel elements were added one at a time to the initial critical configuration in Positions 68, 69, and 65, respectively. Table 8 gives the fuel inventory and the excess reactivity for the various loadings.

The sixty-fifth fuel element had a slightly greater worth than the succeeding two elements. The relative decrease in worth of the sixty-sixth and sixty-seventh element is probably a purely geometric effect. The sixty-fifth fuel element was added on a clean face of the hexagonal core in a region where the thermal flux was peaking. The sixty-sixth and sixty-seventh elements were added to the periphery next to elements already on the face; hence their worth was somewhat less due to the flux depression surrounding the element already in position.

TABLE 8. NUMBER OF FUEL ELEMENTS, FUEL INVENTORY, AND EXCESS REACTIVITY IN CLEAN CORE

Number of Fuel Elements	Fuel Inventory, g	Excess Reactivity, per cent $\frac{\Delta k}{k}$	Element Worth, per cent $\frac{\Delta k}{k}$
64	19,453	+0.258 ± 0.003	
65 (additional element in Position 68)	19,742	+0.514 ± 0.004	+0.245 ± 0.005
66 (additional element in Position 69)	20,031	+0.716 ± 0.004	+0.202 ± 0.006
67 (additional element in Position 65)	20,328	+0.930 ± 0.005	+0.214 ± 0.006

Temperature Coefficient of Reactivity

The temperature coefficient of the reactor system was measured by noting the change in position of a calibrated control rod as the water temperature was increased. The reactivity per deg C is a linear function of temperature in the experimental range studied (see Figure 26). The temperature coefficient becomes negative at about 70 C. Heating the moderator from 20 C to 80 C introduces 0.22 per cent $\frac{\Delta k}{k}$ increase in reactivity.

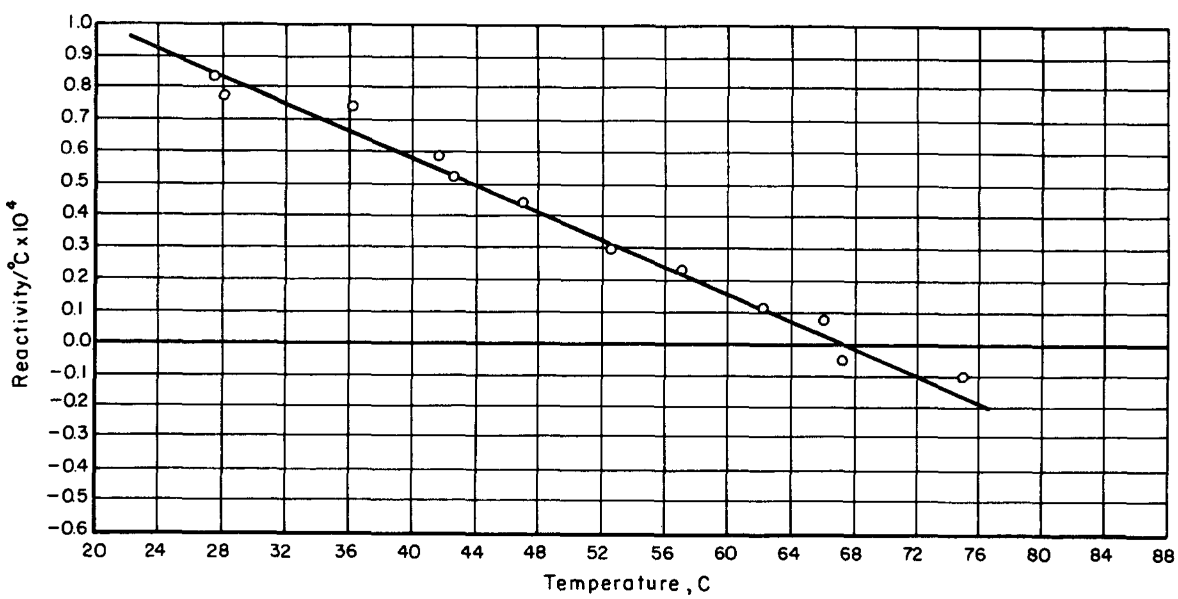

FIGURE 26. TEMPERATURE COEFFICIENT OF REACTIVITY FOR THE CLEAN CORE

[redacted]

In an attempt to measure the fuel-element temperature coefficient separately the just-critical rod position was determined while the moderator-reflector regions were several degrees warmer than the fuel elements. As the fuel element came to temperature equilibrium with the moderator-reflector, the rod position was varied to maintain a critical condition. The magnitude of the change was too small to be measured. This result agrees with the negligible value for the temperature coefficient in the fuel as calculated by Aerojet-General Corporation for GCRE-I[1], i. e., approximately 1×10^{-6} reactivity per deg C.

Reactivity Worth of Mock-Up Safety Blades

Two tungsten blades, one 2 by 0.2 by 24 in. and the other 4 by 0.2 by 12 in., were covered on one side with a 1/16-in.-thick indium sheet and wrapped in 10-mil cadmium to form mock-up safety blades. These blades were centered at Position B-2 in the core (see Figure 13). Table 9 gives the results of this experiment.

TABLE 9. WORTH OF MOCK-UP SAFETY BLADES

Blade Construction	Blade Position[a]	Blade Worth, per cent $\frac{\Delta k}{k}$
2-in.-wide tungsten-indium jacketed with 10 mils of cadmium	B-2, inserted 11.00 in.	-0.452 ± 0.005
2-in.-wide tungsten-indium jacketed with 10 mils of cadmium	B-2, inserted 5.50 in.	-0.126 ± 0.003
4-in.-wide tungsten-indium jacketed with 10 mils of cadmium	B-2, inserted 5.50 in.	-0.193 ± 0.005

(a) See Figure 13.

The ratio of shutdown capacity of the mock-up safety blade at a 11.00-in. insertion to that at 5.50 in. is 3.6. Doubling the width of the blade at 5.50 in. insertion gives 1.5 times as much worth.

Flux- and Power-Distribution Measurements

Measurements were made to examine the flux and power distributions and the distortion in these quantities caused by the cadmium bands on the fuel elements. Full-length bare manganese wires were placed in the fuel elements and in the moderator between fuel elements along Radius AA to measure total axial and radial flux. The process was repeated using cadmium-covered wires, from which the epicadmium flux and subsequently the thermal flux were determined.

Figure 27 gives the axial variation in total and epicadmium flux in the moderator region between the fuel elements and in the reflector region adjacent to the core. Figure 28 gives the axial flux variation in two of the fuel elements. Other positions along this radius exhibit similar shapes.

[redacted]

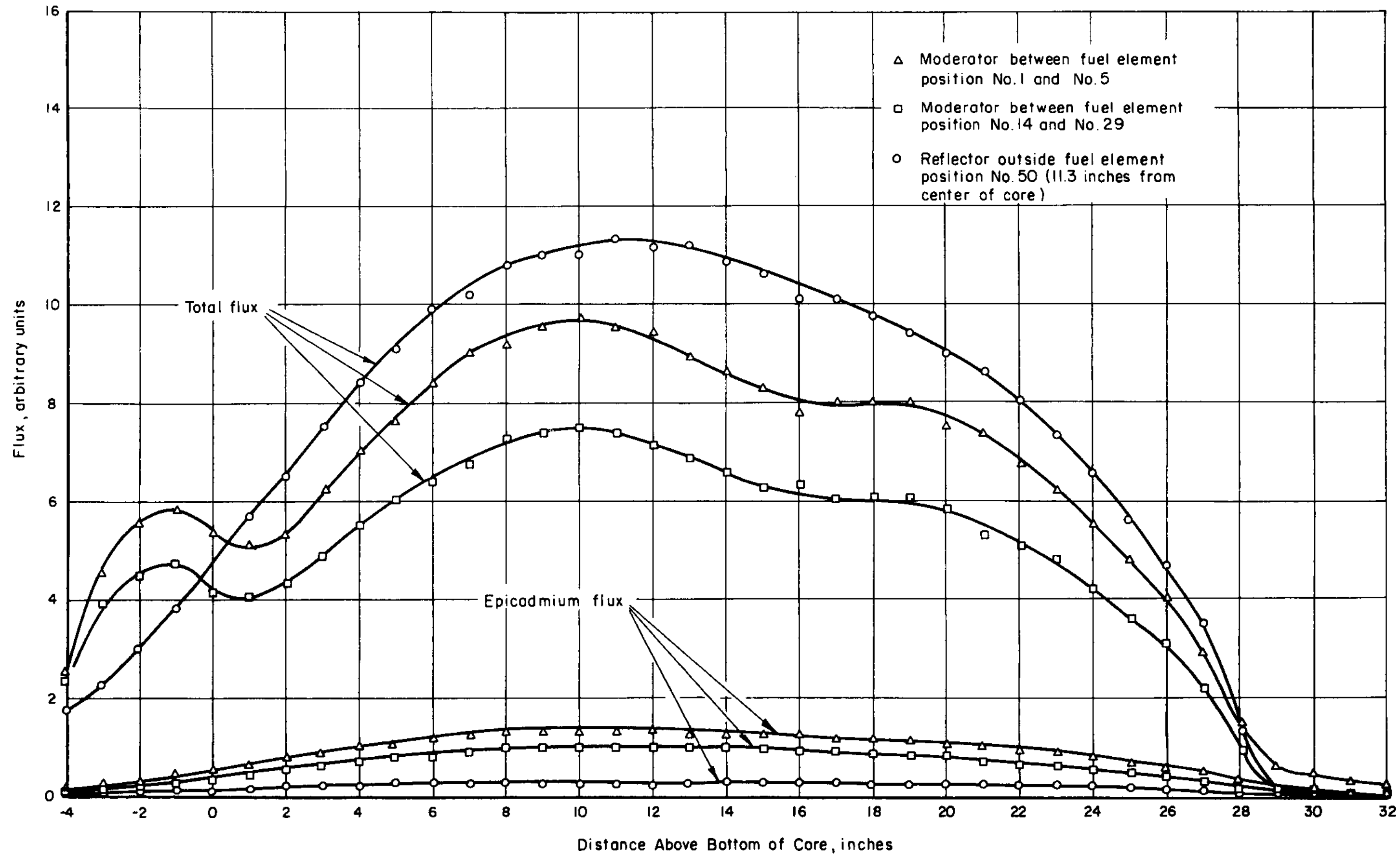

FIGURE 27. AXIAL FLUX DISTRIBUTION IN MODERATOR AND REFLECTOR ALONG RADIUS AA – CLEAN CORE

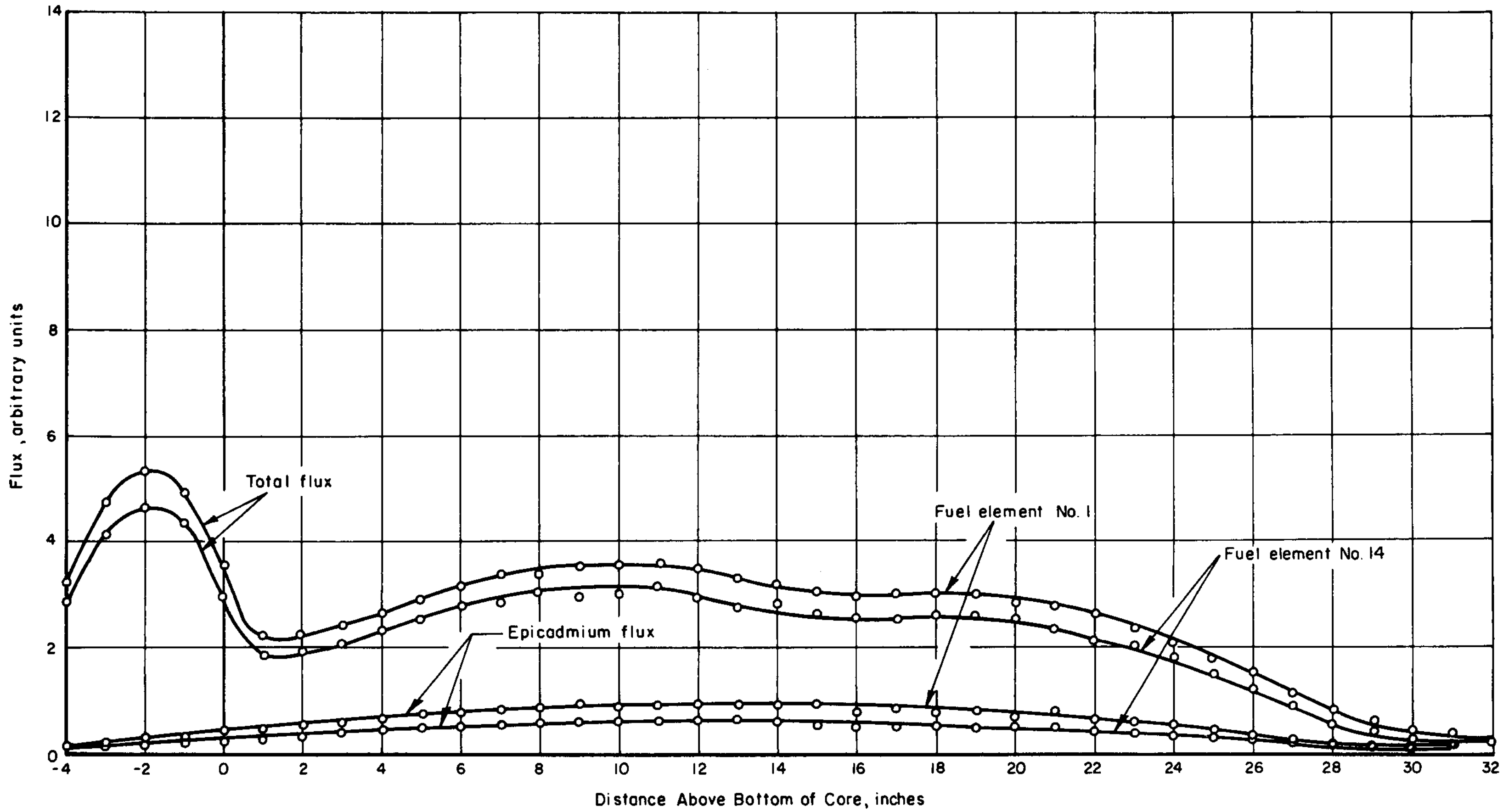

FIGURE 28. AXIAL FLUX DISTRIBUTION AT CENTER OF FUEL ELEMENTS ALONG RADIUS AA – CLEAN CORE

The radial variation of the total flux is presented in Figure 29. The curves for the various axial positions differ because of the flux depression caused by the cadmium band at an axial height of 12.5 to 17.5 in. This causes a sharper peaking in the radial reflector at the 14-in. height.

In addition to flux measurements, the power distribution axially, radially, and azimuthally within fuel elements was examined. Two elements, 1 and 50, at the extreme ends of Radius AA were selected for investigation to determine whether the results were applicable to various regions in the core.

Aluminum catcher foils were arranged axially in columns from 6 in. below to 6 in. above the cadmium-band region. The foil columns were placed at three angular positions on each fuel cylinder. The following sketch shows the angular orientation of the foil columns with respect to adjacent fuel elements.

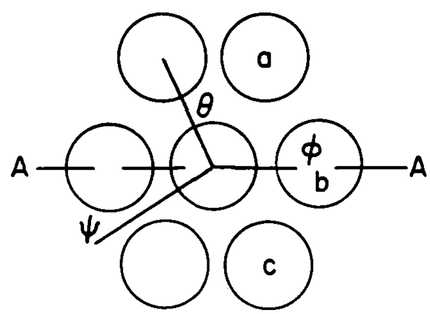

Because of space limitations no foils were placed along the psi axis in the two innermost fuel cylinders. Element 50, at the core perimeter, has no adjoining elements in Positions a, b, and c shown in the sketch.

Figure 30 gives the results of power measurements at three angles in the central fuel element, and shows little azimuthal variation in power for this position. In the corresponding plots for Position 50, Figure 31, the absence of neighboring fuel elements on the side toward the radial reflector causes an azimuthal variation with an increased power on the reflector side.

Figures 30 and 31 also show that axial variation in power is independent of the radial location of the element, i.e., the curves obtained in Positions 1 and 50 are similar. That the influence of the cadmium band is more pronounced on the outer cylinder is also apparent.

The power variation radially within fuel elements in Positions 1 and 50 is shown in Figure 32. The power depression is shown for axial positions above, below, and in the cadmium-band region. These curves show that the power depression is not significantly affected by the cadmium bands.

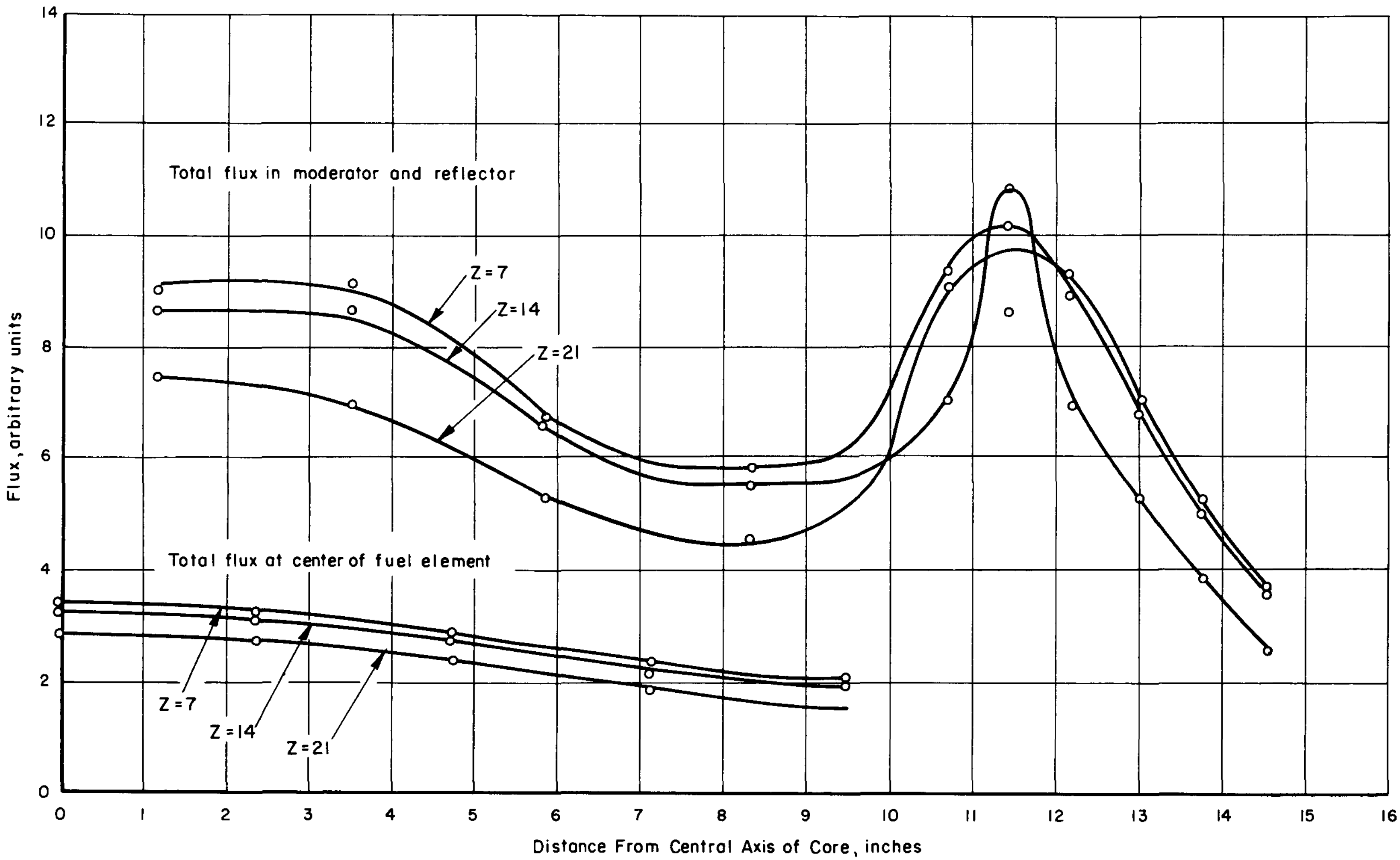

FIGURE 29. RADIAL FLUX DISTRIBUTION ALONG RADIUS AA - CLEAN CORE

Z = distance above bottom of core, in.

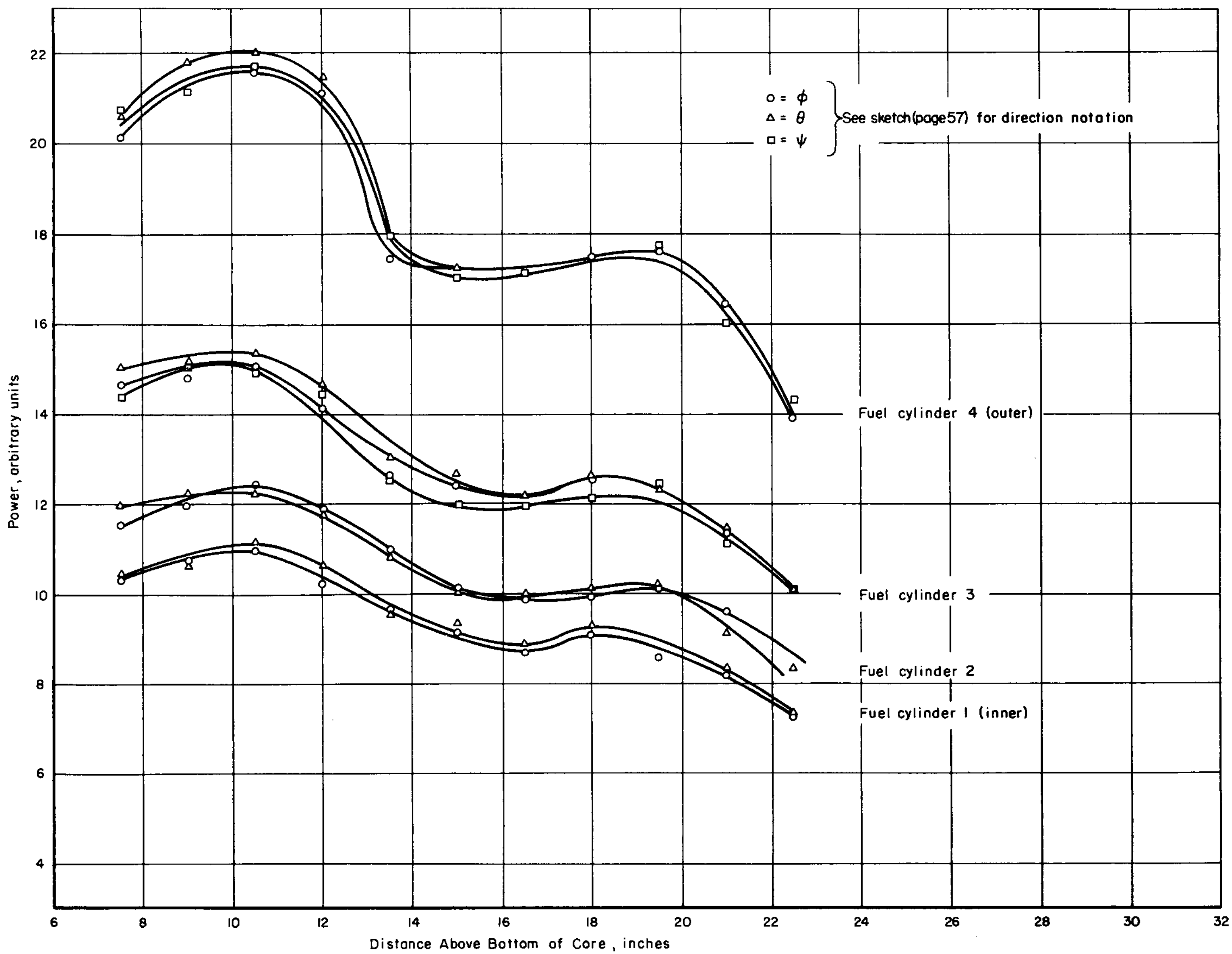

FIGURE 30. AXIAL POWER DISTRIBUTION IN CENTRAL FUEL ELEMENT (POSITION 1) – CLEAN CORE

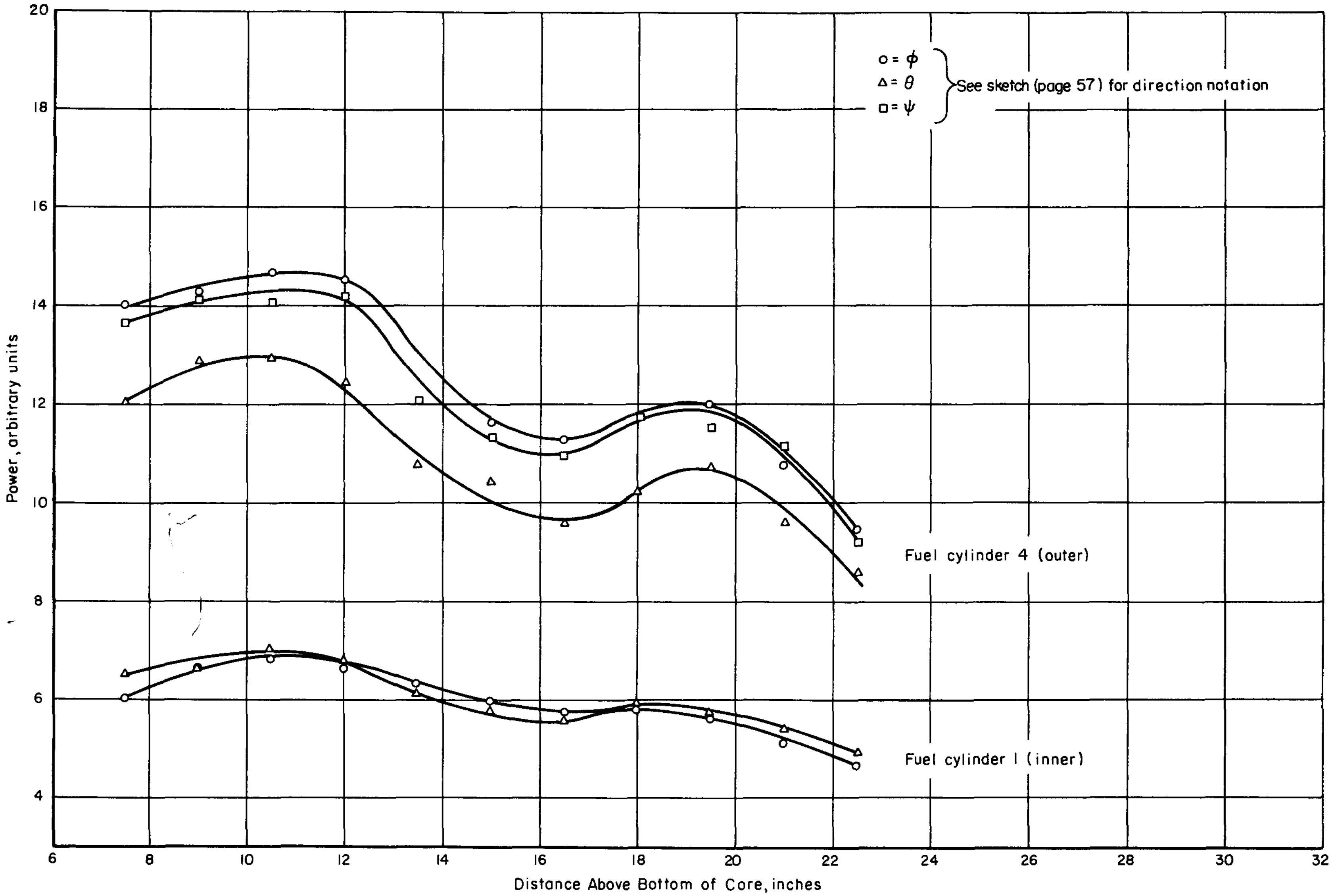

FIGURE 31. AXIAL POWER DISTRIBUTION IN OUTER FUEL ELEMENT (POSITION 50) – CLEAN CORE

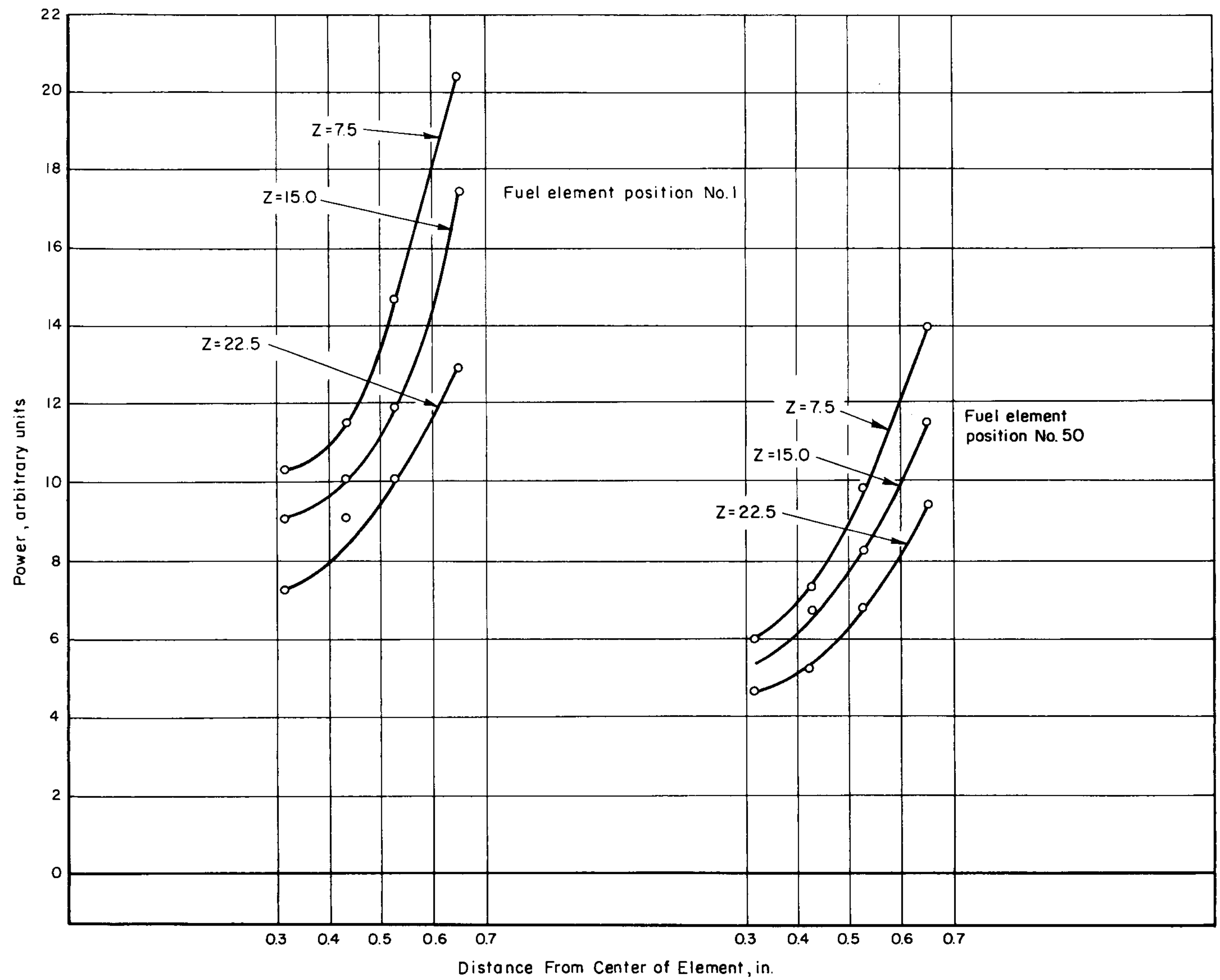

FIGURE 32. VARIATION OF POWER WITHIN FUEL ELEMENTS ALONG RADIUS AA – CLEAN CORE

Z = distance above bottom of core, in.

Lead-Reflected Core

Critical Core Configuration

The first experiments were run with a hexagonal annulus of lead 4 in. thick surrounding 51 fuel elements as shown in Figure 33a. With the lead in this position the core is referred to as the Lead-1 core. The radial lead reflector was 24 in. high and centered axially on the active portion of the fuel about 1/2 in. from the peripheral fuel elements. With the maximum loading of 51 fuel elements the reactor was not critical. Cadmium poison bands were removed from fuel elements in Positions 38, 61, 60, and 59, to attain a critical condition. This case (see Figure 33a) contained 15,616 g of uranium-235 and had excess reactivity of +0.047 ± 0.001 per cent $\frac{\Delta k}{k}$.

After the initial criticality, the lead reflector was moved back to form a hexagon surrounding 61 fuel elements (referred to as the Lead-2 core). In the Lead-2 core the gap between the fuel elements and the lead varied from 1/8 to 3/4 in. In this configuration the fuel inventory was 16,807 g of uranium-235 contained in 55 fuel elements with an excess reactivity of +0.275 per cent $\frac{\Delta k}{k}$ (see Figure 33b). Most of the experiments on the lead-reflected core were performed with the Lead-2 core.

Late in the experiments the lead surrounding the 61 fuel elements was adjusted to give a uniform 1/2-in. gap between the outer fuel elements and the inner face of lead reflector (Lead-3 core). Moving the lead resulted in a 56-element core (see Figure 33c) containing 17,093 g of uranium-235 with 0.495 per cent $\frac{\Delta k}{k}$ excess reactivity. The fifty-sixth fuel element occupied Position 42.

Reactivity Worth of Peripheral Fuel Elements

Table 10 lists the results of measurements of reactivity worth for peripheral fuel elements in the Lead-2 and the Lead-3 cores. The worth of an element did not change when the lead reflector was moved. The similarity of the results is a good indication that measurements made in the Lead-2 core can be compared with similar ones performed in the Lead-3 core.

Temperature Coefficient of Reactivity

The temperature coefficient was measured in the Lead-2 core and the results are shown in Figure 34. This curve is very similar to the temperature-coefficient curve obtained in the Clean-Core configuration. The integral of the curve indicates a reactivity increase of about 0.21 per cent $\frac{\Delta k}{k}$ from 20 to 80 C.

[redacted]

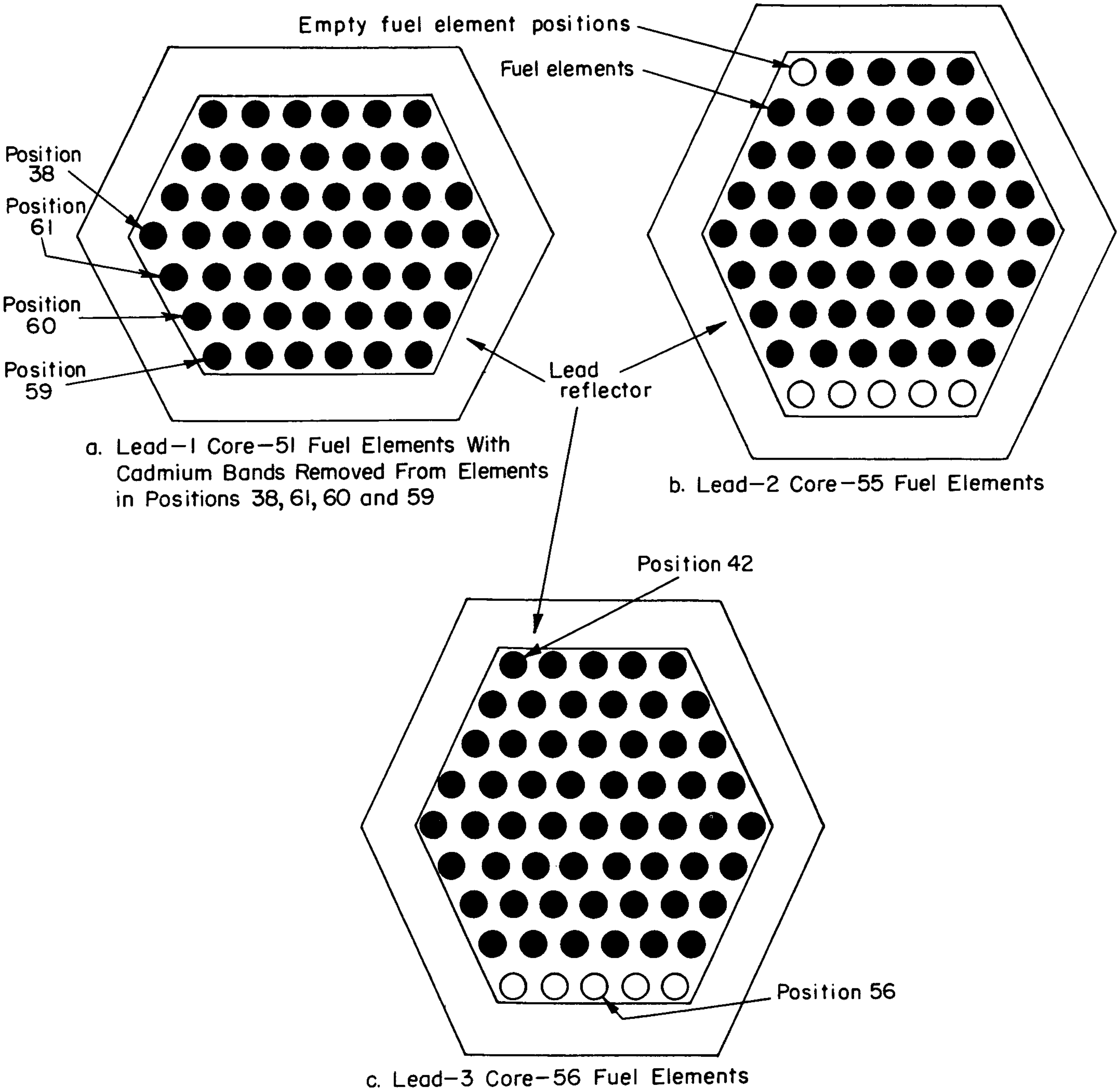

FIGURE 33. INITIAL CRITICAL CONDITION WITH LEAD-REFLECTED CORE

[redacted]

[redacted]

TABLE 10. NUMBER OF FUEL ELEMENTS, FUEL INVENTORY, AND EXCESS REACTIVITY IN LEAD-REFLECTED CORE

Core	Number of Fuel Elements	Fuel Inventory, g	Excess Reactivity, per cent $\frac{\Delta k}{k}$	Element Worth, per cent $\frac{\Delta k}{k}$
Lead-1	51[a]	15,616	+0.047 ± 0.001	
Lead-2	55	16,807	+0.275 ± 0.007	
Lead-2	56 (additional element in Position 42)	17,093	+0.670 ± 0.016	+0.395 ± 0.017
Lead-3[b]	56 (additional element in Position 42)	17,093	+0.495 ± 0.012	
Lead-3	57 (additional element in Position 56)	17,393	+0.887 ± 0.020	+0.392 ± 0.023

(a) Cadmium bands were removed from elements in Positions 38, 61, 60, and 59.

(b) Criticality could have been achieved with 55 elements; however experiments in progress required the excess reactivity, and criticality with the smaller number of elements was not carried out.

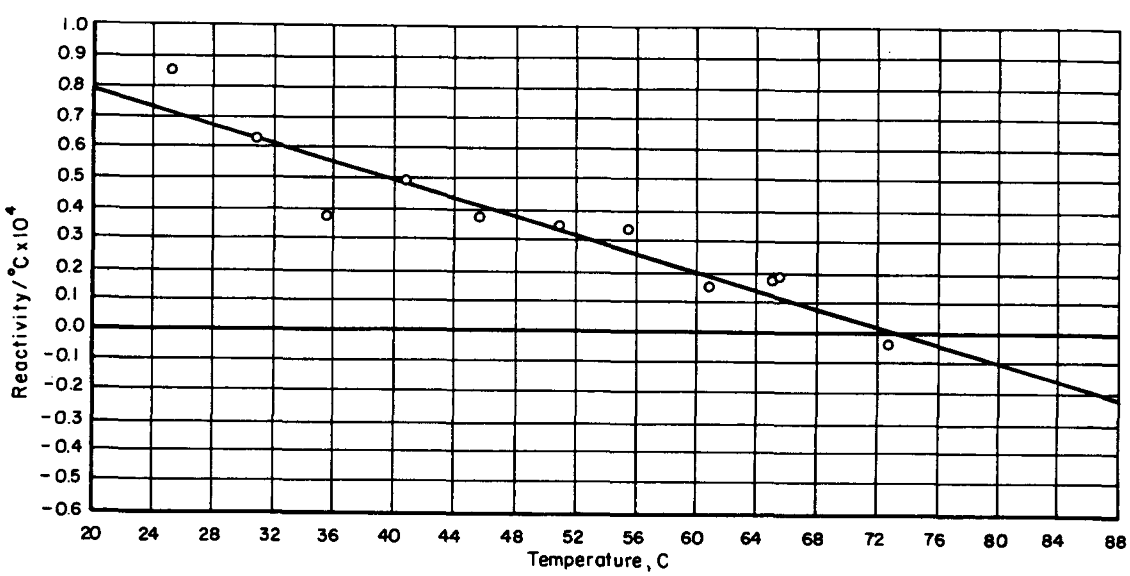

FIGURE 34. TEMPERATURE COEFFICIENT OF REACTIVITY FOR THE LEAD-3 CORE

[redacted]

Reactivity Worth of Mock-Up Safety Blades

The reactivity worths of several mocked-up safety and shutdown rods were measured in the Lead-Reflected Core. The materials, used singly and/or in various combinations, were:

Tungsten	0.20 by 2.0 in.
Aluminum	0.20 by 2.0 in.
Polyethylene	0.20 by 2.0 in.
Indium	0.062 by 2.0 in.
Cadmium	0.010 in. thick, covering both sides and all edges of the materials used in combination with it.

The blades were inserted into the core 11 in. from the 12-in.-radius reference circle at Position B-2 (see Figure 13).

Table 11 gives the results of this set of experiments.

TABLE 11. RESULTS OF TUNGSTEN MOCK-UP BLADE STUDIES IN THE LEAD-2 CORE

Blades inserted 11 in. at Position B-2, all blades 2 in. wide.

Blade Composition	Blade Worth, per cent $\frac{\Delta k}{k}$
Tungsten-indium-cadmium	-0.546 ± 0.013
Tungsten-cadmium	-0.498 ± 0.012
Aluminum-indium-cadmium	-0.476 ± 0.011
Aluminum-cadmium	-0.432 ± 0.010
Polyethylene-cadmium	-0.477 ± 0.011

Several interesting conclusions may be drawn from Table 11. First, the cadmium shell filled with polyethylene has a greater reactivity worth than the cadmium shell filled with aluminum. This occurs because fast and epicadmium neutrons which get through one side of the cadmium may be thermalized by the polyethylene and absorbed by the cadmium before escaping into the core region. This gives the combination of cadmium and polyethylene an effective epithermal worth which cadmium alone does not have. Since the presence of polyethylene increases the effectiveness of cadmium for control, the measurements with other materials cannot be meaningfully compared to the cadmium-polyethylene measurements.

A further conclusion drawn from the data in Table 11 is that the epithermal worth of the tungsten blade is approximately -0.068 per cent $\frac{\Delta k}{k}$ in reactivity. This worth was obtained by comparing the tungsten with aluminum; however, the aluminum is a weak absorber compared with tungsten and the worth of tungsten would not be expected to change much if it was compared with void rather than the aluminum.

[redacted]

The epithermal worth of the indium blade is -0.046 per cent $\frac{\Delta k}{k}$ in reactivity, approximately two-thirds the worth of the tungsten. This value is obtained whether the indium is used in combination with tungsten or aluminum. This indicated that the important resonances in indium do not overlap seriously with those in aluminum or tungsten.

In the composite blade composed of cadmium, tungsten, and indium, the thermal absorption takes place almost entirely in the cadmium. The value of the other materials then depends on their resonance absorption and may be assigned as follows:

	Reactivity Worth, per cent $\frac{\Delta k}{k}$	Per Cent of Total Worth
Cadmium	-0.432	79.1
Tungsten	-0.068	12.5
Indium	-0.046	8.4
Total	-0.547	100

In the absence of the cadmium the worth of the tungsten and indium would be larger because of their thermal absorption.

In a second set of experiments 4 and 8-in.-wide blades of tungsten 1/16 in. thick were tested as mock-up shim blades (i.e., no indium or cadmium materials were used) at position 8 in. below the top of the core (1 in. below Position B-1). The blades were supported from the perimeter of the core by the holder shown in Figure 35.

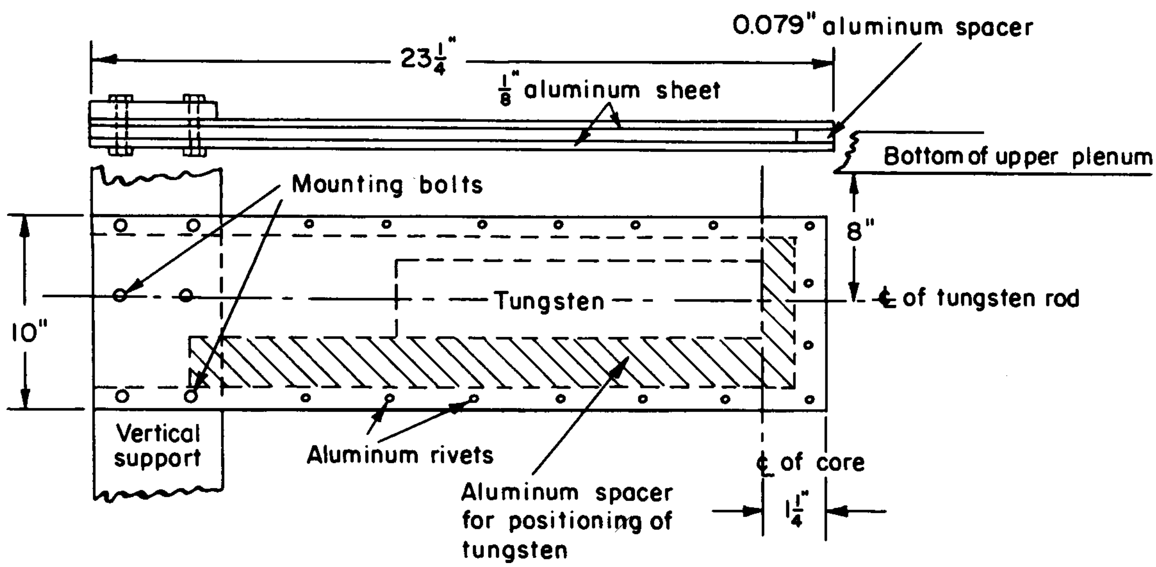

FIGURE 35. SPECIAL MOCK-UP BLADE HOLDER

For polyethylene holder, polyethylene is substituted for aluminum in materials.

[redacted]

Table 12 gives the results of this second set of experiments. Although the aluminum holder had a relatively large effect on the reactivity of the core it had a very small effect on the measured worth of the tungsten blade. The worth of the tungsten was the same within the accuracy of the experiment for the two holders used in the series of experiments.

TABLE 12. RESULTS OF TUNGSTEN MOCK-UP BLADE STUDIES IN LEAD-2 CORE

Blade	Holder	Measured Reactivity Change, per cent	Blade Worth, per cent $\frac{\Delta k}{k}$
None	Aluminum	-0.161 ± 0.004	--
Tungsten, 4 by 0.063 in., inserted 12 in.	Aluminum	-0.485 ± 0.012	-0.324
Tungsten, 4 by 0.063 in., inserted 6 in.	Aluminum	-0.255 ± 0.006	-0.094
Tungsten, 8 by 0.063 in., inserted 6 in.	Aluminum	-0.308 ± 0.007	-0.147
None	Polyethylene	+0.022 + 0.001	--
Tungsten, 4 by 0.063 in., inserted 12 in.	Polyethylene	-0.310 ± 0.007	-0.332

The ratio of the reactivity worth of the 4-in. blade inserted 12 in. to its worth at 6 in. is about 3.5. Doubling the width of the blade at the 6-in. insertion resulted in an increase in reactivity worth of approximately 1.6.

Miscellaneous Reactivity Experiments

Later in the program the water-flooded core condition which occurs during loading operation on the GCRE-1 core was to be mocked up. Water could not be used in the critical assembly because of its corrosive effect on the thin uranium foils; consequently it was necessary to determine the relative merits of various materials as water simulators. An empty fuel can in Position 29 (see Figure 4) was filled successively with water, paraffin, and polyethylene. These experiments were performed with the Lead-2 core containing 56 elements. Following these experiments the Lead-3 core was set up. The reactivity effect of a water-filled can and of a mineral oil-filled can was measured in Position 29.

Table 13 lists the materials and their hydrogen density, and the reactivity associated with the substitution of a can of the material for the normal fuel element. The reactivity effect of the mineral oil has been normalized by eliminating the reactivity change associated with moving the lead.

[redacted]

TABLE 13. COMPARISON OF REACTIVITY EFFECTS AND HYDROGEN DENSITY OF VARIOUS MATERIALS

Material	Hydrogen Atoms per Cm^3 at 20 C	Material Worth Relative to a Fuel Element, per cent $\frac{\Delta k}{k}$	Reactivity Worth, $\frac{\Delta k}{k}$ per hydrogen atom
Water	6.7×10^{22}	-0.598 ± 0.018	--
Mineral oil	7.5×10^{22}	-0.612 ± 0.015	-1.8×10^{-29}
Polyethylene	7.9×10^{22}	-0.640 ± 0.015	-3.1×10^{-29}
Paraffin	8.0×10^{22}	-0.650 ± 0.017	-3.6×10^{-29}

Since identical volumes of materials were used, it can be seen that the mineral oil is 97.7 per cent as effective as water in terms of reactivity effect, whereas both paraffin and polyethylene are about 92 to 93 per cent effective. On the basis of these results and because of its ease of handling, mineral oil was used as the water-simulating material in the Simulated-Flooded Core.

Power-Distribution Measurements

Only power measurements were made in the Lead-Reflected Core. These measurements were designed to study the effects of the mock-up blades and lead reflector on power distribution. Measurements were made of axial and radial power distributions along Radii AA and BB; and of power depressions within the fuel elements with no mock-up blades in the core.

The catcher foils used for measuring local power were located at various axial positions in the elements of interest on the outer fuel cylinder at the point on the circumference most distant from the center of the core (in the element in Position 1 the catcher foils were located on Radius AA or Radius BB). In addition, catcher foils for obtaining axial plots were located in the corresponding positions on the central fuel cylinder of the elements in Position 1 and Position 50 (along Radius AA on the central element). Also, at axial positions 14 and 21 in. above the bottom of the fuel, catcher foils were located on each of the fuel cylinders in each of the elements on Radius AA in the half of the element most distant from the center of the core.

Figure 36 shows the axial variation of power in the fuel elements at Positions 1 and 50. A measurement was made on the central fuel cylinder and the outer fuel cylinder of each of these fuel elements. The two results indicate the similarity of axial power variation in the various fuel cylinders. The axial power distributions in the Lead-Reflected Core show a power depression in the cadmium region similar to the one in the Clean Core.

Figure 37 gives the radial power variation along Radius AA. No unusual variation of radial power caused by the lead reflector is noted. Figure 38 presents the power depression in the fuel cylinders of elements along Radius AA. Comparing these results shows that the general shape of the power depression is independent of axial or radial position in the core. The peak-to-average power ratio within an element was 1.32.

[redacted]

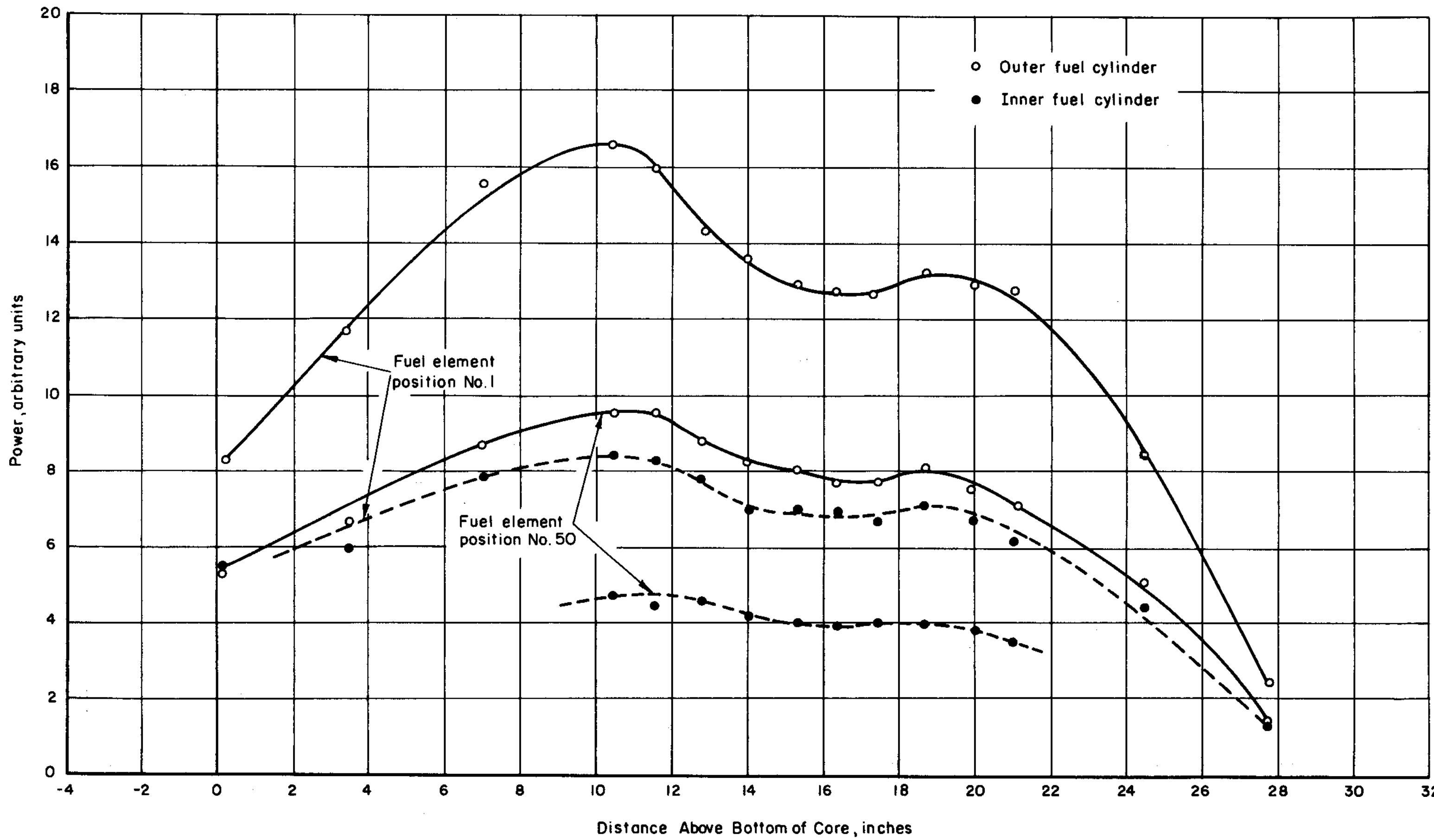

FIGURE 36. AXIAL POWER DISTRIBUTION WITHIN FUEL ELEMENTS ALONG RADIUS AA – LEAD-REFLECTED CORE

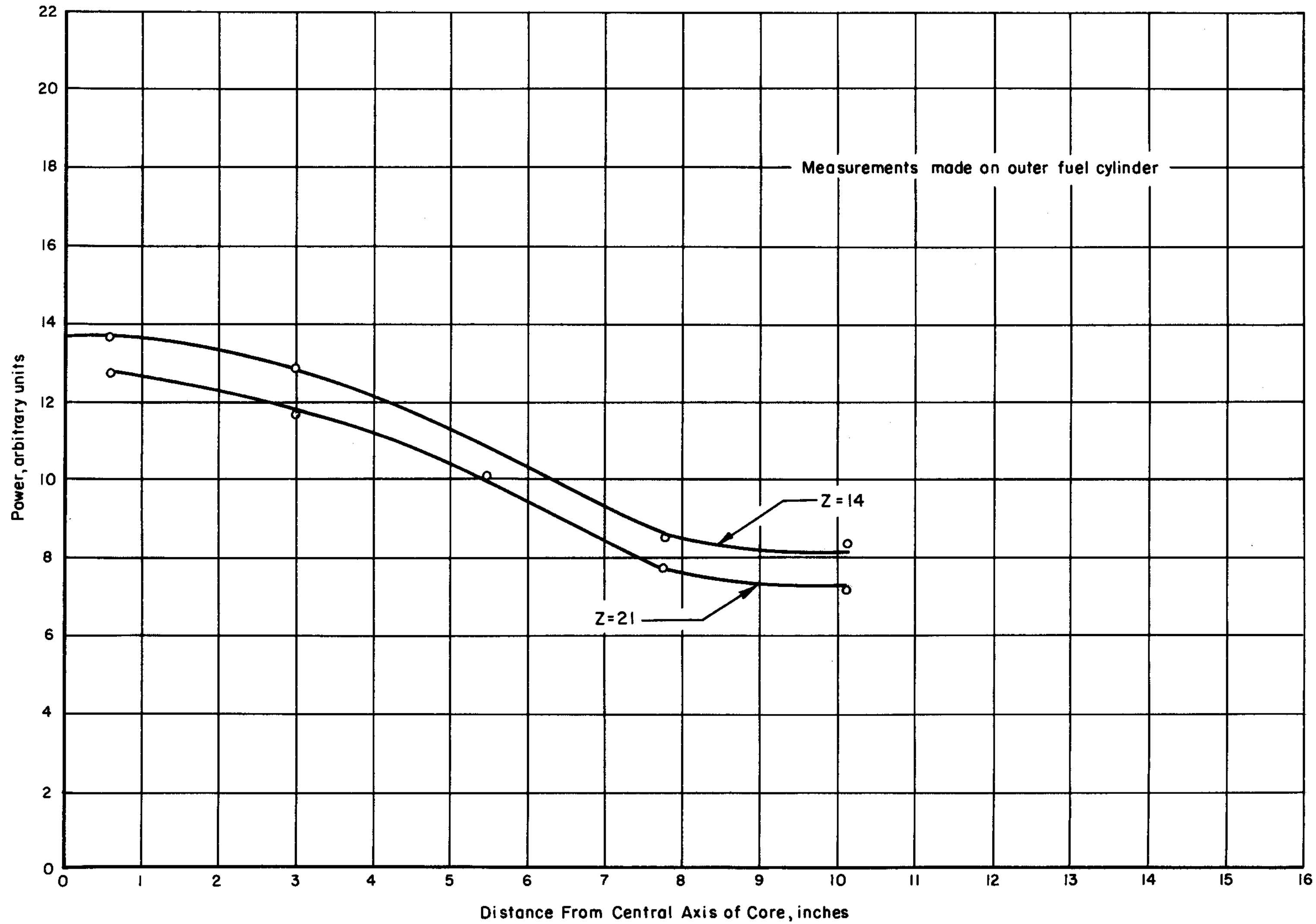

FIGURE 37. RADIAL POWER DISTRIBUTION ALONG THE RADIUS AA - LEAD-REFLECTED CORE

Z = distance above bottom of core, in.

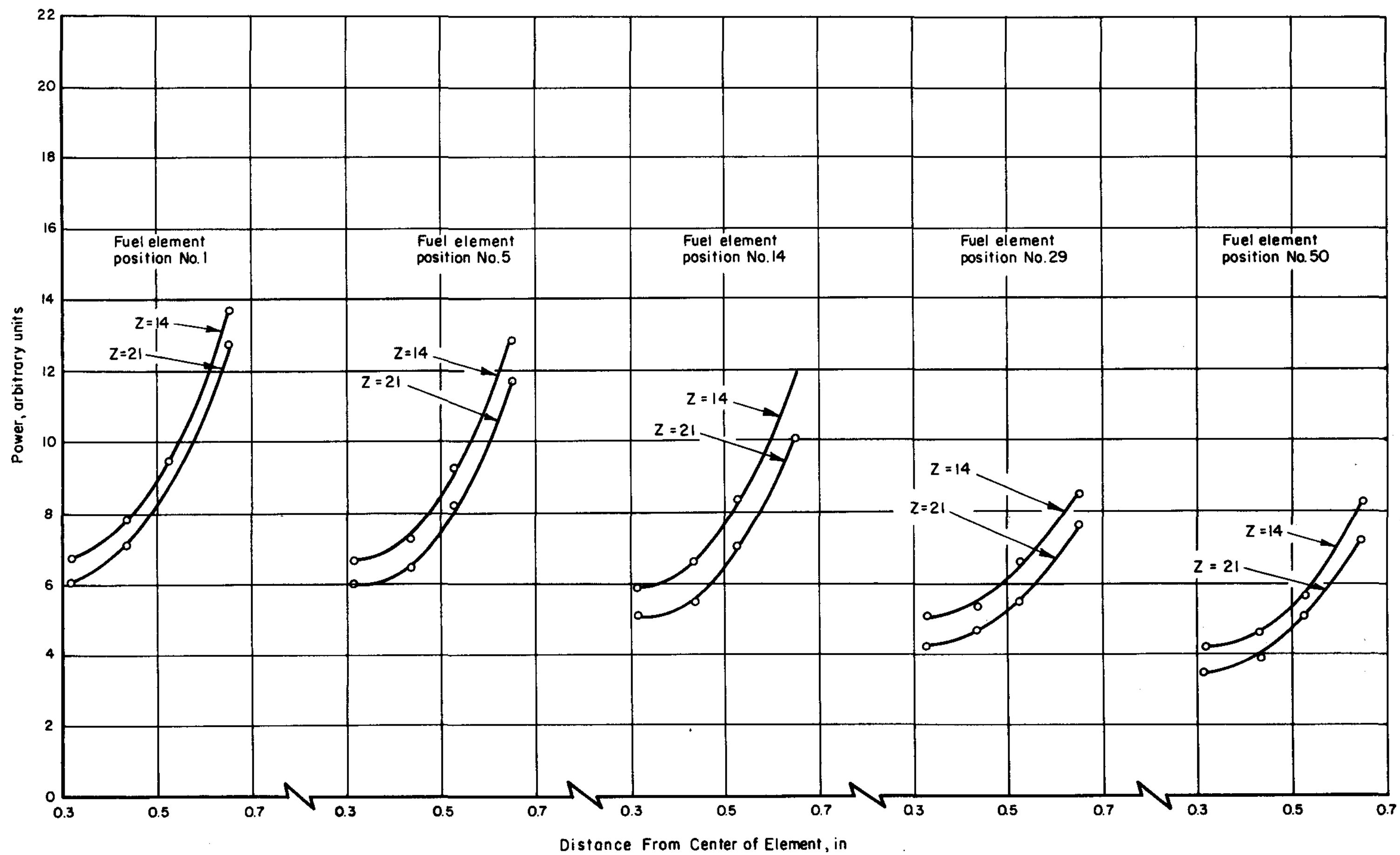

FIGURE 38. VARIATION OF POWER WITHIN FUEL ELEMENTS ALONG RADIUS AA – LEAD-REFLECTED CORE

Z = distance above bottom of core, in.

The data in Figures 36 and 37 were analyzed to determine the ratio of peak-to-average power axially and radially. The axial ratio is 1.38. The radial peak-to-average power ratio is 1.37. This is an average of the ratios at axial heights 14 and 21 in. above the bottom of the fuel. Using the above values the peak-to-average power ratio in the core (including the variation within an element) is 2.50. If the element variation is neglected the ratio becomes 1.89.

To study perturbations caused by mock-up shim-blades in Position B-2, axial columns of foils were placed in the elements occupying Positions 1 and 14. (The element in Position 1 was adjacent to the tip of the mock-up blade and the element in Position 14 was at the midpoint of the mock-up blade.) On each fuel cylinder one column of foils faced the blade and the other was 180 deg away from the blade. These columns extended well above and below the mock-up blades. The measurements were made using the polyethylene holder to support the tungsten. The polyethylene, having nuclear properties close to those of water, produced little perturbation on the system. This case closely simulates the shim-blade configuration for GCRE-1. The results of this study are given in Figure 39. The power at Position 1, obtained without the mock-up blade in the core, is also shown as a comparison. The power variation 180 deg from the blade differs from the unperturbed power variation by 10 per cent, while the power generation on the side of the fuel element facing the mock-up blade is reduced by as much as 30 per cent. With the mock-up blade present, the power variation in a 180-deg sector of the outer fuel cylinder is 25 per cent.

Power measurements were made at the interface between the reflector and the active core region in Positions 38, 40, and 44. The results of the measurements, which were all done in the Lead-2 core, appear in Figure 40. A schematic drawing of the geometry at each location is included in Figure 40. In the region where the lead is close to the fuel elements (on the order of a 1/8-in. gap) the power distribution is affected on the side toward the reflector. However, in regions where the lead is located about 1/2 in. from the core perimeter the power depression is almost symmetrical. In a corner region of the reflector where the water thickness is 1/2 in. or greater, the power depression is unaffected by the lead. In the last two cases the power depression is the same as that found in elements away from the lead reflector (see Figure 38).

Simulated-Flooded Core

For the Simulated-Flooded Core the lead reflector enclosed 61 element positions (the Lead-3 core configuration). The coolant channels were filled with mineral oil to simulate water flooding of the core.

Critical Core Configuration

With the fuel elements filled with mineral oil the reactor was critical with a hexagonal arrangement of the central 37 fuel elements. In this configuration the reactor was just critical with all control rods removed, i.e., no excess reactivity. The uranium-235 inventory was 11,318 g.

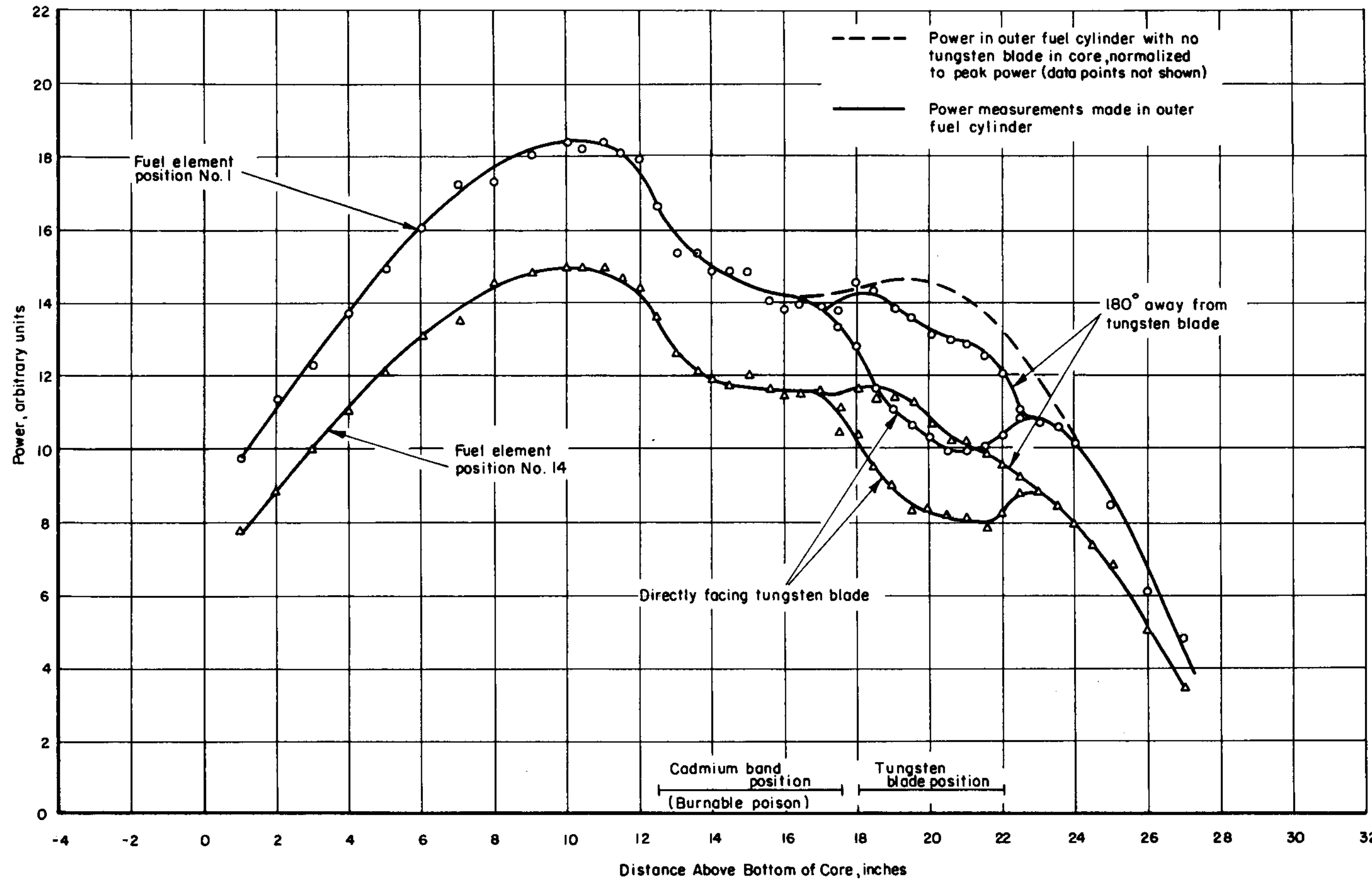

FIGURE 39. AXIAL POWER DISTRIBUTION IN THE VICINITY OF A MOCK-UP SHIM CONTROL BLADE - LEAD-REFLECTED CORE

Tungsten blade 4.0 in. wide by 0.063 in. thick.

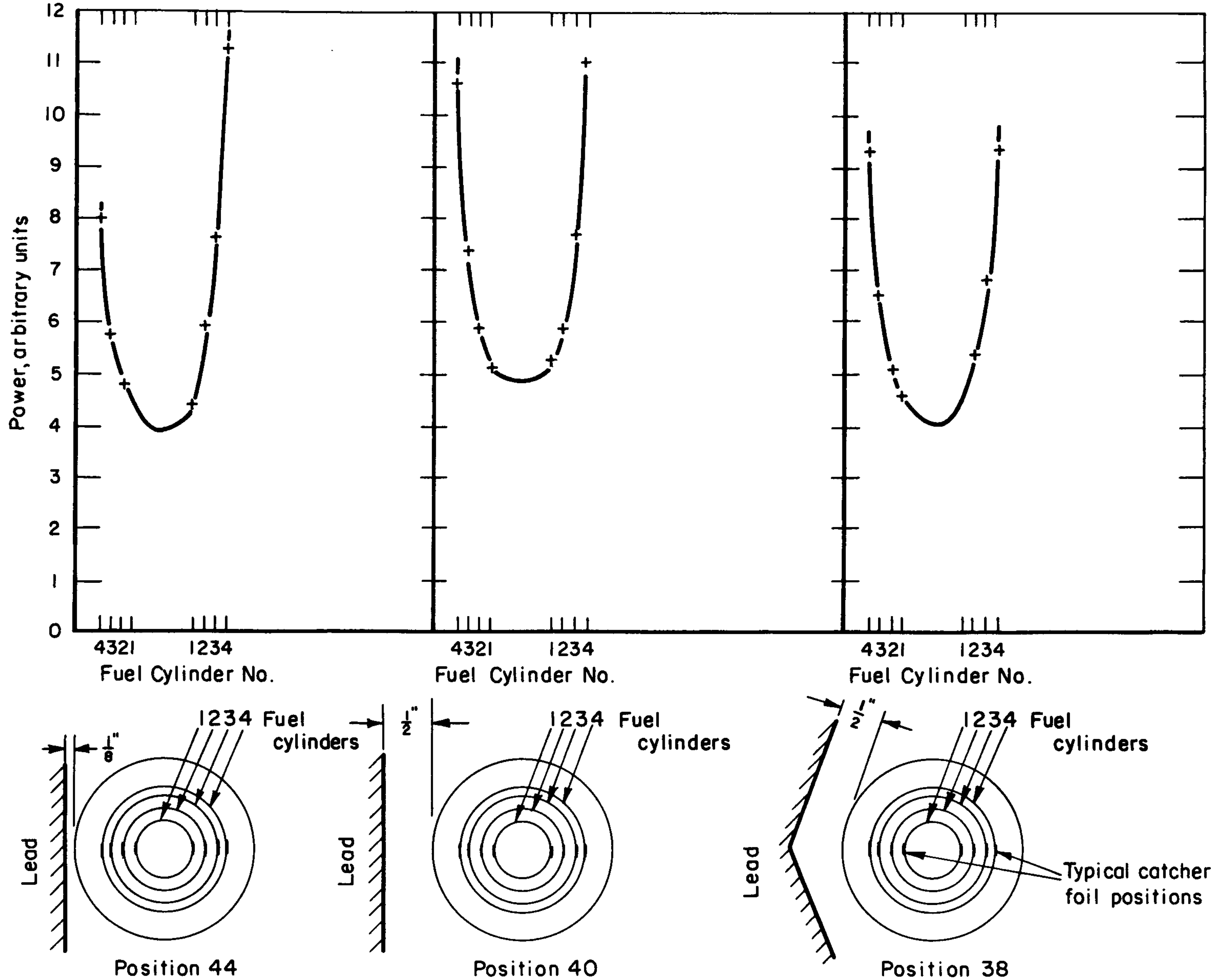

FIGURE 40. COMPARISON OF POWER DEPRESSIONS ON FUEL CYLINDERS NEAR LEAD REFLECTOR, LEAD-1 CORE

Reactivity Worth of Peripheral Fuel Elements

Two elements were added to the core periphery. The thirty-eighth fuel element was inserted into Position 60 and the thirty-ninth fuel element was inserted into Position 59, as shown in Figures 41a and 41b.

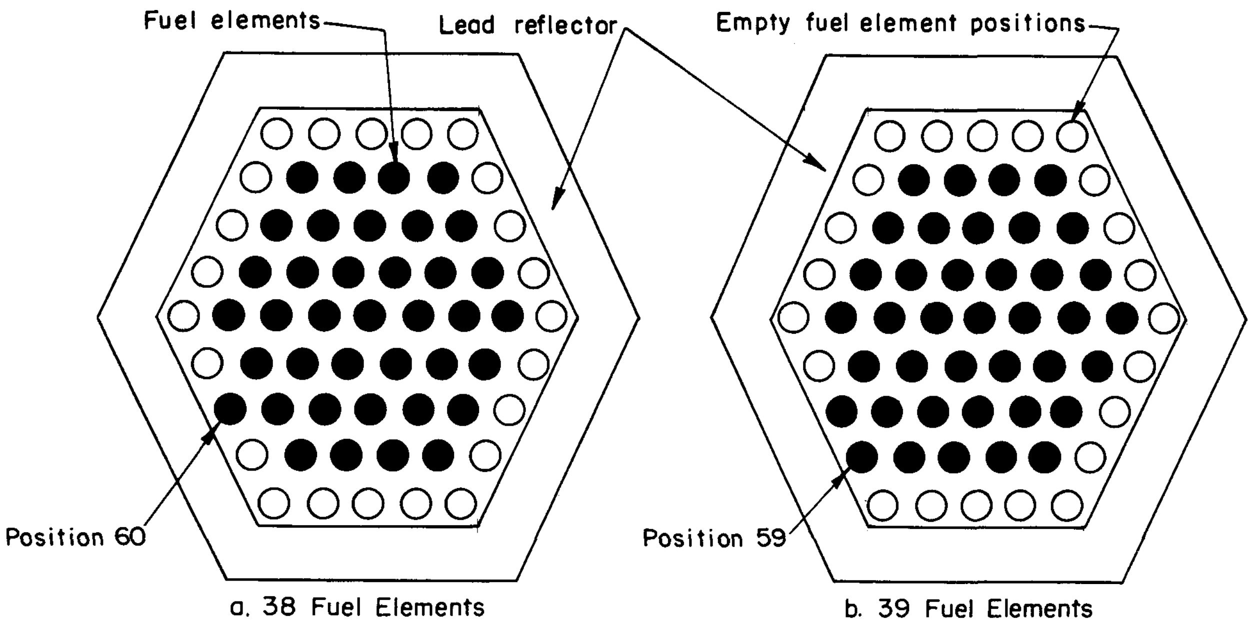

FIGURE 41. CRITICAL CONFIGURATION FOR SIMULATED-FLOODED CORE

The worths of the peripheral fuel elements in the flooded core are given in Table 14.

TABLE 14. NUMBER OF FUEL ELEMENTS, FUEL INVENTORY, AND EXCESS REACTIVITY IN FLOODED CORE

Number of Fuel Elements	Fuel Inventory, g	Excess Reactivity, per cent $\frac{\Delta k}{k}$	Element Worth, per cent $\frac{\Delta k}{k}$
37	11,318	$+0.000 {+0.020 \atop -0.000}$	
38 (additional element in Position 60)	11,636	+0.430 ± 0.010	0.430 ± 0.002
39 (additional element in Position 59)	11,936	+0.809 ± 0.019	0.379 ± 0.021

[redacted]

The worth of the two additional fuel elements is different, i.e., +0.430 per cent for the thirty-eighth fuel element and +0.379 per cent for the thirty-ninth. The thirty-eighth fuel element was alone in the reflector region, whereas the thirty-ninth element was added in the perturbed-flux region of the thirty-eighth.

Reactivity Worth of Mock-Up Safety and Control Blades

The Lead-Reflected Core in the flooded condition is critical with only 37 fuel elements. Since the full core would have 61 fuel elements, the shutdown blades must have a negative reactivity at least equivalent to the reactivity added by 24 elements if they are to shut down the flooded reactor.

A number of shutdown-blade arrangements have been checked in the Simulated-Flooded Core configuration. Table 15 lists rod configurations along with the number of fuel elements required for criticality and the excess reactivity in the core when the reactor was made critical for the first set of experiments. All the blades were inserted to a position 1.5 in. beyond the core center line.

TABLE 15. WORTH OF MOCK-UP BLADES IN THE SIMULATED-FLOODED CORE

Rod Width and Position[a]	Number of Fuel Elements	Per Cent Excess Reactivity Left in Core
8-in. blades at A-2 and D-2	46	+0.159 ± 0.004
8-in. blades at A-1, A-2, C-1, and C-2	49	+0.171 ± 0.004
8-in. blades at A-1, A-2, B-1, and B-2	49	+0.254 ± 0.006
8-in. blades at A-1, A-2, and B-1 7-in. blade at B-2	49	+0.507 ± 0.012
8-in. blades at A-1, A-2, D-1, and D-2	49	+0.441 ± 0.011
8-in. blades at A-2, B-2, C-2, and D-2	54	+0.175 ± 0.004

(a) See Figure 13 for position designations.

The shutdown-rod configuration originally proposed for the GCRE-1 consisted of 8-in. blades in the eight positions listed in Table 15. From a consideration of the second, third, and fifth case in Table 15, it appears that a complete set of shutdown rods would control 22-1/2 additional elements, providing there were negligible interaction between sets of blades. However, the interaction between blades is not known, and is in a direction which will decrease their total effectiveness. From these experiments it is concluded that this set of shutdown rods could not control more than a 59-element flooded core. This is not sufficient.

The next experiments were to measure the reactivity worth of several large shutdown blades arranged as shown in Figure 42. Blades E and F were cadmium-covered indium-tungsten sandwiches measuring 24 by 15 in. Blade H was of similar construction measuring 14 by 15 in. Blade G was a cadmium-covered aluminum-indium sandwich 10 by 24 in. supported from a holder on the perimeter of the core. Blades E, F, and H rested on polyethylene blocks and were supported from the sides by the fuel cans and small polyethylene spacers.

[redacted]

[redacted]

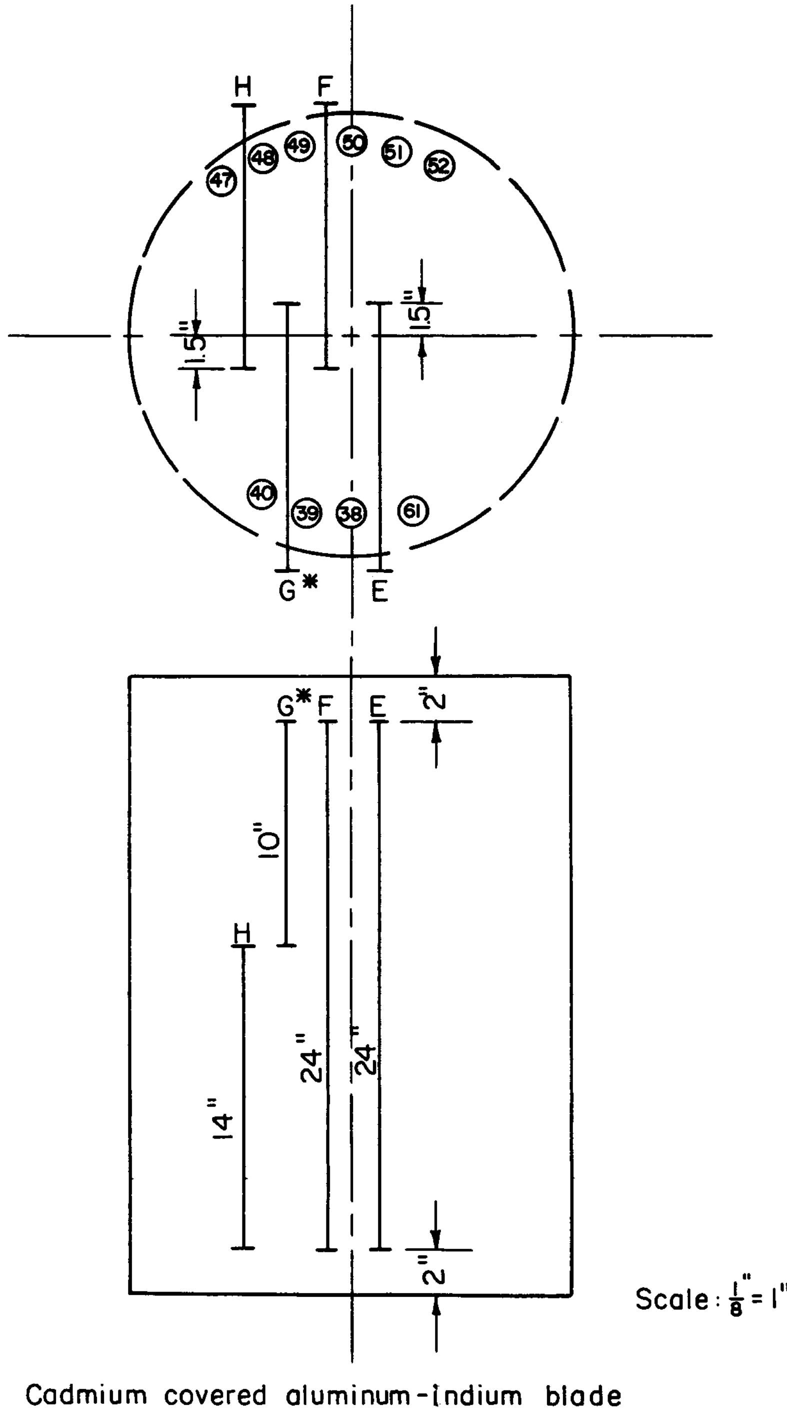

FIGURE 42. LARGE SHUTDOWN-BLADE ARRANGEMENT, SIMULATED-FLOODED CORE

[redacted]

[redacted]

The initial core loading of 41 fuel elements was subcritical. Attempts to achieve criticality were made thereafter in three-element increments. This procedure was continued until a core loading of 61 fuel elements (the maximum loading possible with the lead reflector in place) was obtained. Figure 43 is a curve of the normalized and averaged inverse count rates from several channels versus fuel-element loading. The extrapolation of inverse count rate versus fuel loading is at best only a rough approximation and becomes increasingly difficult the more subcritical the reactor is. The data were fitted to an equation representing the inverse count rate as the critical condition was approached[6]. This fitted curve extrapolates to a critical loading of 66 elements.

Additional measurements of the amount of subcriticality of the core were made by the source-jerk method.[4] Figure 44 is a plot of the experimental data obtained during one of the source-jerk experiments when the core loading was 55 elements. Upon applying Equation (2) a value of 0.963 is obtained for k_{eff}. Values of k_{eff} found for several fuel loadings are plotted in Figure 45. The data, fitted by the method of least squares to the one-group critical equation, resulted in the curve shown. This curve extrapolates to a value of 67 fuel elements for the critical loading.

On the basis of the two experimental methods used, a value of 66.5 ± 1 fuel elements would be the critical configuration. Since the flooded core was critical with 37 fuel elements, it may be concluded that the mock-up rod configuration used in this particular experiment would control 29 fuel elements. This is five more elements than can be loaded in this core, which is equivalent to 1.2 to 2.4 per cent $\frac{\Delta k}{k}$ reactivity.

Flux Measurements

Only flux measurements were made for the Simulated-Flooded Core. Figure 46 gives the results of activating a bare manganese wire in the mandrel of the central fuel element (Position 1) to obtain the axial flux variation. Flooding of the core introduces reflector material above the fuel elements, producing a partial upper axial reflector which causes the flux to peak above the core.

Thermal Utilization Measurements

For calculating thermal utilization, extensive total and epicadmium flux data were taken in the region of the central fuel element at the points shown in Figure 47 at axial positions 10.5 and 16.0 in. above the bottom of the fuel. Typical radial plots of thermal flux in a unit cell are shown in Figure 48. Using the data of Tables 16 and 17, the thermal utilization was calculated to be 0.715.

[redacted]

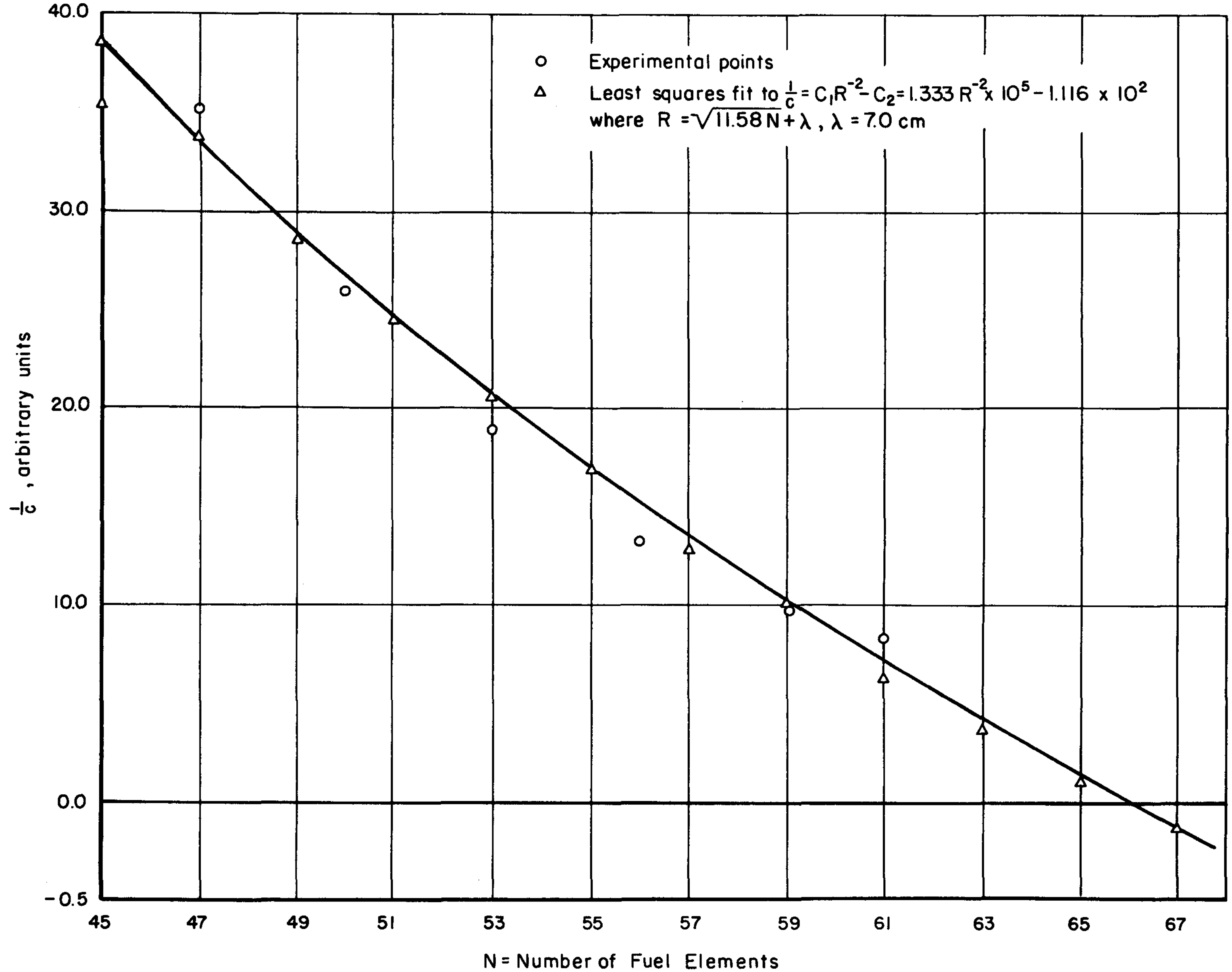

FIGURE 43. INVERSE COUNT RATE VERSUS FUEL-ELEMENT LOADING

[redacted]

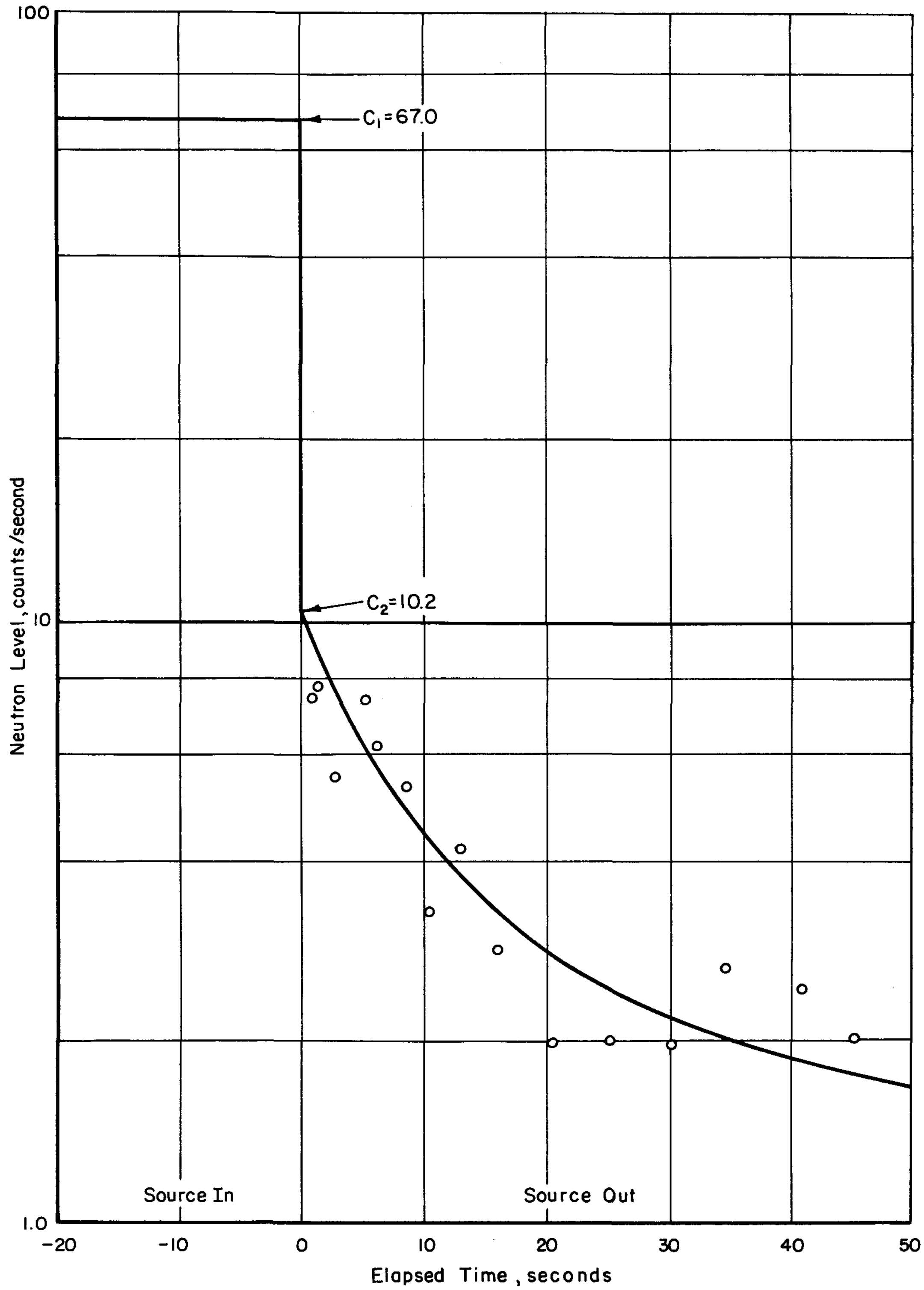

FIGURE 44. NEUTRON LEVEL VERSUS ELAPSED TIME FOR A TYPICAL SOURCE-JERK EXPERIMENT

[redacted]

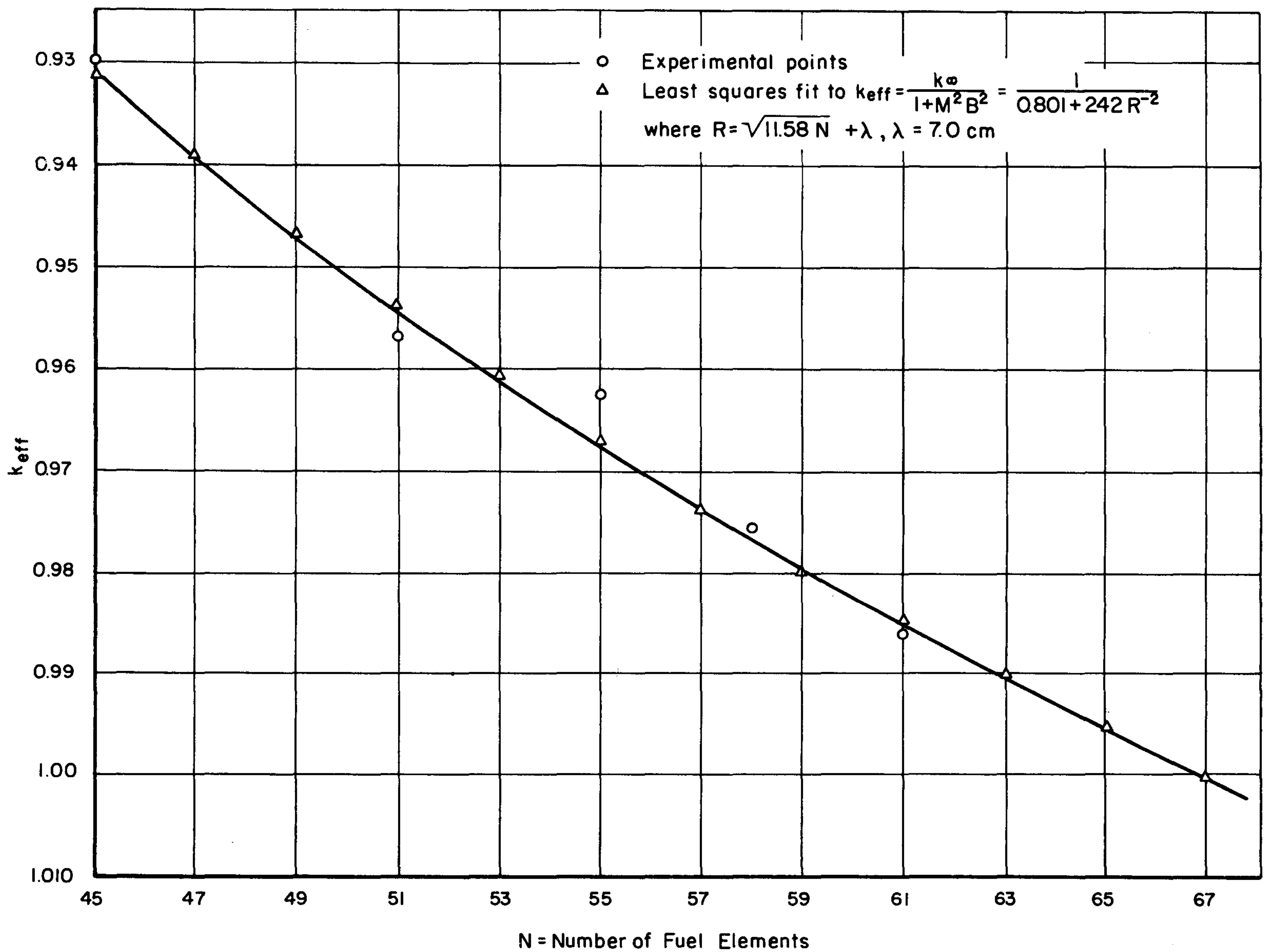

FIGURE 45. k_{eff} VERSUS FUEL-ELEMENT LOADING

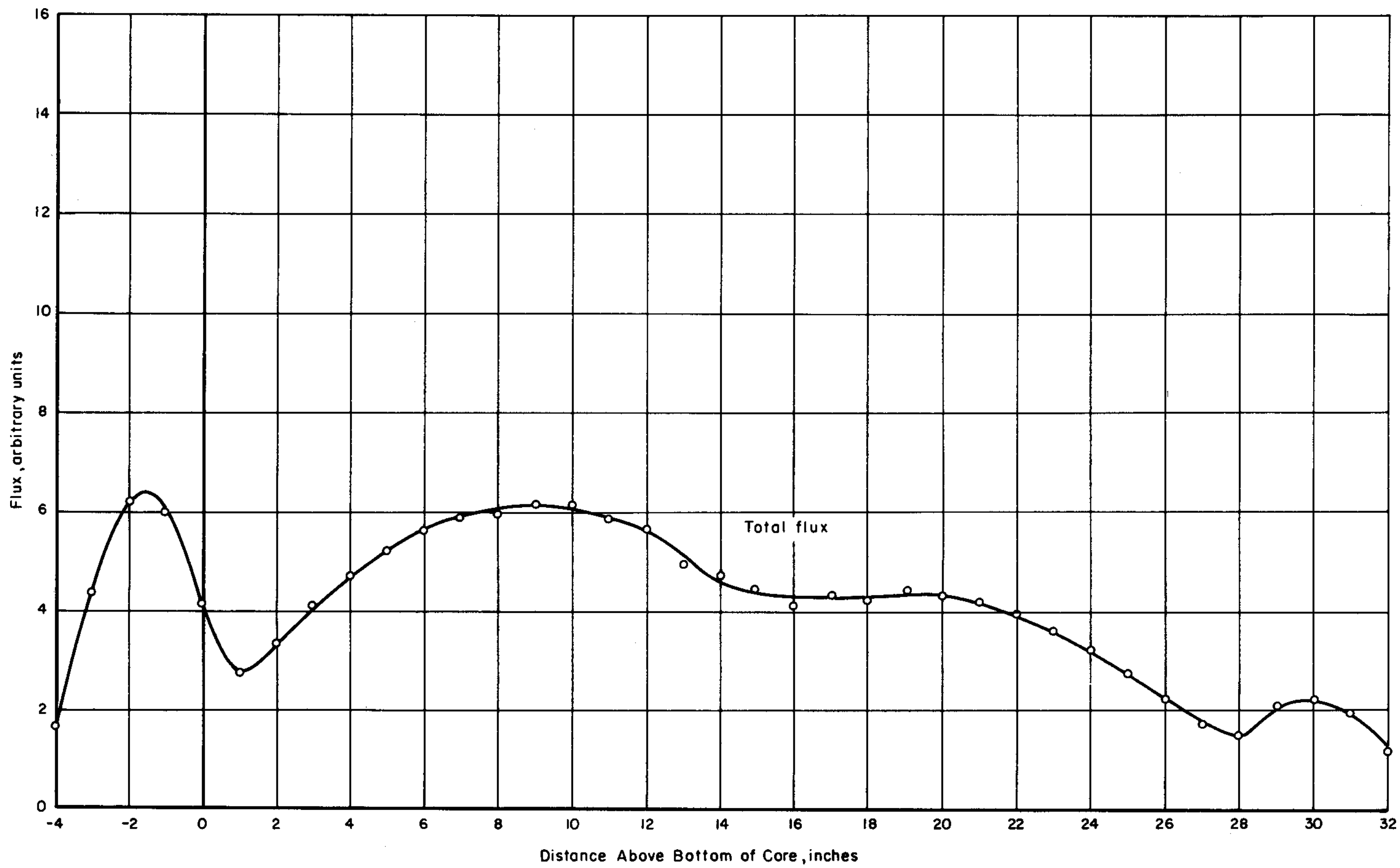

FIGURE 46. AXIAL FLUX DISTRIBUTION IN THE CENTER OF THE CENTRAL FUEL ELEMENT-SIMULATED-FLOODED CORE

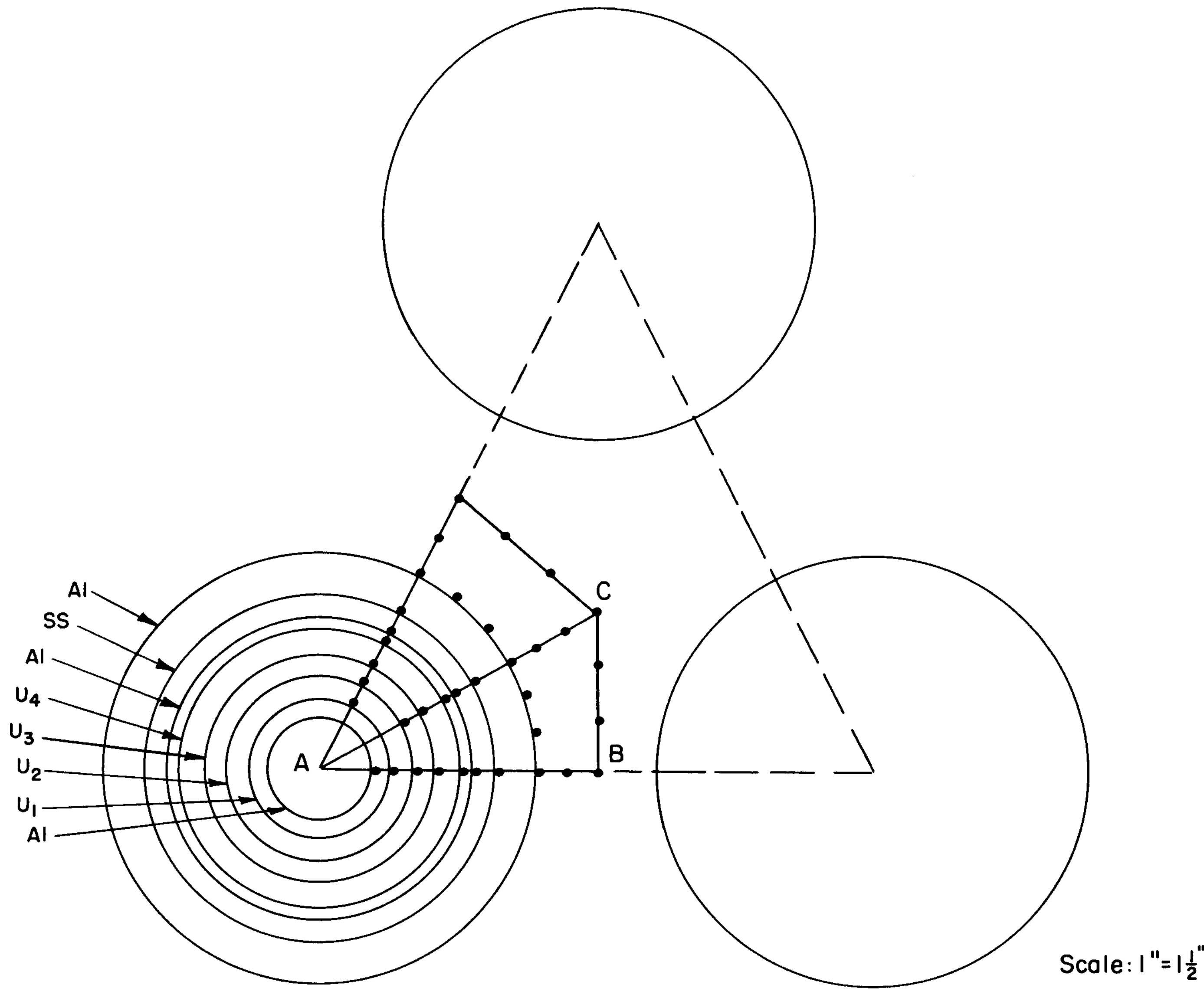

FIGURE 47. LOCATION OF MANGANESE WIRES FOR DETAILED FLUX MAPPING WITHIN AND ADJACENT TO A FUEL ELEMENT IN THE FLOODED CORE

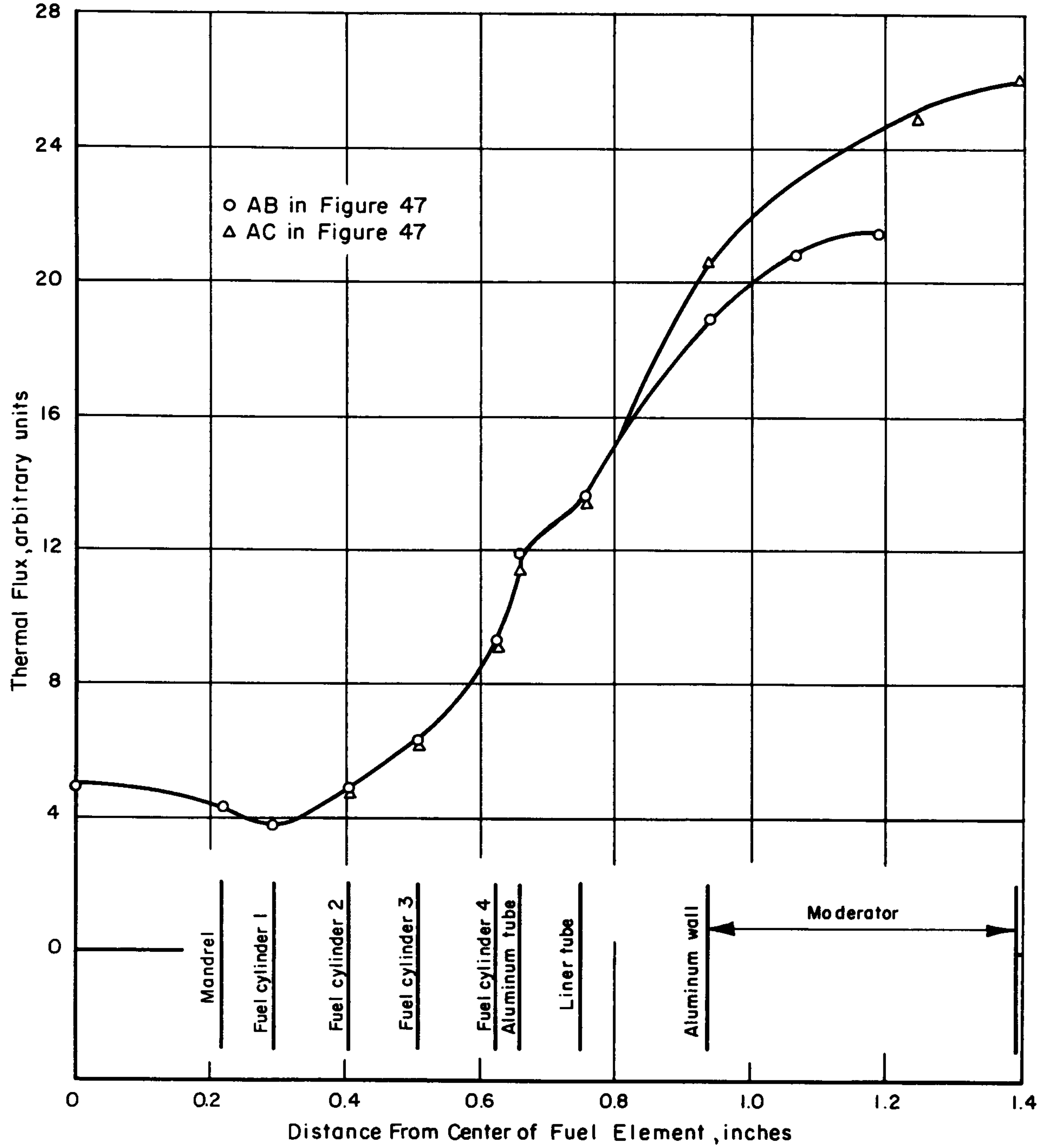

FIGURE 48. THERMAL FLUX THROUGH THE CENTRAL FUEL-ELEMENT CELL, FLOODED CORE

Measurements made at Z = 10.5 in. Outer surface of element components shown.

[redacted]

TABLE 16. PARAMETERS USED IN THERMAL UTILIZATION CALCULATIONS

Cell Material	Per Cent of Total Volume	Ratio to Fuel Volume	Cross Section: $\sigma^{(a)}$, barns	Cross Section: Σ, cm^{-1}	Ratio to Fuel Cross Section
Total cell	100.00	--	--	--	--
Water	51.05	83.48	0.589	0.0197	0.000690
Mineral oil	29.80	48.73	12.42	0.0223	0.000781
Aluminum	9.84	16.09	0.204	0.0123	0.000431
Stainless steel	8.63	14.12	2.66	0.222	0.00777
Uranium	0.675	1.105	--	--	--
Fuel (uranium-235)	0.612	1.00	599[b]	28.56	1.0

(a) Corrected for Maxwellian distribution.
(b) Corrected for non-1/v dependence.

TABLE 17. THERMAL UTILIZATION DATA

	Values at Indicated Distance From Bottom of Fuel in Position 1: 10.5 In.	Values at Indicated Distance From Bottom of Fuel in Position 1: 16.0 In.
Average Thermal Flux		
Uranium-235	6,680	4,288
Water	22,894	15,641
Mineral oil	9,748	6,554
Aluminum	15,745	10,422
Stainless steel	7,371	4,773
Ratio of Flux in Material to Flux in Fuel		
Water	3.427	3.648
Mineral oil	1.459	1.528
Aluminum	2.357	2.431
Stainless steel	1.103	1.113
Calculated Values of Thermal Utilization	0.719	0.711

[redacted]

[redacted]

DISCUSSION

The following sections compare experimental results from similar experiments on the different cores. Not all cores have comparable data so that the comparisons are limited in some cases.

Temperature Coefficient of Reactivity

Curves showing the temperature coefficients of reactivity for the Clean and Lead-Reflected Cores appear in Figures 26 and 34, respectively. These curves are similar in shape and magnitude, and the reactivity changes resulting from the temperature rising from 20 to 80 C are the same (0.22 per cent $\frac{\Delta k}{k}$) within experimental error.

Reactivity Worth of Peripheral Fuel Elements

The reactivity worth of adding fuel elements to the core perimeters has been tabulated for each core. These data are summarized on Figure 49 as curves of fuel-element additions versus excess reactivity. In each case, within the range investigated, a linear variation adequately fits the data. There is a tendency for the slope of these curves to decrease for larger values of the critical number of fuel elements (the fractional change in equivalent core radius and in geometrical buckling per element is smaller for larger cores; therefore, the reactivity change is expected to be smaller).

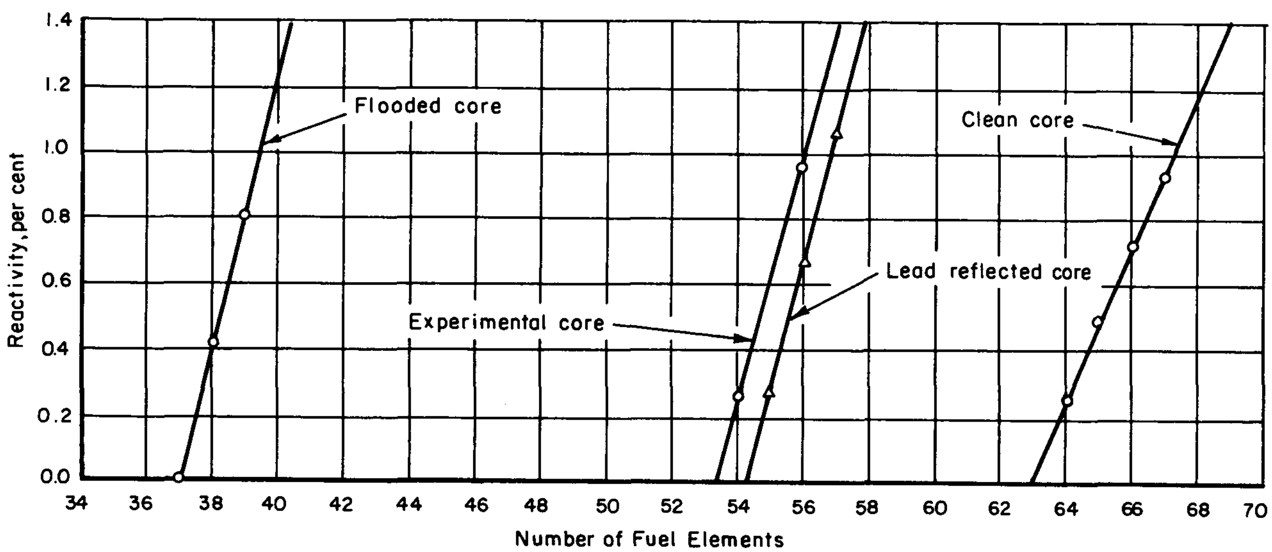

FIGURE 49. EXCESS REACTIVITY VERSUS FUEL-ELEMENT ADDITIONS FOR ALL CORE CONFIGURATIONS

Both the Experimental and Lead-Reflected Cores had comparable critical numbers of fuel elements. In these core configurations the worth of additional elements followed the same linear variation (within experimental error).

[redacted]

[redacted]

Flux- and Power-Distribution Measurements

The axial distribution of flux (total) in the center fuel element in the Experimental, Clean, and Simulated-Flooded Cores appears in Figure 50. These data are normalized to give the same average flux value over the active fuel region. The influence of the cadmium band is apparent; also the addition of a partial upper axial reflector in the Simulated-Flooded Core is seen (the moderator water was at normal height; the mineral oil level was above the fuel, forming a partial axial reflector). The flux distributions show a change in importance of the lower axial reflector between these core configurations. The highest relative peak in the lower axial reflector occurs with the Clean Core, next is the Experimental Core, and finally the Simulated-Flooded Core. The general shape of these curves within the fuel regions shows that the lower axial reflector savings is consistent with this variation in reflector flux peaking; i. e., the higher the peak, the greater is the return of neutrons by the bottom reflector, and the larger is the reflector savings.

Figure 51 compares the flux depression through a fuel element-moderator unit cell of the Experimental and Simulated-Flooded Cores. The data have been normalized to the flux value at the third fuel cylinder. These data were taken at different axial positions; however, the variation in flux depression was found to be constant with axial position so that these curves may be compared directly. The difference in thermal utilization between these two core configurations is apparent from these flux variations.

The curves of Figure 52 compare the power variation within the central fuel element in the Lead-Reflected and Experimental Cores (normalized to the power value on the outer fuel cylinder). This comparison shows that the Lead-Reflected Core has less power depression within the fuel element than does the Experimental Core. This may be indicative of a "harder" neutron spectrum within the Lead-Reflected Core.

SUMMARY

Critical Core Configurations

Four different cores were studied. These were (1) the Experimental Core, (2) the Clean Core, (3) the Lead-Reflected Core and, (4) the Simulated-Flooded Core. The first core contained an array of tubes containing the fuel elements, and was water moderated and reflected. In the second core the simulated burnable poison was added to the fuel element. The third core had a 4-in.-thick lead reflector surrounding the water-moderated core at a distance 1/2 in. from the peripheral fuel elements. The fourth core configuration used mineral oil to simulate water in flooding the coolant channels of the Lead-Reflected Core. The critical core configurations and associated excess reactivity are given in Table 18.

[redacted]

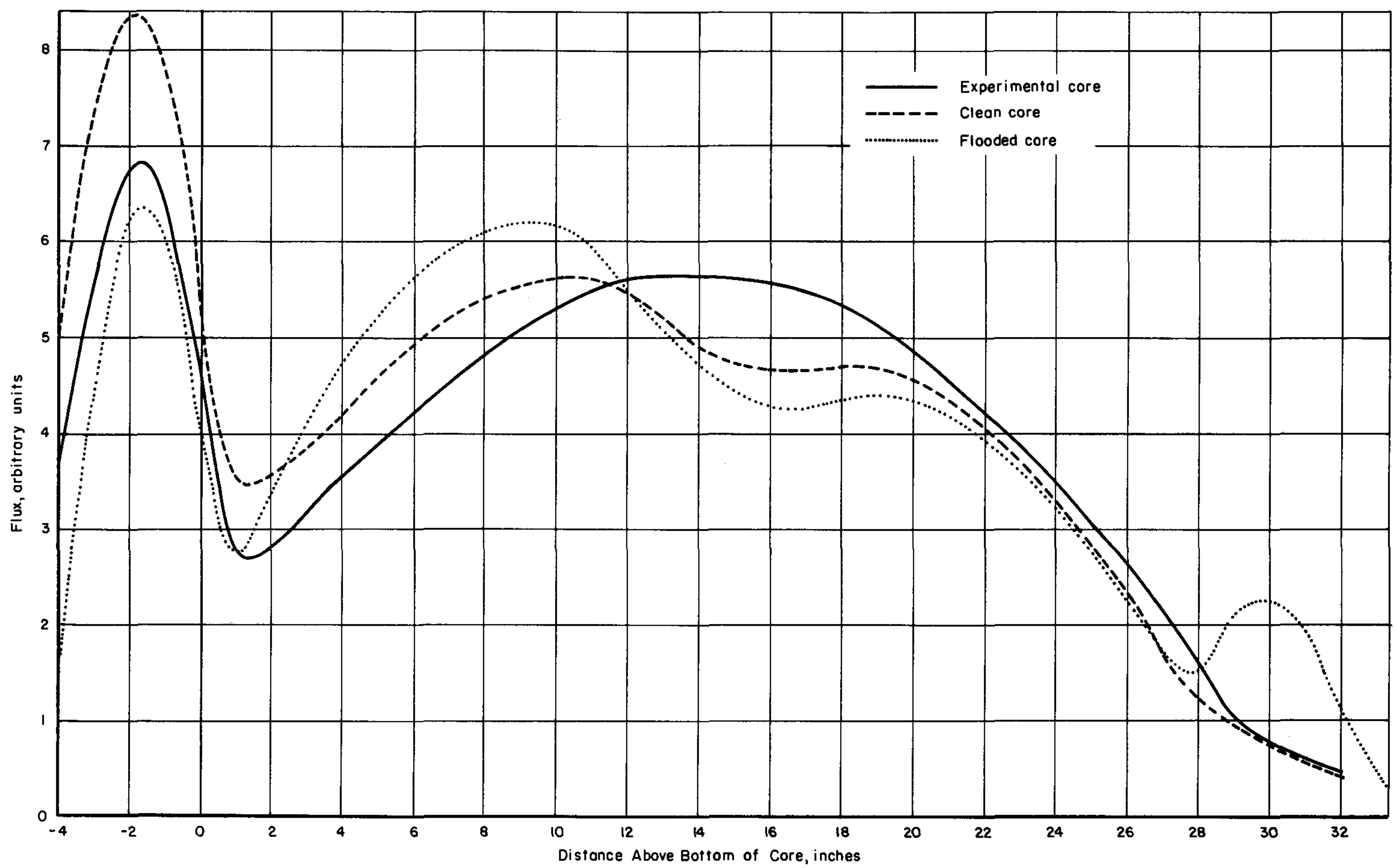

FIGURE 50. COMPARISON OF AXIAL FLUX DISTRIBUTIONS IN CENTER OF CENTRAL FUEL ELEMENTS IN VARIOUS CORES

Data normalized to have equal axial averages over the fuel region.

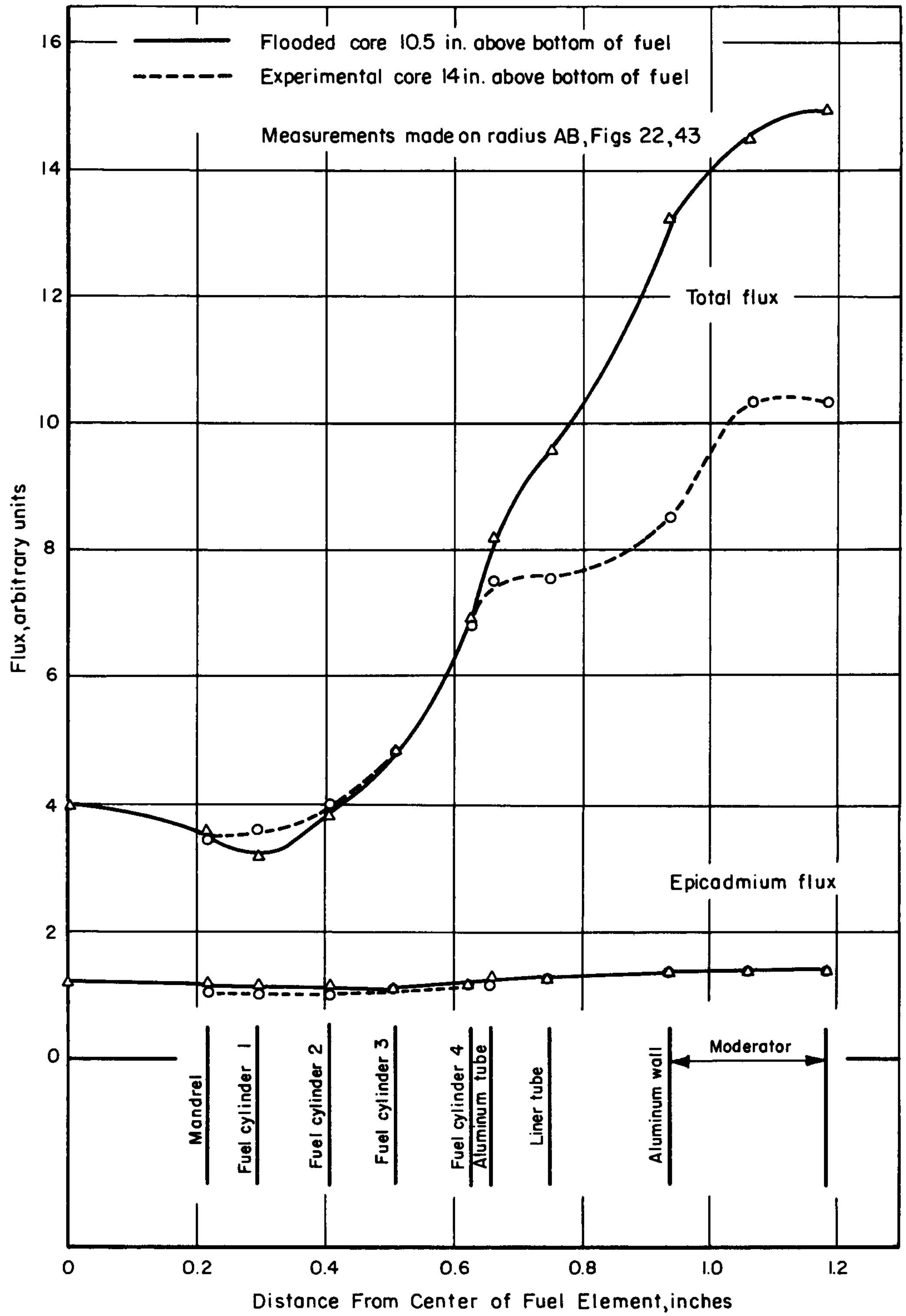

FIGURE 51. COMPARISON OF FLUX THROUGH THE CENTRAL FUEL-ELEMENT CELL

[redacted]

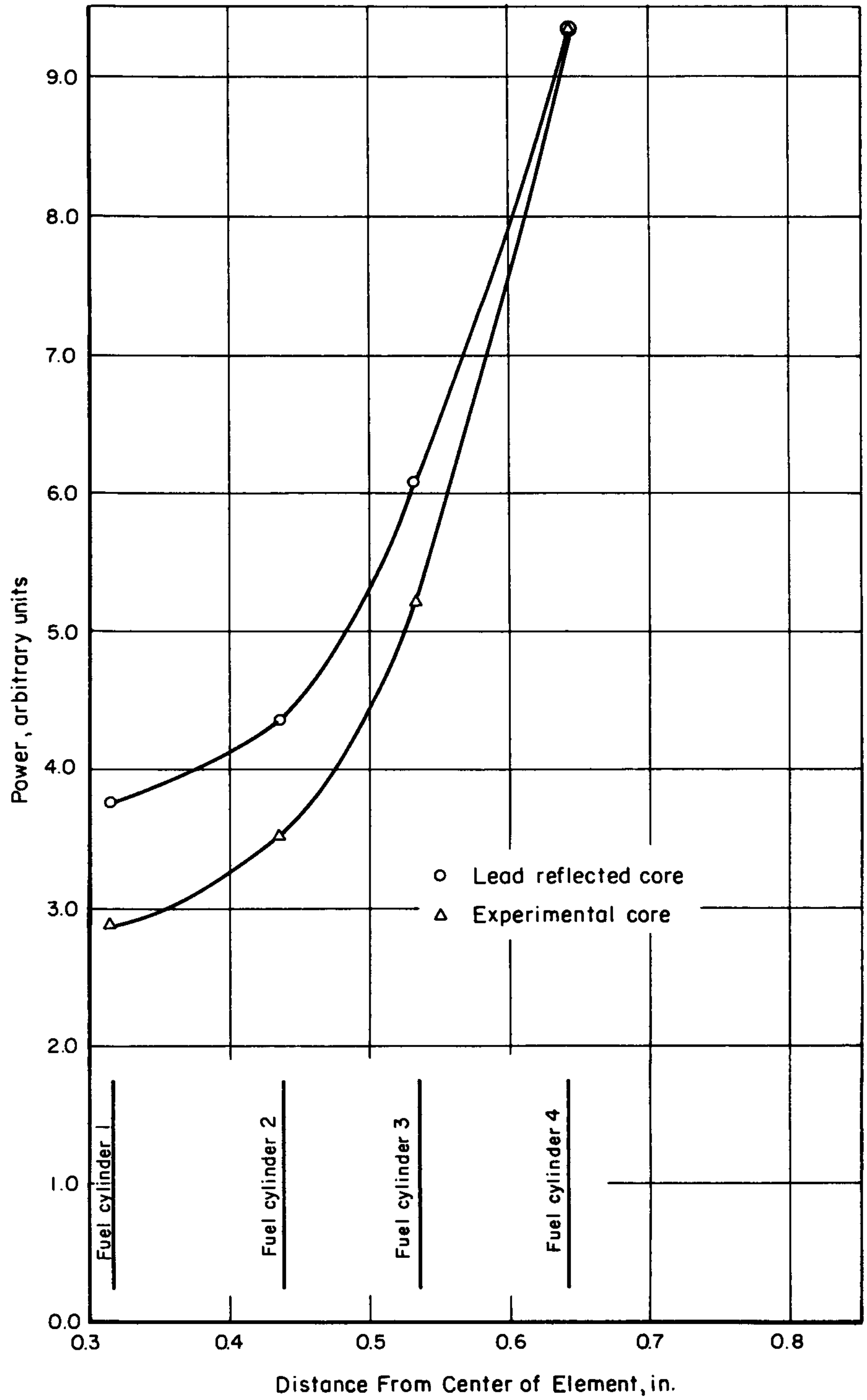

FIGURE 52. POWER DEPRESSION IN THE CENTRAL FUEL ELEMENT

Power normalized to peak power on outer fuel cylinder.

[redacted]

TABLE 18. NUMBER OF FUEL ELEMENTS, FUEL INVENTORY, AND EXCESS REACTIVITY IN GCRE-1 CRITICAL-ASSEMBLY CORES

Core Configuration	Number of Elements	Fuel Inventory, g	Excess Reactivity in Core, per cent $\frac{\Delta k}{k}$
Experimental Core	54	16,383	+0.250
Clean Core	64	19,453	+0.258
Lead-Reflected Core[(a)]	56	17,093	+0.495
Simulated-Flooded Core	37	11,318	0.000

(a) Criticality could have been achieved with 55 fuel elements; however, experiments in progress required an excess reactivity and hence the minimum number of fuel elements was not used.

Reactivity Measurements

In the Experimental Core the worth of the upper axial reflector was measured to be about 0.4 per cent $\frac{\Delta k}{k}$ for 2 in. of reflector. In addition, the worth of a 2-3/4-in. upper axial annular reflector surrounding the upper grid plate was measured to be 0.08 per cent $\frac{\Delta k}{k}$.

The temperature coefficient of reactivity was measured in both the Clean Core and Lead-Reflected Core. A linear variation of the coefficient with temperature was noted in both cases. The values were approximately equal, +0.22 per cent $\frac{\Delta k}{k}$, for a temperature change from 20 to 80 C.

Measurements were made of the worth of peripheral fuel elements in each core. Table 19 summarizes these results.

TABLE 19. WORTH OF FUEL ELEMENTS ADDED TO CORE PERIMETER

Core Configuration	Worth of Fuel-Element Additions, per cent $\frac{\Delta k}{k}$ per element
Experimental Core	0.350
Clean Core	0.221
Lead-Reflected Core	0.380
Simulated-Flooded Core	0.435

Measurements were made of the worth of fuel cans (without fuel) filled with various water-simulating organic materials in Position 29 in the Lead-Reflected Core. These experiments were done as an aid to selecting a water substitute for the Simulated-Flooded Core mock-up. The results are summarized in Table 20. The change in reactivity is roughly proportioned to change in hydrogen density in magnitude, but opposite in sign.

[redacted]

[redacted]

TABLE 20. COMPARISON OF THE REACTIVITY WORTH AND HYDROGEN DENSITY OF VARIOUS MATERIALS

Material	Hydrogen Atoms per Cm^3 at 20 C	Material Worth Relative to Water, per cent $\frac{\Delta k}{k}$
Water	6.7×10^{22}	--
Mineral oil	7.5×10^{22}	-0.014
Polyethylene	7.9×10^{22}	-0.042
Paraffin	8.0×10^{22}	-0.052

Migration Area

The migration area was measured in the Experimental Core. Values of 59.3 and 59.7 cm^2 were obtained by using as the axial reflector savings 12.7 cm obtained by extrapolating flux plots; a value of 55.9 cm^2 was obtained from an analysis using only the data from the migration-area experiment.

Flux-Distribution Measurements

Complete flux mapping was done in the Experimental Core and the Clean Core using manganese-wire activation techniques. The results show a large flux peaking in the radial and lower axial reflectors and a depression in the region of the simulated burnable poison.

Detailed flux measurements were made in a fuel-element unit cell, including the moderator region adjacent to the fuel element, for the purpose of calculating thermal utilizations. This was done in the Experimental and Simulated-Flooded Cores; the thermal utilizations were 0.780 and 0.715, respectively.

Power-Distribution Measurements

Power distributions were measured by the catcher-foil technique. The axial and radial core power variations agree favorably with the flux variations.

Power distributions were also measured within fuel elements. Typical determinations of the variation of the power generated on the four fuel cylinders of a given fuel element are presented in Table 21. There were no major deviations from these power ratios throughout the core.

[redacted]

[redacted]

TABLE 21. POWER VARIATION WITHIN FUEL ELEMENTS

Core Configuration	Ratio of Power Generation in Indicated Fuel Cylinder to That of Outer Cylinder: Inner	Second	Third	Outer
Experimental Core	0.452	0.506	0.651	1.00
Lead-Reflected Core	0.529	0.576	0.723	1.00

The core axial and radial peak-to-average power ratios and the radial peak-to-average power ratio within an element were computed. Using these values, the peak-to-average power variation for the core was computed with and without the variation within the fuel element. In these calculations the separability of the power variations was assumed; this was found to be generally true for all cores from the flux and power measurements which were made. These ratios appear in Table 22.

TABLE 22. PEAK-TO-AVERAGE POWER RATIOS

	Ratio of Peak-to-Average Power: Experimental Core	Lead-Reflected Core
Within an Element	1.42	1.32
Axially	1.39	1.38
Radially	1.42	1.37
Core (Neglecting the Power Variation Within an Element)	1.97	1.89
Core (Including Element Variation)	2.80	2.50

The local variation of power-generation rate in the vicinity of a mock-up shim-control blade was measured. It was noted that the local power density varied by 25 per cent from the side of the outer fuel cylinder facing the shim blade to the opposite side.

Mock-Up Control-Blade Experiments

The control blades for the GCRE-1 will enter the core horizontally, passing between rows of elements on lines parallel to Radius AA (Figure 4). The shim, setback, and fine-control rods are expected to be of tungsten, which is not as black to thermal neutrons as cadmium or boron. A 2-in.-wide blade of tungsten inserted at midheight has a reactivity worth of 0.4 to 0.7 per cent $\frac{\Delta k}{k}$, depending upon core configuration and rod insertion distance.

The shutdown and safety rods are only to shut the reactor down in an emergency and to hold it subcritical for changing elements, etc. A thermally black rod with many absorption peaks in the resonance region is desirable to produce maximum shutdown. A sandwich construction of tungsten and indium between two sheets of cadmium was found to produce 25 per cent greater reactivity control than cadmium alone and

[redacted]

approximately the same increase over the use of tungsten alone. The original GCRE-1 design having eight blades, 8 in. wide, was found to be insufficient to control the 61-element lead-reflected flooded core. Further experiments showed that a combination of two 24-in., one 14-in., and one 10-in. blade would make the 61-element lead-reflected Simulated-Flooded Core from 1.2 to 2.4 per cent $\frac{\Delta k}{k}$ subcritical, the exact value depending upon the worth of the additional elements, which was not obtained.

REFERENCES

(1) "GCRE Hazard Summary Report", IDO-28506 (March, 1958). Confidential.

(2) Hanna, G. C., Milton, J. D. C., Sharp, W. T., Stevens, N. M., and Taylor, E. A., Proceedings of the Symposium on the Physics of Fission Held at Chalk River, Ontario, May 14 to 18, 1956, CRP-642A (May, 1956).

(3) Worthing, Archie G., and Geffner, Joseph, Treatment of Experimental Data, John Wiley and Sons, Inc., New York (1943).

(4) Jankowski, F. J., Klein, D., and Miller, T. M., Nuclear Science and Engineering, 2, 287-302 (1957).

(5) Proceedings of the International Conference on the Peaceful Uses of Atomic Energy, Vol. 5, United Nations, New York (1956), pp 206-7.

(6) Proceedings of the International Conference on the Peaceful Uses of Atomic Energy, Vol. 5, United Nations, New York (1956), p 195.

DAD:WCB:RWK:RAE:FJJ:JWC/mmk

[redacted]

APPENDIX A

CRITICAL-ASSEMBLY CONTROL-ROD CALIBRATIONS

[redacted]

[redacted]

APPENDIX A

CRITICAL-ASSEMBLY CONTROL-ROD CALIBRATIONS

Since most of the experiments were based on reactivity measurements, it was necessary to calibrate some of the critical-assembly rods for each of the four core configurations studied. Figures A-1 through A-6 give the results of these calibrations. Figure A-1 gives the differential reactivity worth of Rod 2 in each core. (Figure 4 in the text of this report gives the location of each rod.) The corresponding integral worths are given in Figure A-2. Similar curves for Rod 3 are given in Figures A-3 and A-4. The perturbing influence of the cadmium band is quite apparent from the curves of differential worth of both Rods 2 and 3. The variations in total worth and shape of the calibration curve for a given rod occur because in going from one core configuration to another the changing core configuration produces changes of importance for the regions through which the rod passes, and the changing core diameter produces a relative change in rod location.

The above rod worths were all found with no mock-up blades present. Figures A-5 and A-6 give the differential and integral reactivity worths of Rod 2 in the flooded core with various mock-up blade configurations.

One curve on Figure A-5 is the differential rod worth for Rod 2 with no mock-up blades present. The other curve and the two isolated points show the effect on control-rod worth of mock-up blades (see Figure 13 for mock-up blade locations).

[redacted]

[redacted]

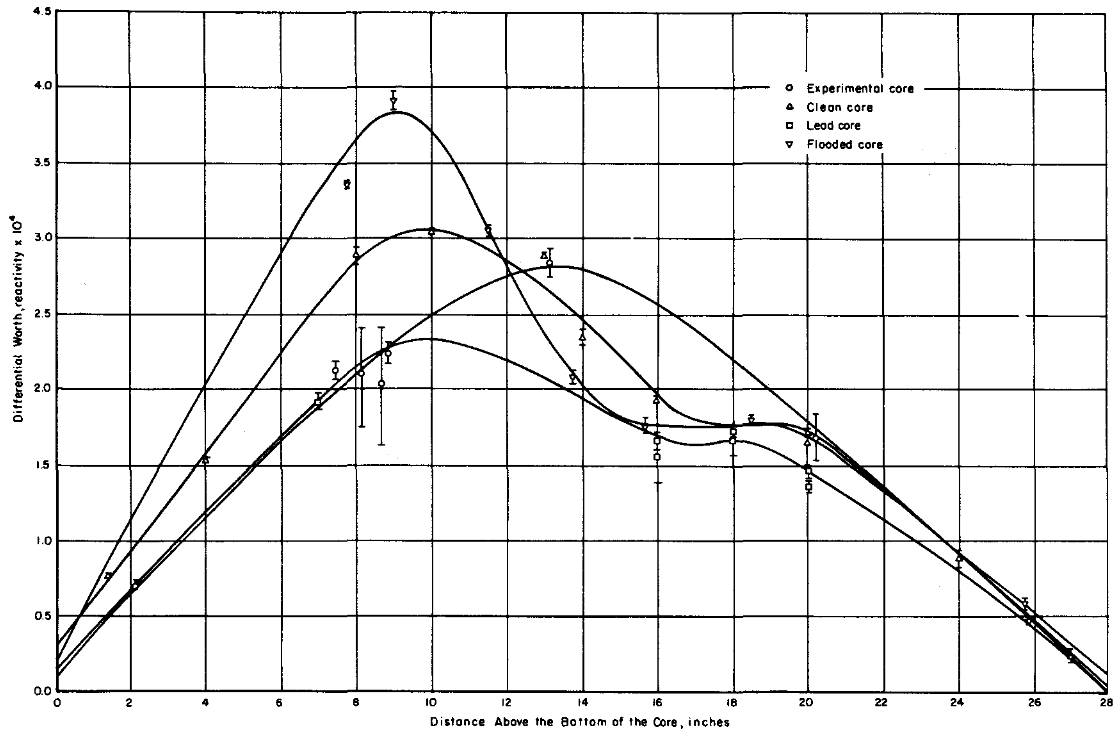

FIGURE A-1. DIFFERENTIAL WORTH OF CRITICAL-ASSEMBLY CONTROL-ROD 2

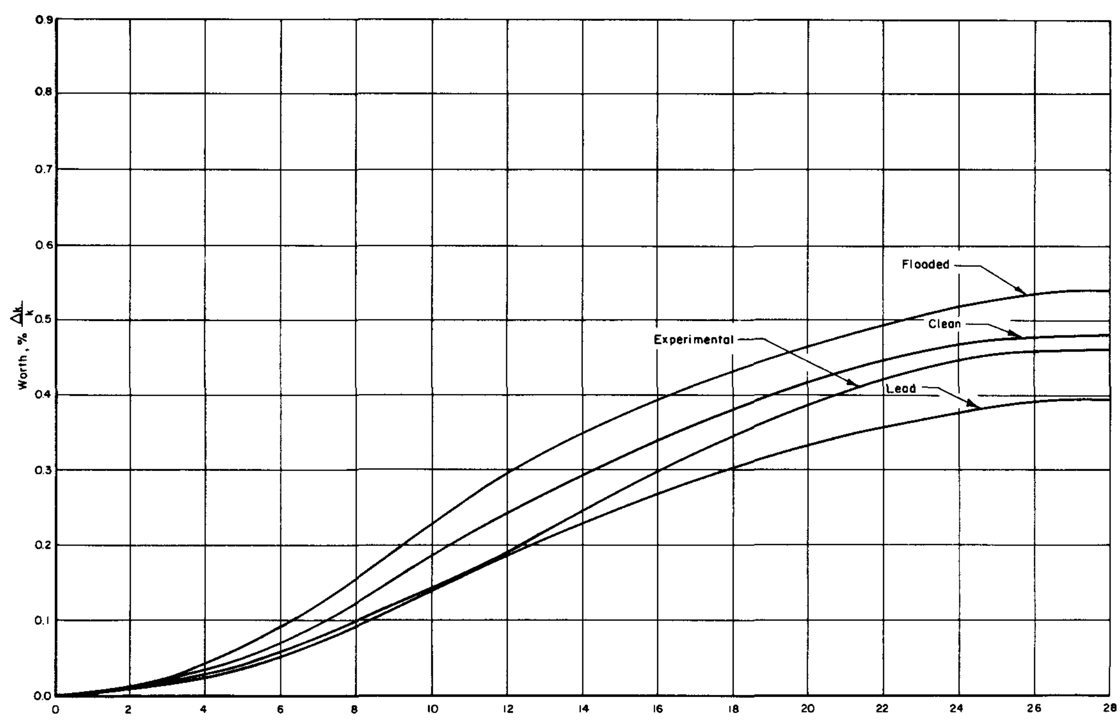

FIGURE A-2. INTEGRAL WORTH OF CRITICAL-ASSEMBLY CONTROL-ROD 2

[redacted]

[redacted]

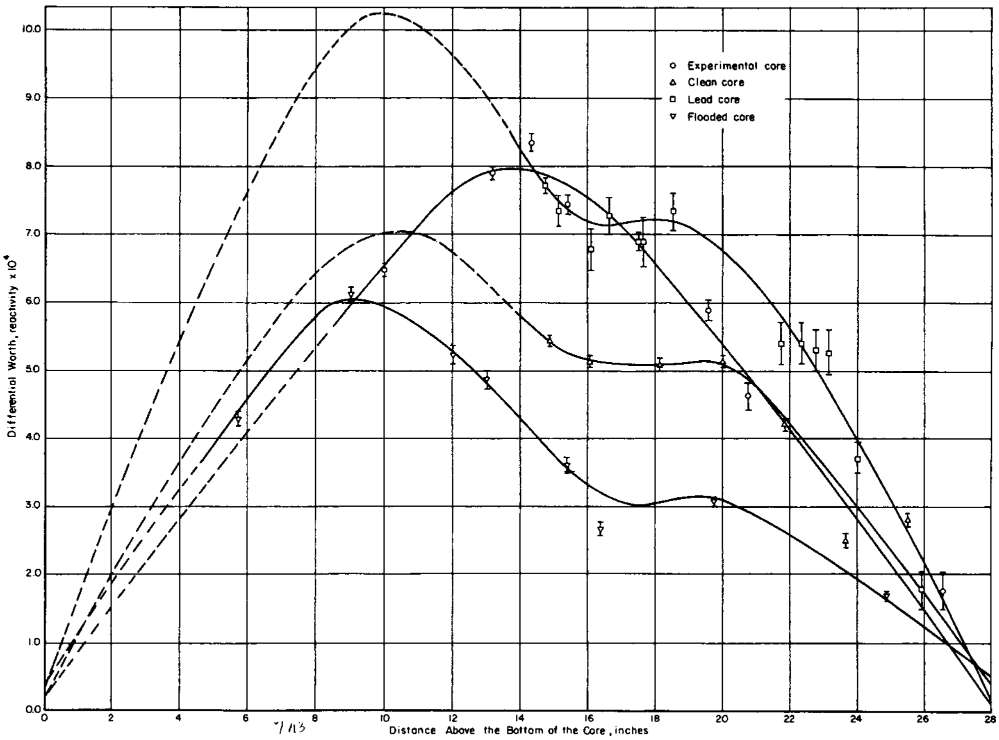

FIGURE A-3. DIFFERENTIAL WORTH OF CRITICAL-ASSEMBLY CONTROL-ROD 3

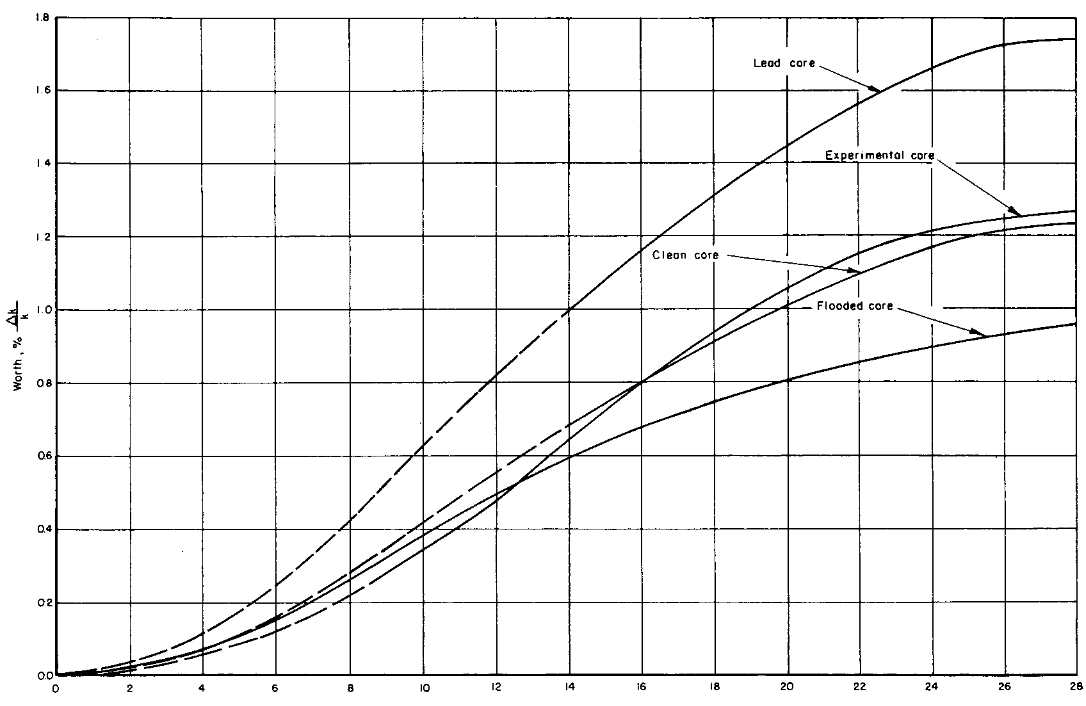

FIGURE A-4. DIFFERENTIAL WORTH OF CRITICAL-ASSEMBLY CONTROL-ROD 3

[redacted]

[redacted]

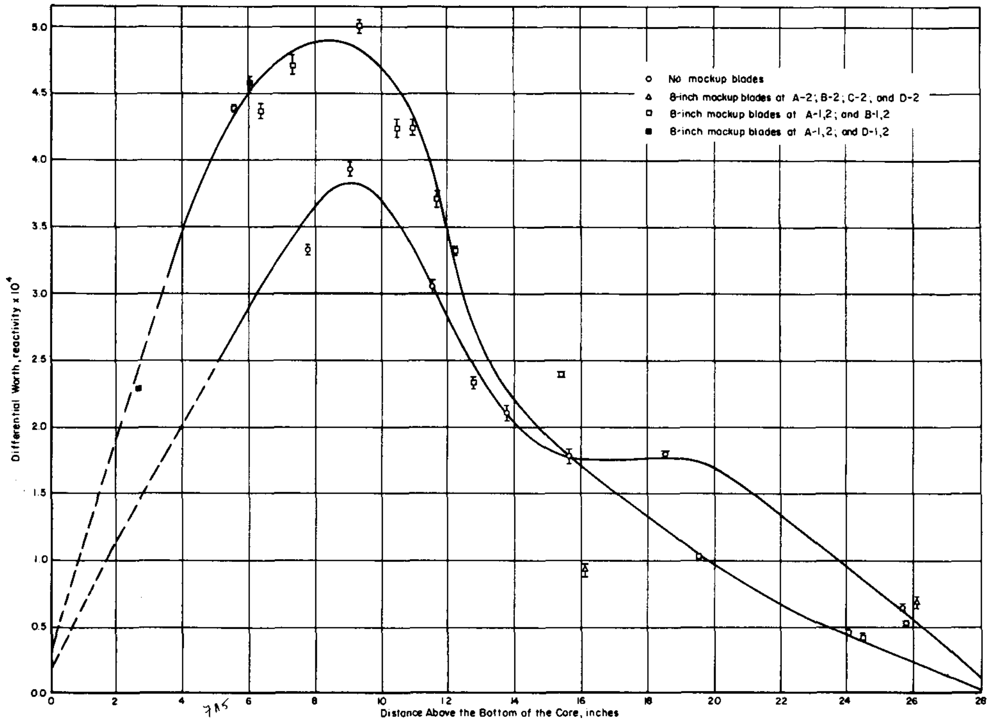

FIGURE A-5. DIFFERENTIAL WORTH OF CRITICAL-ASSEMBLY CONTROL-ROD 2 IN THE FLOODED CORE WITH MOCK-UP CONTROL BLADES

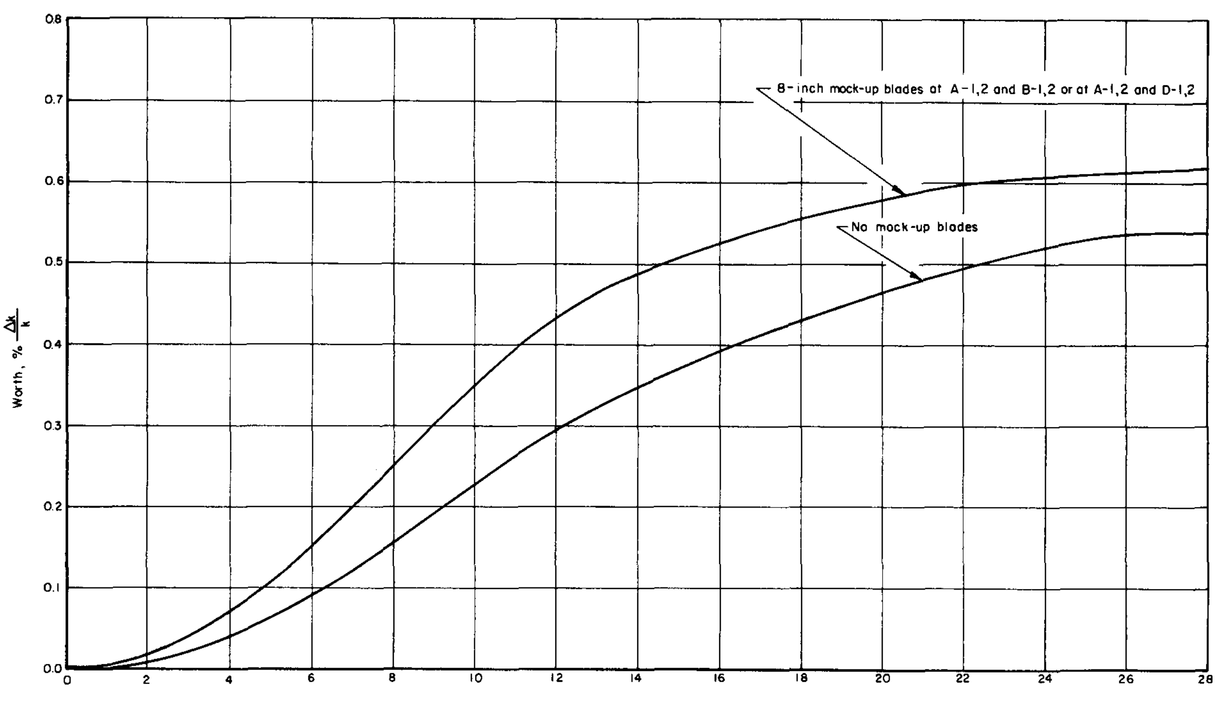

FIGURE A-6. INTEGRAL WORTH OF CRITICAL-ASSEMBLY CONTROL-ROD 2 ON THE FLOODED CORE WITH MOCK-UP CONTROL BLADES

[redacted]